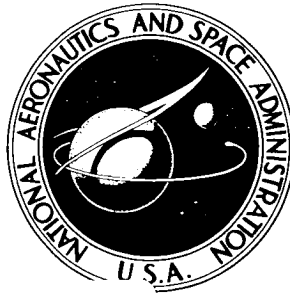


NASA TECHNICAL NOTE



NASA TN D-2690

NASA TN D-2690

FACILITY FORM 602

N65 18212	
(ACCESSION NUMBER)	(THRU)
123	1
(PAGES)	(CODE)
	02
(NASA CR OR TMX OR AD NUMBER)	(CATEGORY)

GPO PRICE \$

OTS PRICE(S) \$ 4.00

Hard copy (HC)

Microfiche (MF) 1.00

# LANDING GEAR LOADS OBTAINED DURING SIMULATED LANDING TESTS OVER VARIOUS OBSTACLES

*by Robert C. Dreher*

*Langley Research Center*

*Langley Station, Hampton, Va.*

LANDING-GEAR LOADS OBTAINED DURING SIMULATED  
LANDING TESTS OVER VARIOUS OBSTACLES

By Robert C. Dreher

Langley Research Center  
Langley Station, Hampton, Va.

NATIONAL AERONAUTICS AND SPACE ADMINISTRATION

---

For sale by the Office of Technical Services, Department of Commerce,  
Washington, D.C. 20230 -- Price \$4.00

LANDING-GEAR LOADS OBTAINED DURING SIMULATED  
LANDING TESTS OVER VARIOUS OBSTACLES

By Robert C. Dreher  
Langley Research Center

SUMMARY

18212

An investigation was made at the Langley landing-loads track to obtain information on the loads induced on an airplane by rough terrain. The investigation consisted of simulated landing-impact tests, taxiing tests, and slow-rolling tests over obstacles of various sizes and shapes by using a main landing gear of the OV-1C Mohawk airplane. This landing gear is of the cantilever type, and the shock strut was equipped with a standard metering pin and orifice. The nominal diameter of the tire was 26 inches. The size of the obstacles varied up to 4 inches in height and 120 inches in length; a sand bed 8 inches in height and 720 inches in length was also used. Forward speeds from 40.0 to 88.7 knots were attained during the landing-impact tests. Speeds during the slow-rolling tests were in the neighborhood of 2 feet per second. The data are presented in the form of tables and time histories of the various parameters measured.

INTRODUCTION

AUTHOR

A considerable amount of interest has been shown recently by the military services, as well as aircraft and tire manufacturers, concerning the operation of airplanes on rough or unprepared terrain. A major problem to be considered in operations of this type is the loads induced on the airplane by the rough terrain. These loads will dictate the landing-gear design, as well as other design criteria, for airplanes to be used for operations on rough terrain. The U.S. Army has authorized a study contract with industry to investigate by analytical methods the loads induced on the OV-1C Mohawk airplane during landings on terrain of varying degrees of roughness. In order to obtain experimental data to be used to confirm the analytical computations of this study, the National Aeronautics and Space Administration had conducted simulated landing-impact tests and taxiing tests with a main landing gear of this airplane over obstacles of various sizes and shapes which simulate rough terrain. In addition to being used with analytical studies, it was believed that experimental data would provide empirical relationships not readily obtained by analytical methods. These data obtained by using one type of landing gear could be useful also as a basis for comparison with other types that may be developed for operations on rough terrain.

Very little information is available on the behavior of tires as they traverse obstacles. In analytical analyses, various assumptions have to be made concerning the behavior of the tires. Therefore, in an attempt to obtain some insight on the characteristics of a tire as it passes over an obstacle, this investigation included slow-rolling tests over various obstacles.

This investigation was made at the Langley landing-loads track and employed a main landing gear of the OV-1C Mohawk airplane. This landing gear is a cantilever type and was equipped with a 26-inch-diameter tire. Except for the sand bed, maximum heights of the obstacles were 2, 3, and 4 inches, and the lengths varied from 3 to 120 inches. The forward speed ranged from 40.0 to 88.7 knots during the landing-impact tests, and the vertical velocity at touchdown ranged from 5.9 to 12.0 feet per second. The point of touchdown occurred at various distances near and ahead of the obstacles during the landing-impact tests. During the taxiing tests, the point of touchdown occurred well ahead of the obstacles. Forward speeds during the slow-rolling tests were approximately 2 feet per second.

The purpose of this paper is to present the data obtained during the tests. The data are presented in the form of tables and time histories of the various parameters measured, and no attempt at analysis is made.

## APPARATUS

### Test Vehicle

The tests were made by using the test facility at the Langley landing-loads track. The test vehicle of this facility is the carriage shown in figure 1. It is 60 feet long and 30 feet wide and weighs approximately 100 000 pounds. The carriage straddles a concrete runway and is catapulted to the desired forward speed by means of a hydraulic-jet catapult. Further information on the operation of this facility is given in reference 1 and on the hydraulic jet in reference 2. The landing gear was attached to a truss which, in turn, was attached to a vertical drop carriage incorporated in the main carriage. A means for simulating wing lift is incorporated in the drop carriage; this means consists of applying an upward force after the desired vertical velocity is attained. In these tests the total drop weight was 6 618 pounds, and a simulated wing lift of approximately 0.85g was used.

### Landing Gear

The landing gear used in the tests is shown in figure 2 and, as mentioned previously, is the main gear used on the OV-1C Mohawk airplane. It was equipped with a ribbed tread 8.50 x 10, type III, 10-ply-rating tire during the landing-impact and taxiing tests and with an 8-ply-rating tire during the slow-rolling tests. These tires have a nominal diameter of 26 inches. A tire inflation pressure of 90 pounds per square inch was used for all tests. The manufacturer's load-deflection curve for the 10-ply-rating tire at 90 pounds per square inch and for the 8-ply-rating tire at 85 pounds per square inch are



shown in figure 3. The circular symbols represent values obtained experimentally during this investigation with the 8-ply-rating tire at an inflation pressure of 90 pounds per square inch. The oleopneumatic shock strut had a stroke of 15 inches and contained a standard metering pin and orifice. Dimensions of this metering pin are given in figure 4. The strut was filled with hydraulic fluid up to the upper port of the strut when it was in the fully compressed position. Air was bled from the fluid by cycling the strut slowly. Then, with the strut in the fully extended position and free of the ground, it was inflated with nitrogen to a pressure of 100 pounds per square inch. The landing gear was inclined  $5^{\circ}45'$  forward and  $2^{\circ}13'$  outboard, as shown in figure 5. Weights of the different components of the landing gear and other pertinent information are given in table I. The air volume of 208.5 cubic inches with the strut fully extended was computed from values of strut stroke and air pressures given on the strut-servicing decal on the landing gear.

### DESCRIPTION OF OBSTACLES

Seven types of obstacles employing 23 configurations were used in this investigation (one of these types was holes or depressions in the runway surface). The profile shape, maximum height, length, and material of which the obstacle was constructed are given in table II. The obstacles were constructed of these materials and fastened securely to the runway surface so that a rigid profile would be maintained as the landing-gear wheel passed over the obstacle. Photographs of several of the obstacles are shown in figure 6; the direction of motion as the landing gear traversed the obstacle is noted on the photographs.

The obstacles having a one-minus-cosine ( $1 - \cos$ ) profile and a length of 30 inches, the semicylinder, and the hemisphere had a base  $3/4$  inch thick and were mounted on top of the runway surface. Therefore, in order for the surface ahead of these obstacles to be at the same height as the beginning of the profiles, a ramp having a steel surface 16 feet in length was fastened to the runway surface adjoining and ahead of these obstacles. The first 2 feet of this ramp tapered from  $1/4$  inch to  $3/4$  inch. There was a  $3/4$ -inch drop to the runway surface at the rear of these obstacles. This ramp was also placed ahead of the first obstacle in the configuration consisting of the  $1 - \cos$  undulations and of the  $1 - \cos$  shaped obstacles which were spaced 9 feet apart (tests 20 to 26).

The obstacles constructed of reinforced concrete were mounted on a  $1/4$ -inch steel plate which was fastened to the runway surface. The front and rear edges of this plate were shaped so that they were included in the profile of the obstacle. The plywood step-shaped obstacles (table II) had a steel block 3 inches in length at the beginning of the step. Obstacles in the form of holes or depressions were obtained by removing a portion of the concrete runway and replacing it in the desired shape. The obstacle consisting of soft sand was a bed approximately 9 feet wide and 60 feet long. This bed was obtained by placing mortar sand which weighed 96.4 pounds per cubic foot on the runway surface and by leveling it to a depth of 8 inches.

## INSTRUMENTATION

The locations on the landing gear of the various instruments used during the tests are shown in figure 5. Strain gages mounted along the half-fork of the landing gear measured the loads developed normal and parallel to the shock strut. Accelerometers mounted inside the wheel axle measured accelerations in the drag and vertical directions which were used to obtain the lower mass inertia loads developed on the strut. The strut oil pressure transducer was mounted in the metering-pin support plate which is located inside the inner cylinder of the shock strut. The air pressure transducer was mounted in the upper port of the outer cylinder. The outputs of these instruments were recorded on an 18-channel oscillograph.

In addition to the instruments mounted on the landing gear, instrumentation was provided to determine the horizontal speed and displacement of the test carriage as it traveled along the runway. The vertical velocity and vertical displacement of the drop carriage were also measured. The instrument used to determine the horizontal displacement of the test carriage was also used to indicate on the oscillograph record the position of the wheel axle (in the static position) in relation to the obstacles.

## TEST PROCEDURE

Test conditions during the landing-impact tests over the various obstacles are given in table III. The forward speeds are the speeds at the time the landing gear passed over the obstacle and the values of vertical velocity are those measured at the time of touchdown. A wing lift of approximately 0.85g was applied to the drop carriage for all the landing-impact tests. After the test carriage was brought up to the test speed, the vertical drop carriage was released at a preselected point along the runway, allowing the landing-gear tire to contact the runway at various distances near and ahead of the obstacles. During the taxiing tests, the wheel was allowed to contact the runway well ahead of the obstacles, and no wing lift force was applied. All tests were made on a dry runway, except as noted in table III. During taxiing tests 17 and 30, the shock strut was blocked in the fully extended position so that it could not telescope.

In the slow-rolling tests, the tug shown in figure 1 was used to push the test carriage over the obstacles at approximately 2 feet per second. For these tests, the vertical drop carriage of the main carriage and the shock strut were restrained so that neither could move vertically. As the landing gear passed over the obstacle, all vertical displacement other than structural deflections occurred in the tire. Three series of tests were made over five types of obstacles, as shown in table IV. The series differed in the initial tire deflection. In the first series, the drop carriage was blocked in a position so that the tire barely touched the runway surface ahead of the obstacle. The next series was made with the tire deflected 1 inch before being pushed over

the obstacle. Similarly, the third series was made with an initial tire deflection of  $2\frac{1}{4}$  inches.

## PRESENTATION OF DATA

### Landing-Impact and Taxiing Tests

The data obtained during landing-impact and taxiing tests over the various obstacles are shown in figures 7 to 34. These data consist of loads, accelerations, displacements, velocities, and pressures and are presented in the form of time histories from the time of touchdown (for the landing-impact tests) until after the landing gear has traversed the obstacle. In the taxiing tests and the tests where touchdown occurred at an appreciable time ahead of the obstacle, the data are presented only during the time pertinent to the obstacle. The data have been reduced in time increments of 0.001 second.

The upward, aft, and outboard directions of the loads and accelerations are indicated by positive values. Positive values of the drop-carriage vertical displacement, the wheel-axle displacement, and the drop-carriage velocity indicate a downward direction. For the telescoping displacement and telescoping velocity of the strut, positive values indicate that the strut is being compressed. The time at which the center of the wheel axle (in the static position) was over the peak of the obstacles having a smooth contour (tests 1 to 32) and the time at which it was over the beginning of the ramp, the step-shaped obstacles, the holes, and the sand bed (tests 33 to 49) are noted on the figures by the notations "peak of obstacle" and "start of obstacle," respectively.

Ground loads.- The vertical ground loads were obtained from the algebraic sum of the vertical components of the axial shock-strut load, the axial lower mass inertia load, and the side shock-strut load minus the algebraic sum of the vertical components of the normal shock-strut and normal lower mass inertia loads. The horizontal (drag) ground loads were obtained in a similar manner by adding the algebraic sum of the horizontal components of the normal shock-strut and normal lower mass inertia loads to the algebraic sum of the horizontal components of the axial shock-strut and lower mass inertia loads.

Shock-strut loads.- The axial and normal shock-strut loads were obtained by strain gages placed along the half-fork of the landing gear. These loads were corrected mathematically for interaction. During the tests in which touchdown occurred on the steel plate placed ahead of the obstacles having a  $\frac{3}{4}$ -inch base, the values of the normal shock-strut load and hence the horizontal ground load during the time of wheel spin-up were smaller than those obtained where spin-up occurred on dry concrete because of the difference in the coefficient of friction of the two surfaces.

Inertia loads.- The axial lower mass inertia loads were obtained by multiplying the lower mass weight of 127 pounds by the axial accelerations obtained from the accelerometer mounted inside the wheel axle. The normal lower mass

inertia loads were obtained in a similar manner by using the accelerations normal to the shock strut. However, by free vibration of the landing gear, the effective weight of the lower mass was found to be 75 pounds in the horizontal direction. Therefore, this weight was multiplied by the normal accelerations in order to obtain values for the normal lower mass inertia loads.

Accelerations.- The upper mass accelerations were obtained from accelerometers mounted on the upper portion of the landing gear, as shown in figure 5. These accelerometers were oriented so that they measured the accelerations parallel and normal to the shock strut. The values of the accelerations parallel to the shock strut are increments above the lg datum.

Displacements.- The drop-carriage vertical displacement is the vertical distance the drop carriage travels after touchdown. The strut telescoping displacement is the strut stroke, and 15 inches is the maximum. The wheel-axle vertical displacement is the drop-carriage displacement minus the strut stroke. On a smooth runway this value is an indication of tire deflection if wheel-axle deflection is neglected.

Velocities.- The strut telescoping velocity is the rate of closure or extension of the shock strut. The drop-carriage velocity is the vertical velocity of the total dropping weight. The value at zero time is the vertical velocity at touchdown.

Pressures.- The strut oil and strut air pressures are those measured inside the shock strut. It should be remembered that the shock strut had an initial pressure of 100 pounds per square inch. Therefore, the values shown in the figures are increments above this initial pressure.

Side inertia loads and upper mass side accelerations.- The lower mass inertia side loads and the upper mass side accelerations obtained during tests over two obstacles are shown in figure 34 in order to present representative values of these quantities obtained with this landing gear. Figure 34(a) shows the values of the loads and accelerations obtained with a 1 - cos profile, 2-inch-high, 30-inch-long obstacle, whereas figure 34(b) shows the values obtained with an obstacle of the same size and shape but oriented  $45^{\circ}$  to the direction of motion. An effective weight of 90 pounds was used with the lower mass side accelerations to obtain the lower mass inertia loads. This effective weight was obtained by free vibration of the landing gear.

### Slow-Rolling Tests

As mentioned previously, the slow-rolling tests were made in order to obtain information on the behavior of a tire as it passes over an obstacle. Since both the shock strut and the upper mass were restrained from moving in the vertical direction, the results are not indicative of those to be expected from an airplane rolling slowly over obstacles. Even though the tests were not made under dynamic conditions, it was believed that the information obtained could be useful in studies involving tire behavior over obstacles, especially

\*since these obstacles included some which had a radius less than the tire radius, as well as step-shaped obstacles in which a sharp corner deflected the tire.

Table IV gives the maximum vertical ground loads measured as the landing gear was pushed over each of 12 obstacles. The tire was initially deflected 0, 1, and  $2\frac{1}{4}$  inches before being pushed over each obstacle.

Time histories of the vertical ground loads obtained during slow-rolling tests over four different obstacles are shown in figure 35. The time at which the center of the wheel axle was over the beginning of the obstacle is denoted by zero on the time scale; the time at which the wheel axle passed over the end of the obstacle is noted on the figure. Time histories obtained with different initial tire deflections for the same obstacle are not equal in length because the approximate speed of 2 feet per second varied for each test. The 1 - cos, 3-inch-high, 30-inch-long obstacle had a base which was  $\frac{3}{4}$  inch thick. A ramp that tapered from 0 to  $\frac{3}{4}$  inch in the length of 1 foot was placed ahead of this obstacle.

The vertical ground loads obtained during the slow-rolling tests given in table IV and figure 35 were measured by a strain gage mounted on the bottom of the wheel axle. This gage was statically calibrated by varying a downward force on the vertical drop carriage and by measuring the vertical load at the bottom of the tire by means of a ground-reaction platform. Corrections for drag and side interactions are not included in the values given.

#### CONCLUDING REMARKS

A detailed discussion of results obtained in the investigation of simulated landing tests over various obstacles has been omitted in order to expedite publication of these data. However, the following general observations concerning the results of the present investigation are made.

Vertical loads as large as four and five times the static weight were induced on the landing gear by some of the obstacles used in this investigation. The magnitude of the induced loads appears to be affected by, among other parameters, the time during the landing impact at which the obstacle is encountered. In the slow-rolling tests the obstacles having the same maximum height but a length less than the tire radius induced smaller loads on the tire than those having a longer length. This statement appears to be true for the radius-shaped obstacles as well as the step-shaped obstacles and is apparently due to the ability of the tire to absorb or swallow the smaller obstacles.

Langley Research Center,  
National Aeronautics and Space Administration,  
Langley Station, Hampton, Va., November 30, 1964.

## REFERENCES

1. Joyner, Upshur T.; Horne, Walter B.; and Leland, Trafford J. W.: Investigations on the Ground Performance of Aircraft Relating to Wet Runway Braking and Slush Drag. AGARD Rept. 429, Jan. 1963.
2. Joyner, Upshur T.; and Horne, Walter B.: Considerations on a Large Hydraulic Jet Catapult. NACA TN 3203, 1954. (Supersedes NACA RM L51B27.)

TABLE I.- LANDING-GEAR DATA

## Weight, lb:

## Lower mass:

Inner cylinder . . . . .	64
Wheel and tire . . . . .	41
Brake assembly . . . . .	16
Instrumentation . . . . .	6
Total . . . . .	127

## Upper mass:

Outer cylinder . . . . .	56
Side brace . . . . .	18
Instrumentation . . . . .	10
Total . . . . .	84

Attachment truss . . . . .	660
Drop carriage . . . . .	5747

Total drop weight . . . . . 6618

## Natural frequency in drag direction, cps, for:

## Strut extension, in., of:

15 . . . . .	12.8
$7\frac{1}{2}$ . . . . .	15.6
1 . . . . .	18.2

## Area, sq in.:

Pneumatic . . . . .	12.566
Hydraulic . . . . .	9.289 - (Metering-pin area)
Orifice . . . . .	0.4418

## With strut in fully extended position:

Air volume, cu in. . . . .	208.5
Distance between upper and lower bearings, in. . . . .	10.65
Distance between lower bearing and wheel axle, in. . . . .	39.97

## Metering pin:

Extension upstream through orifice with strut fully extended, in. . .	0.51
Extension downstream with strut fully compressed, in. . . . .	0.85

TABLE II.- PROFILE SHAPE AND SIZE OF OBSTACLES

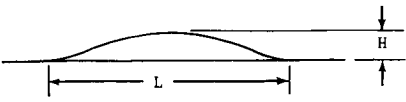
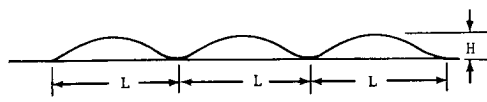
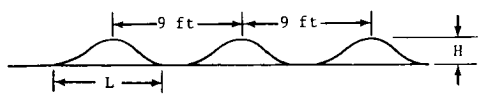
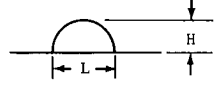
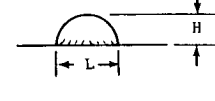
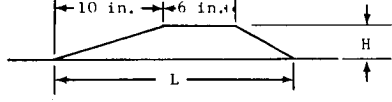
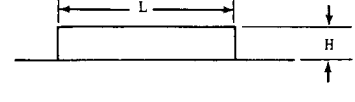
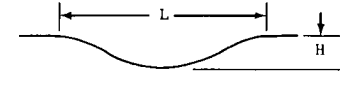
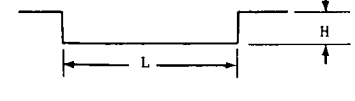
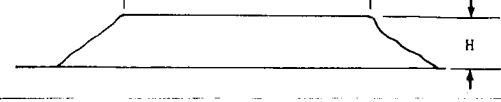
Profile		Size, in.		Material
Shape	Description	Height, H	Length, L	
	1 - cos	2 and 3	30	Cast aluminum
		2, 3, and 4	10	Concrete
	1 - cos (oriented 45° to runway)	2 and 3	30	Cast aluminum
	1 - cos (undulations)	2 and 3	30	Cast aluminum
	1 - cos (9 feet apart)	3	30	Cast aluminum
	Semicylinder	3	6	Steel
	Hemisphere	3	6	Steel
	Ramp	3	21	Concrete
	Step	2 and 3 3 3 2, 3, and 4	3 10 1/2 24 120	Steel Plywood ↓
	1 - cos (hole)	3	15	Concrete
	Step (hole)	3	15	Concrete
	Bed	8	720	Sand



TABLE III.- TEST CONDITIONS DURING LANDING-IMPACT TESTS OVER OBSTACLES

Test	Figure	Obstacle dimension, in.		Forward speed, knots	Vertical velocity, fps (a)	Time at which peak is reached, sec (b)	Touchdown ahead of obstacle, ft	Remarks
		Height	Length					
Shape: 1 - cos								
1	7(a)	2	10	86.3	12.0	0.106	15.4	Wet runway  

<sup>a</sup>At time of touchdown.<sup>b</sup>Time when center of wheel axle is over peak of smooth-contour obstacles or at start of step-shaped obstacles and holes.

TABLE IV.- LOADS OBTAINED DURING SLOW-ROLLING TESTS OVER OBSTACLES

[Forward speed  $\approx$  2 feet per second]

Shape	Obstacle dimensions, in.		Initial tire deflection, in.	Maximum vertical ground load, lb	
	Maximum height	Length		Ahead of obstacle	Over obstacle
Step	2	3	0 1 $2\frac{1}{4}$	0 2 548 6 671	3 639 5 459 8 856
Step	2	120	0 1 $2\frac{1}{4}$	586 3 163 6 794	5 270 8 786 13 237
Step	3	3	0 1 $2\frac{1}{4}$	185 2 653 6 632	5 357 6 995 10 371
Step	3	$10\frac{1}{2}$	0 1 $2\frac{1}{4}$	240 2 997 6 593	7 792 11 029 13 667
Step	3	21	0 1 $2\frac{1}{4}$	242 2 911 6 794	7 642 11 160 16 013
Ramp	3	21	0 1 $2\frac{1}{4}$	121 2 425 6 308	6 794 9 826 14 313
Semicylinder	3	6	0 1 $2\frac{1}{4}$	359 3 116 6 593	6 533 8 633 12 347
Hemisphere	3	6	0 1 $2\frac{1}{4}$	359 2 938 6 353	4 075 6 234 10 070
1 - cos	2	10	0 1 $2\frac{1}{4}$	0 2 585 7 017	2 903 5 541 9 235
1 - cos	2	30	0 1 $2\frac{1}{4}$	0 3 046 7 388	6 168 9 789 13 667
1 - cos	3	10	0 1 $2\frac{1}{4}$	185 2 593 6 632	4 893 6 632 9 889
1 - cos	3	30	0 1 $2\frac{1}{4}$	0 2 532 6 995	9 049 11 517 15 555

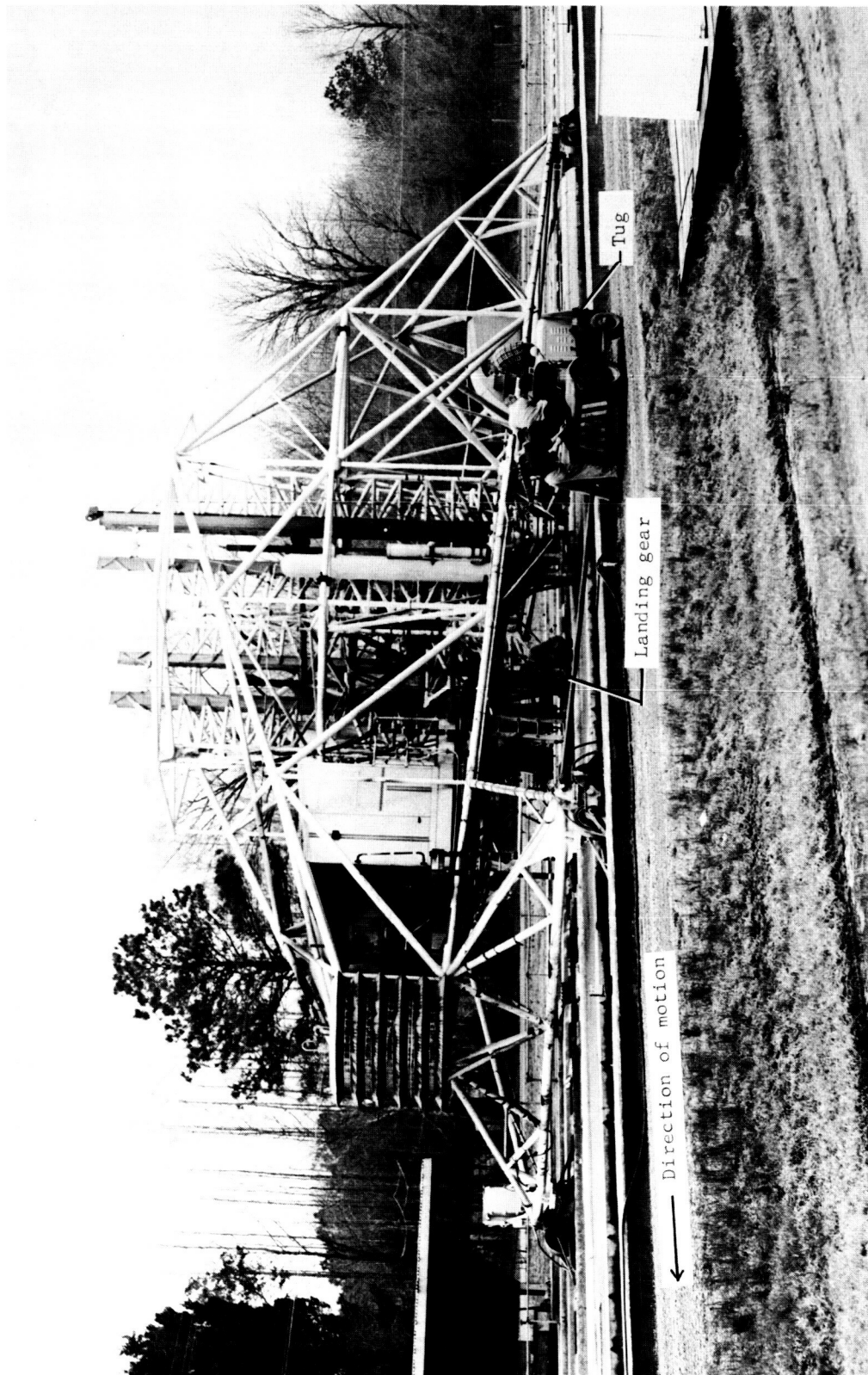
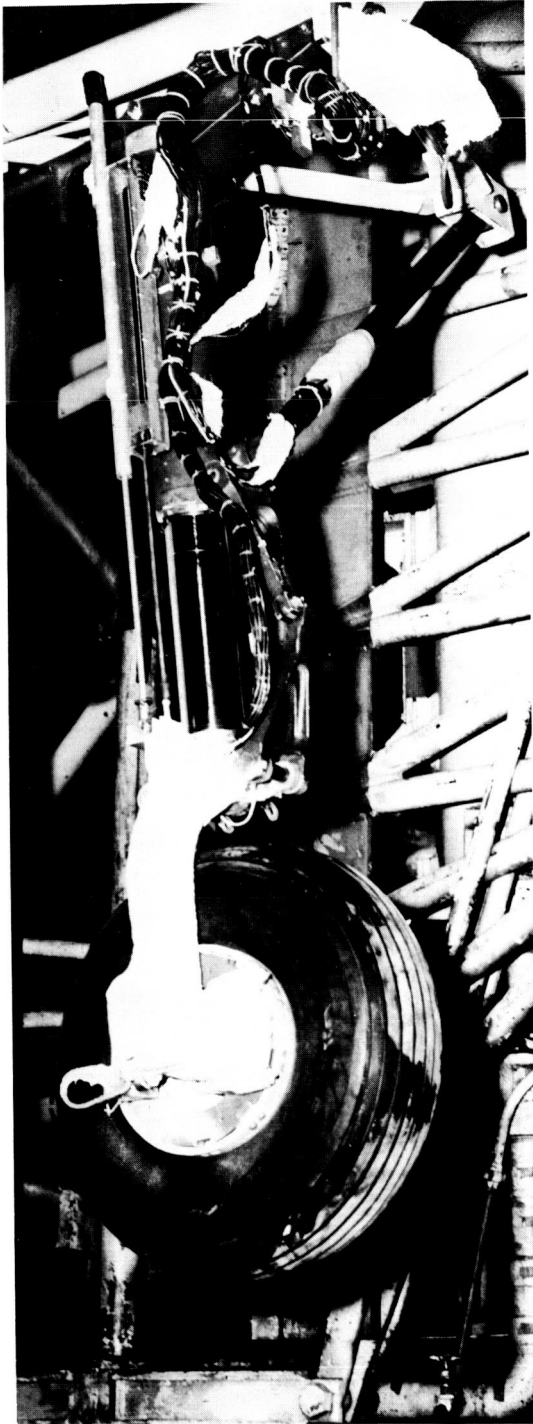
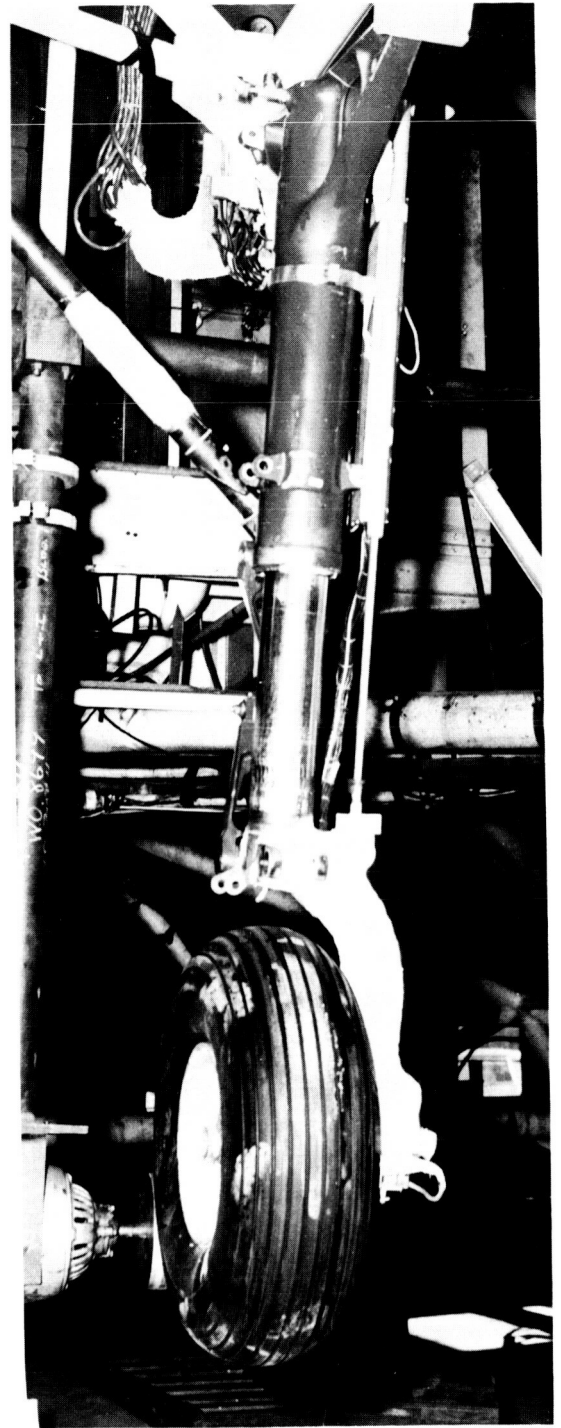


Figure 1.- View of Langley landing-loads track carriage.

L-64-10213



(a) Side view.



(b) Rear view.

L-64-10214

Figure 2.- Landing gear used in tests.

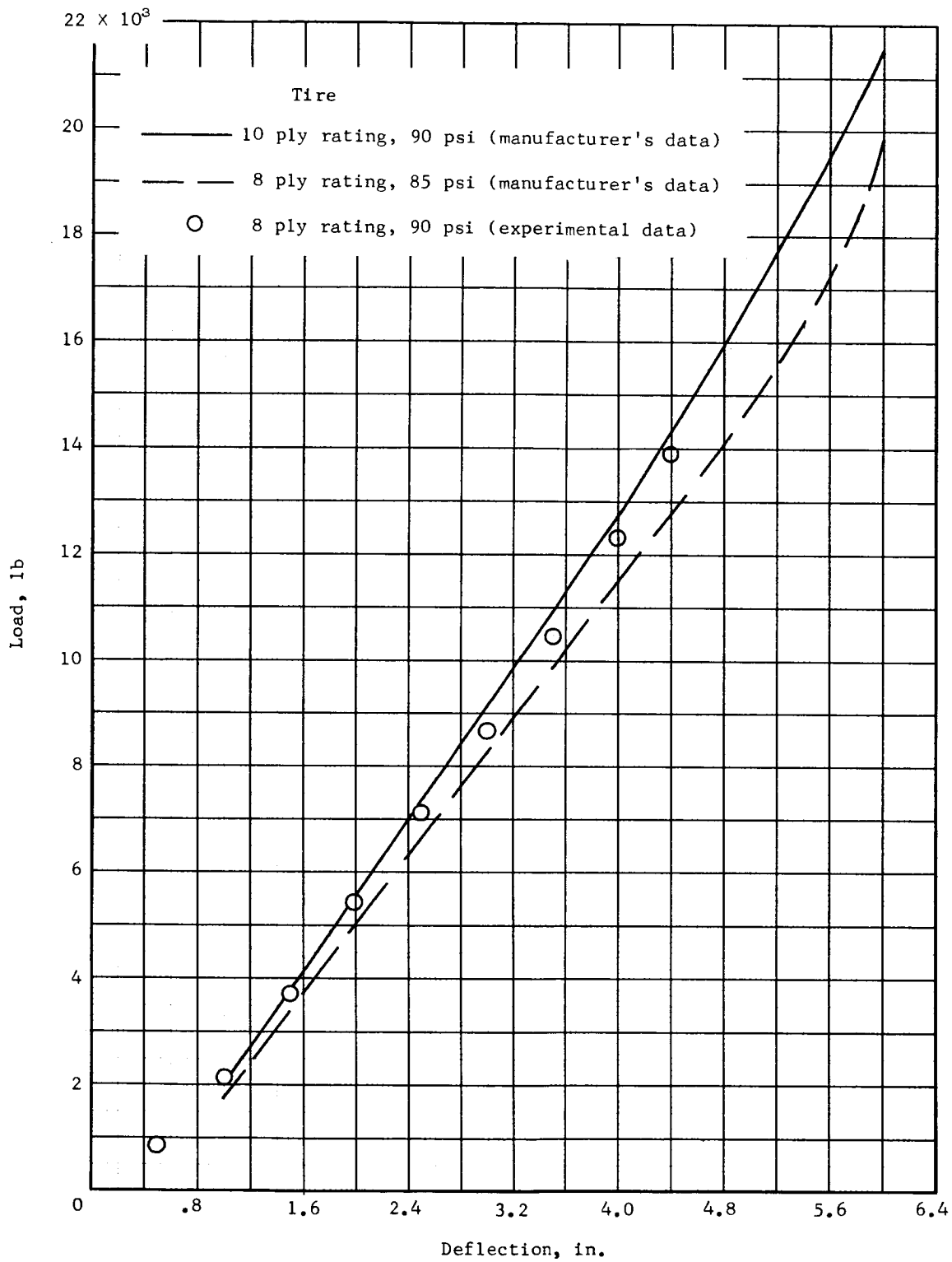


Figure 3.- Load-deflection curves for three 8.50 x 10, type III, 8- and 10-ply-rating tires.

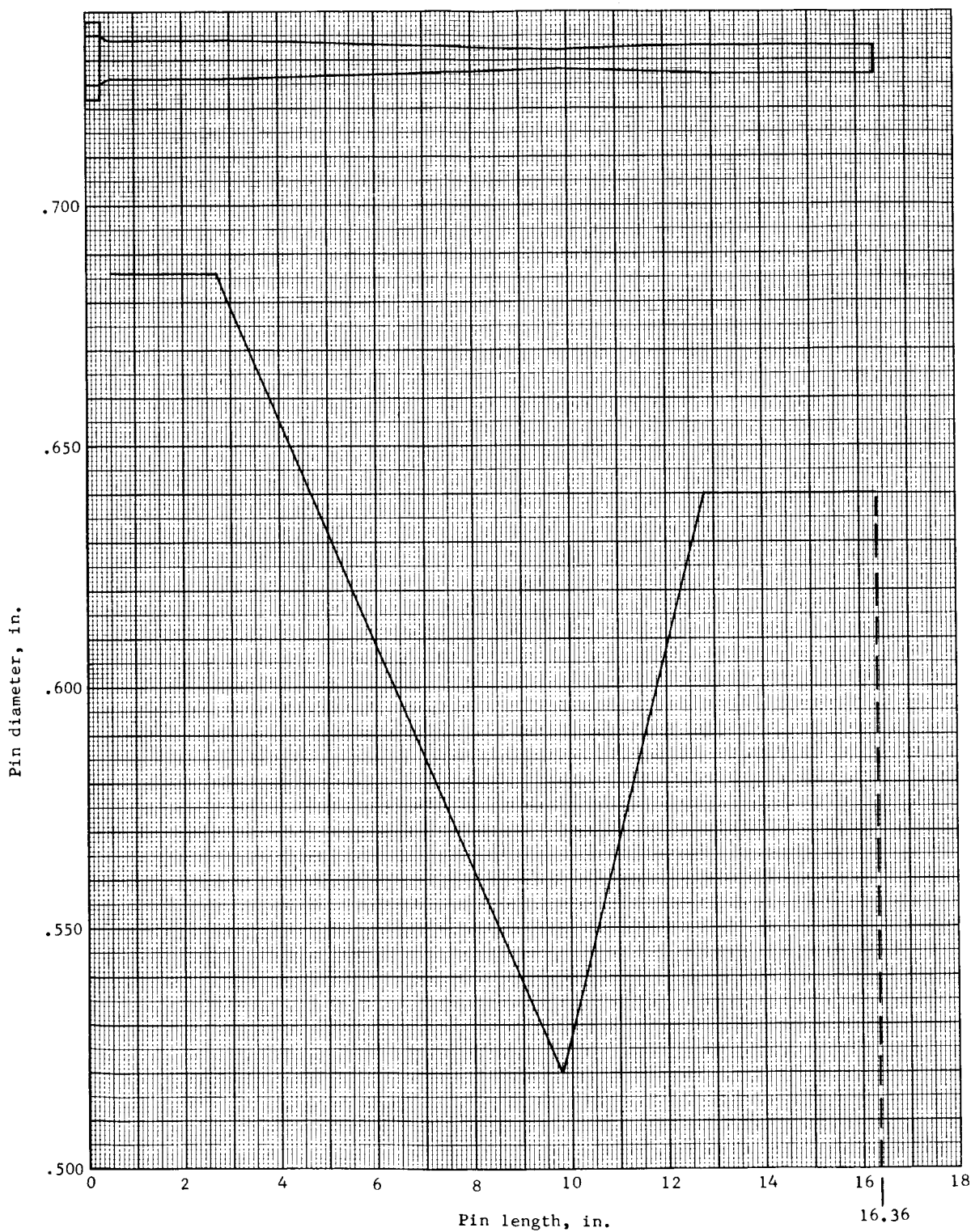


Figure 4.- Dimensions of metering pin; orifice diameter = 0.75 inch.

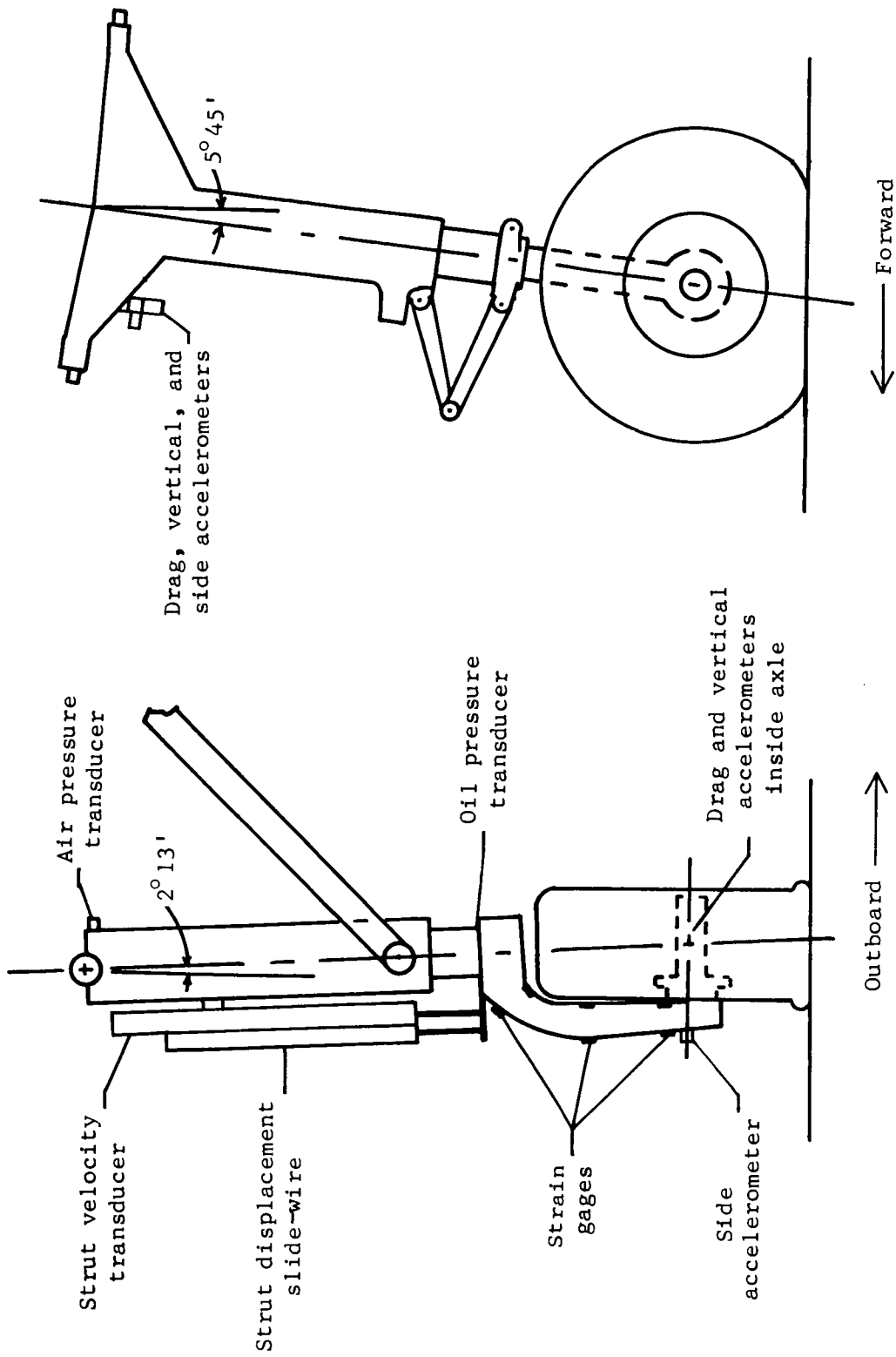
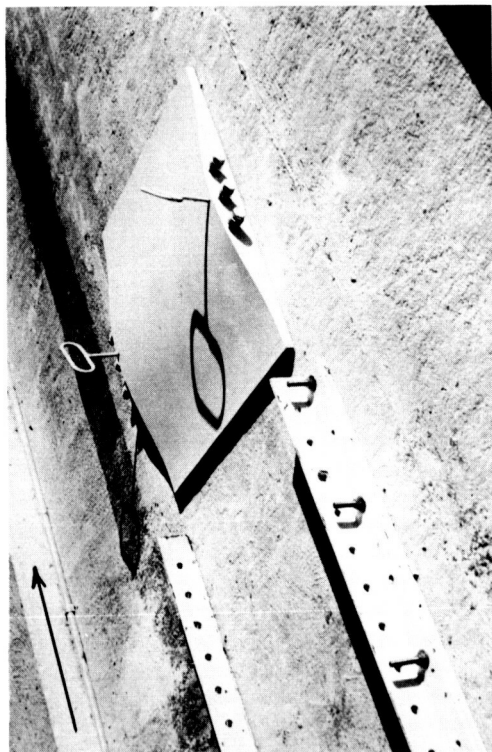
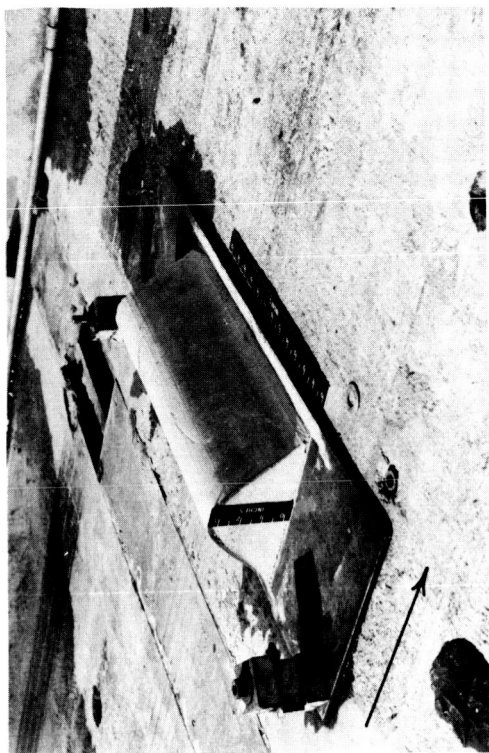


Figure 5.- Sketch showing instrumentation of landing gear.



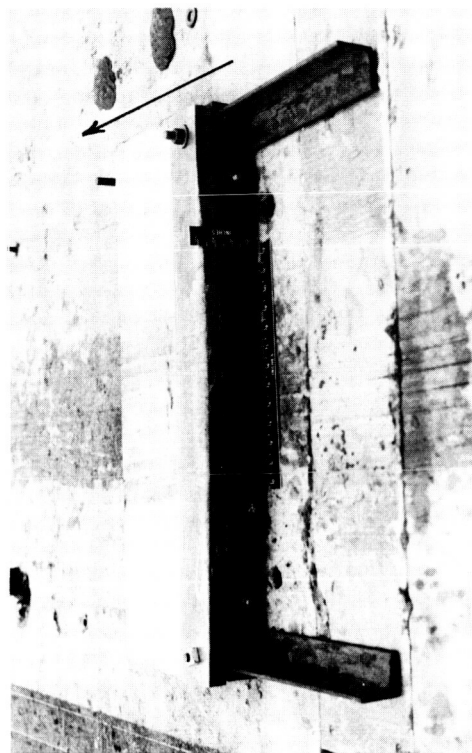
(a) 1 - cos: 2 inches high, 30 inches long.



(b) 1 - cos: 4 inches high, 10 inches long.



(c) Step: 4 inches high, 120 inches long.

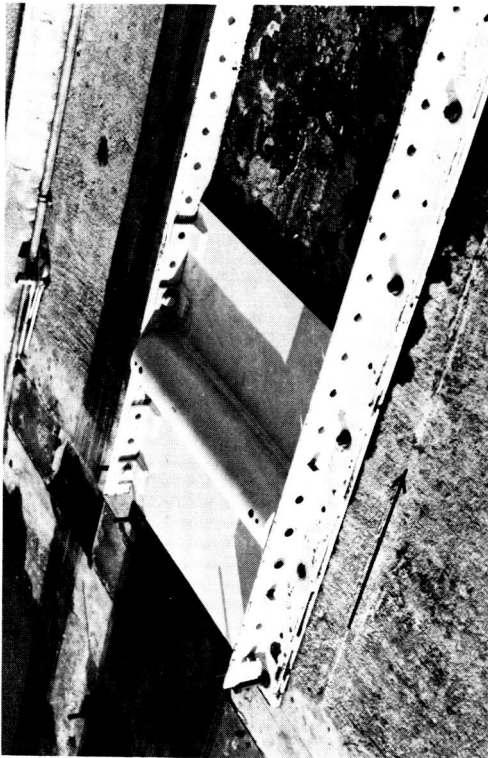


(d) Step: 3 inches high,  $10\frac{1}{2}$  inches long.

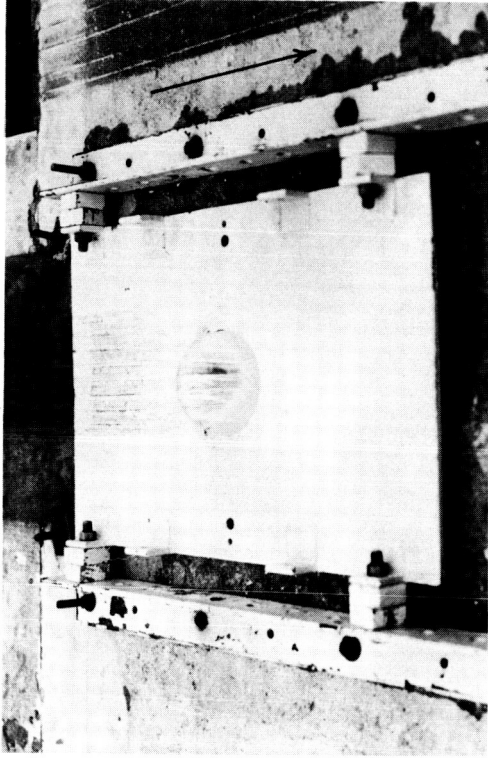
Figure 6.- Types of obstacles used during tests. (Arrows indicate direction of motion.)

I-64-10215

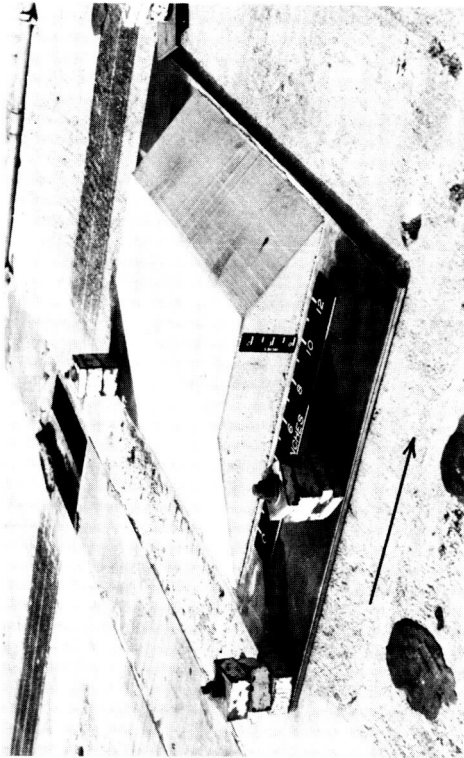




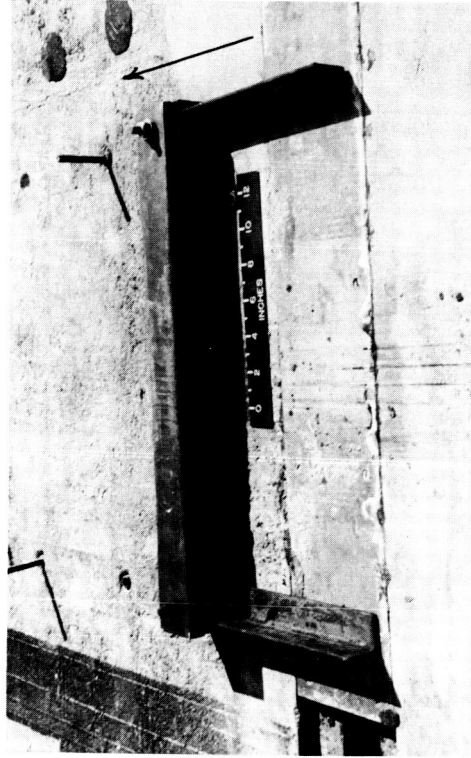
(e) Semicylinder: 3 inches high, 6 inches long.



(f) Hemisphere: 3 inches high, 6 inches long.



(g) Ramp: 3 inches high, 21 inches long.



(h) Step: 3 inches high, 3 inches long.

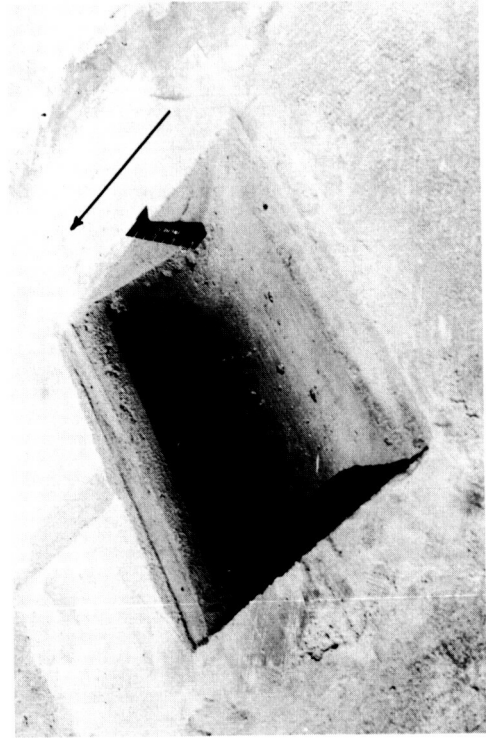
Figure 6.- Continued.



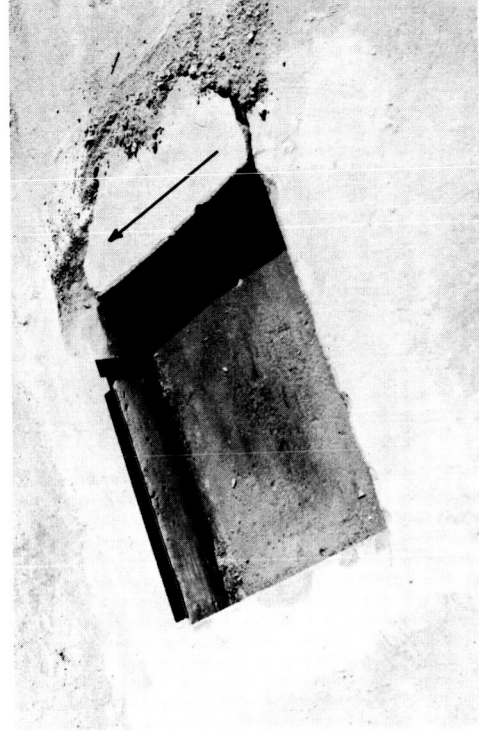
(i) 1 - cos (oriented  $45^{\circ}$  to runway):  
2 inches high, 30 inches long.



(j) Soft sand: 8 inches deep, 720 inches long.

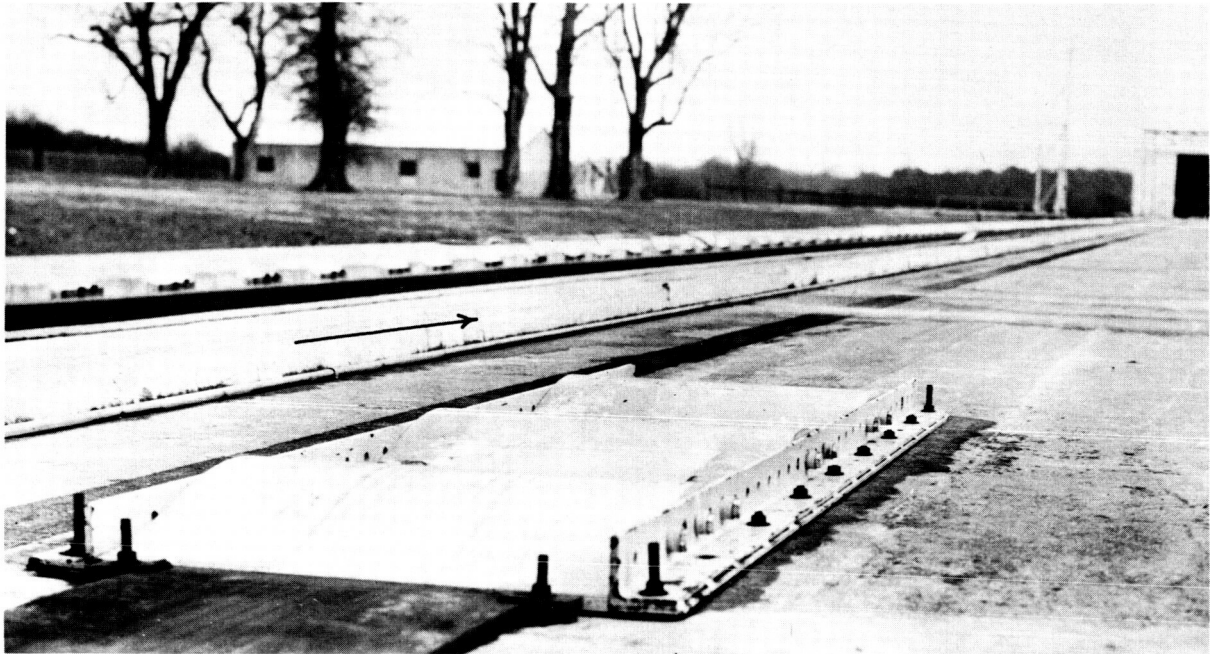


(k) 1 - cos hole: 3 inches deep, 15 inches long.

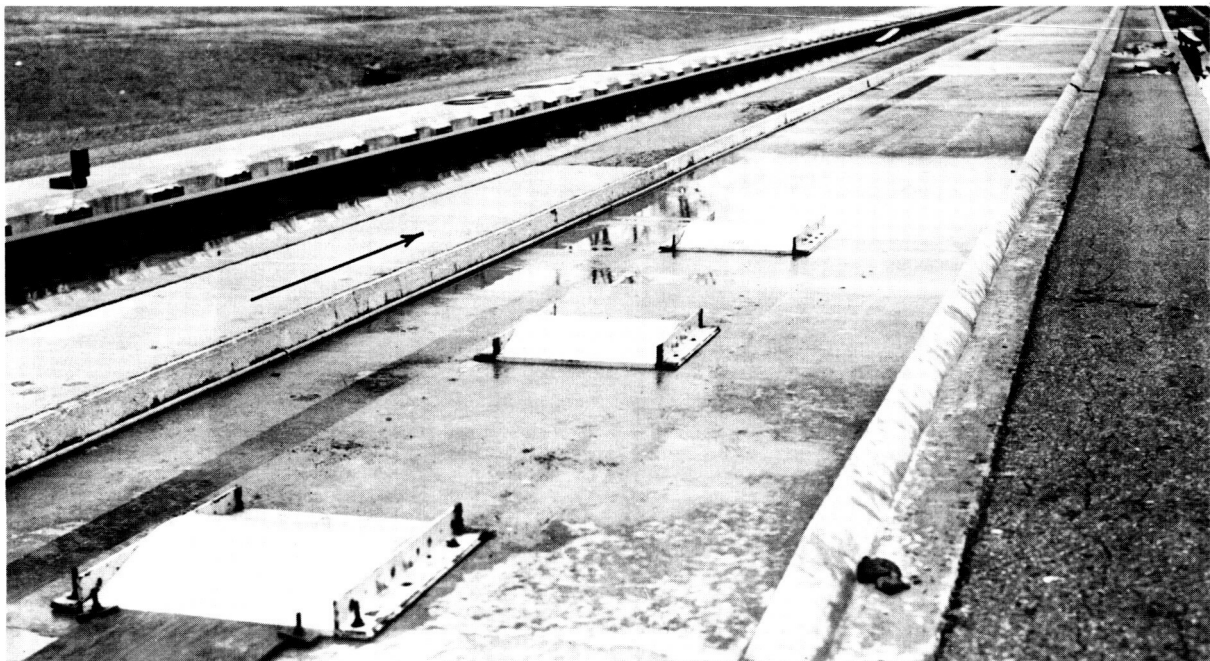


(l) Step hole: 3 inches deep, 15 inches long.

I-64-10217



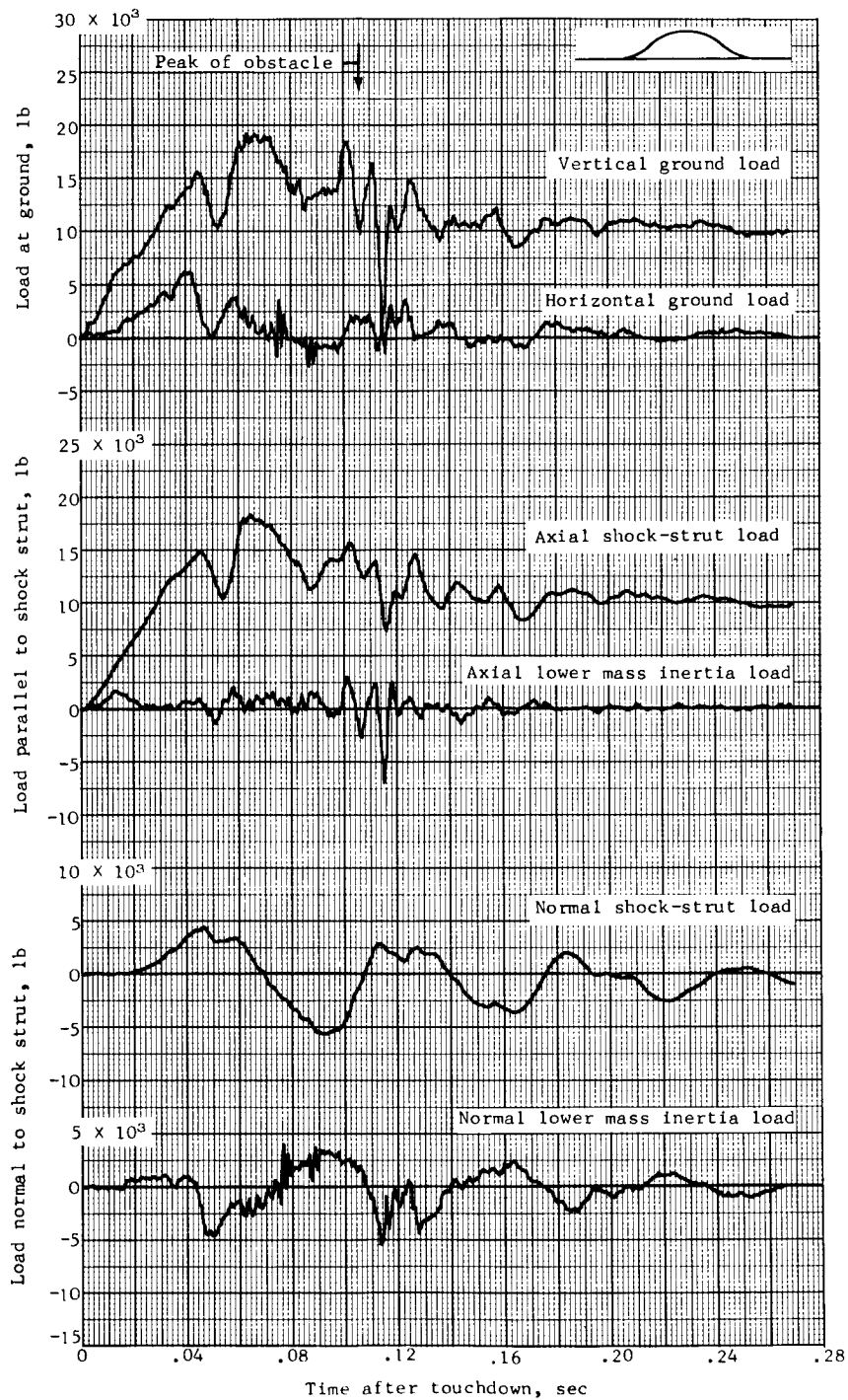
(m) 1 - cos undulations: 3 inches high, 30 inches long.



(n) 1 - cos, spaced 9 feet apart: 3 inches high, 30 inches long.

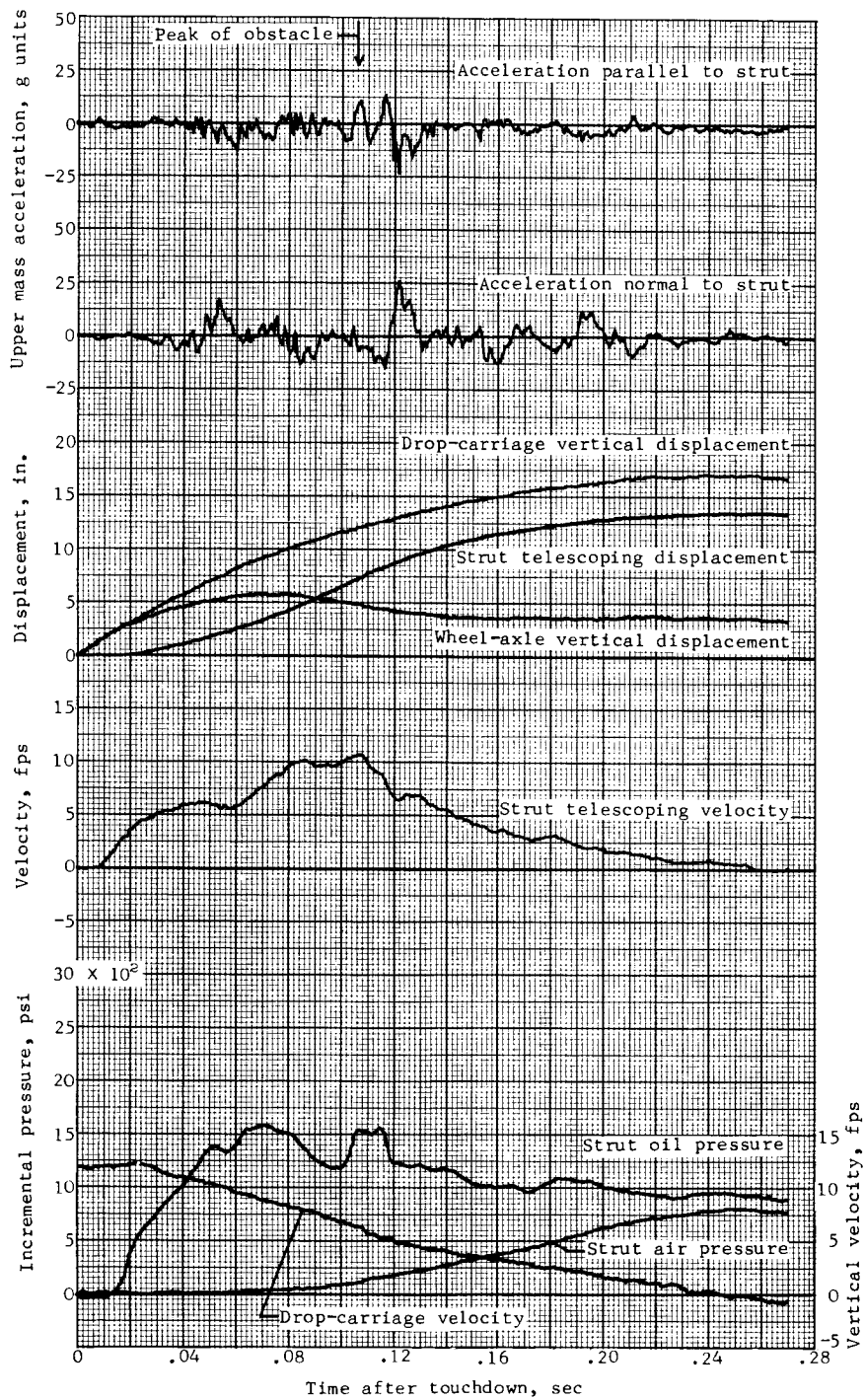
L-64-10218

Figure 6.- Concluded.



(a) Test 1.

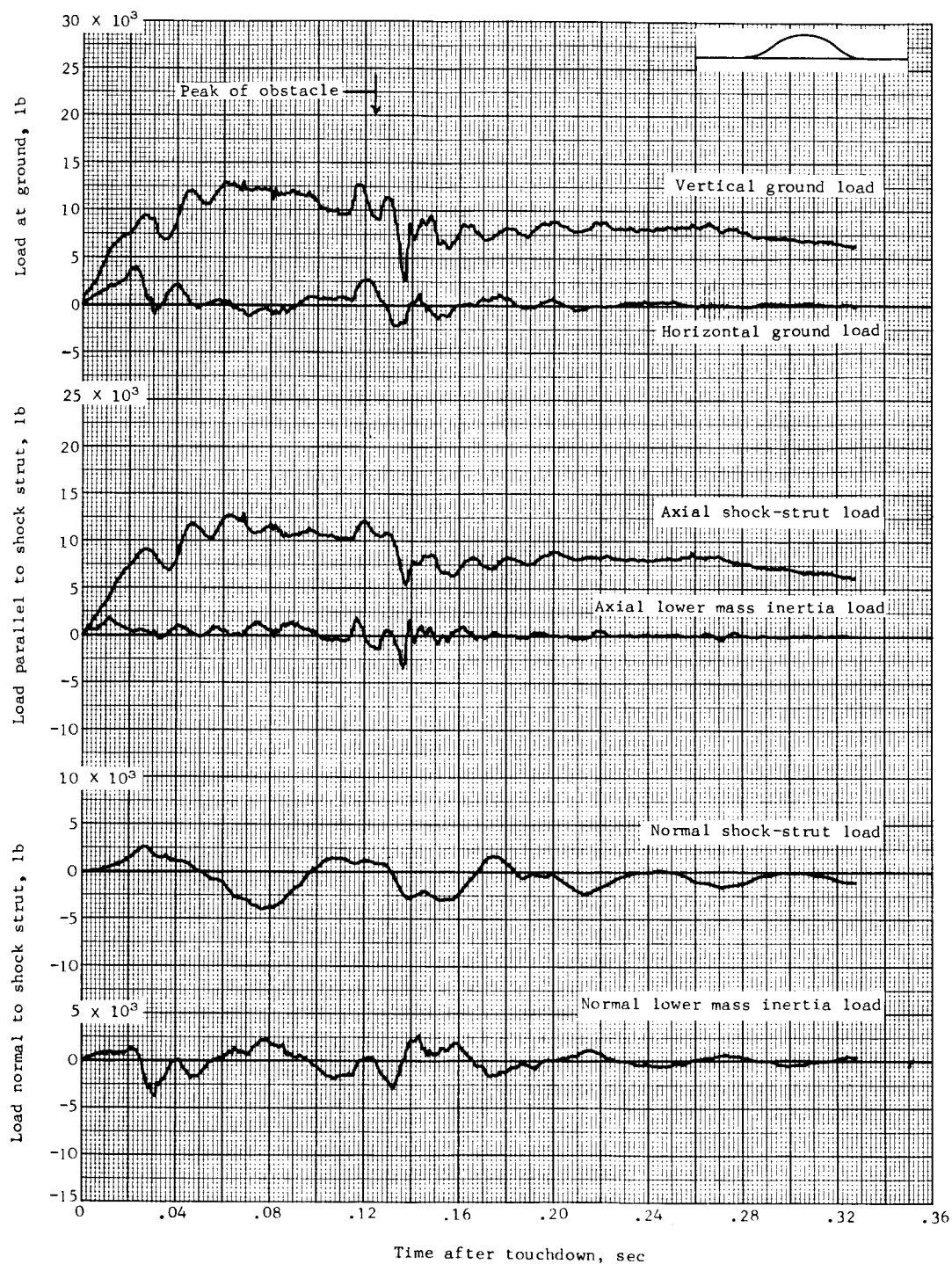
Figure 7.- Time histories of loads and other quantities obtained during landing impact over a 1 - cos, 2-inch-high, 10-inch-long obstacle.



(a) Concluded.

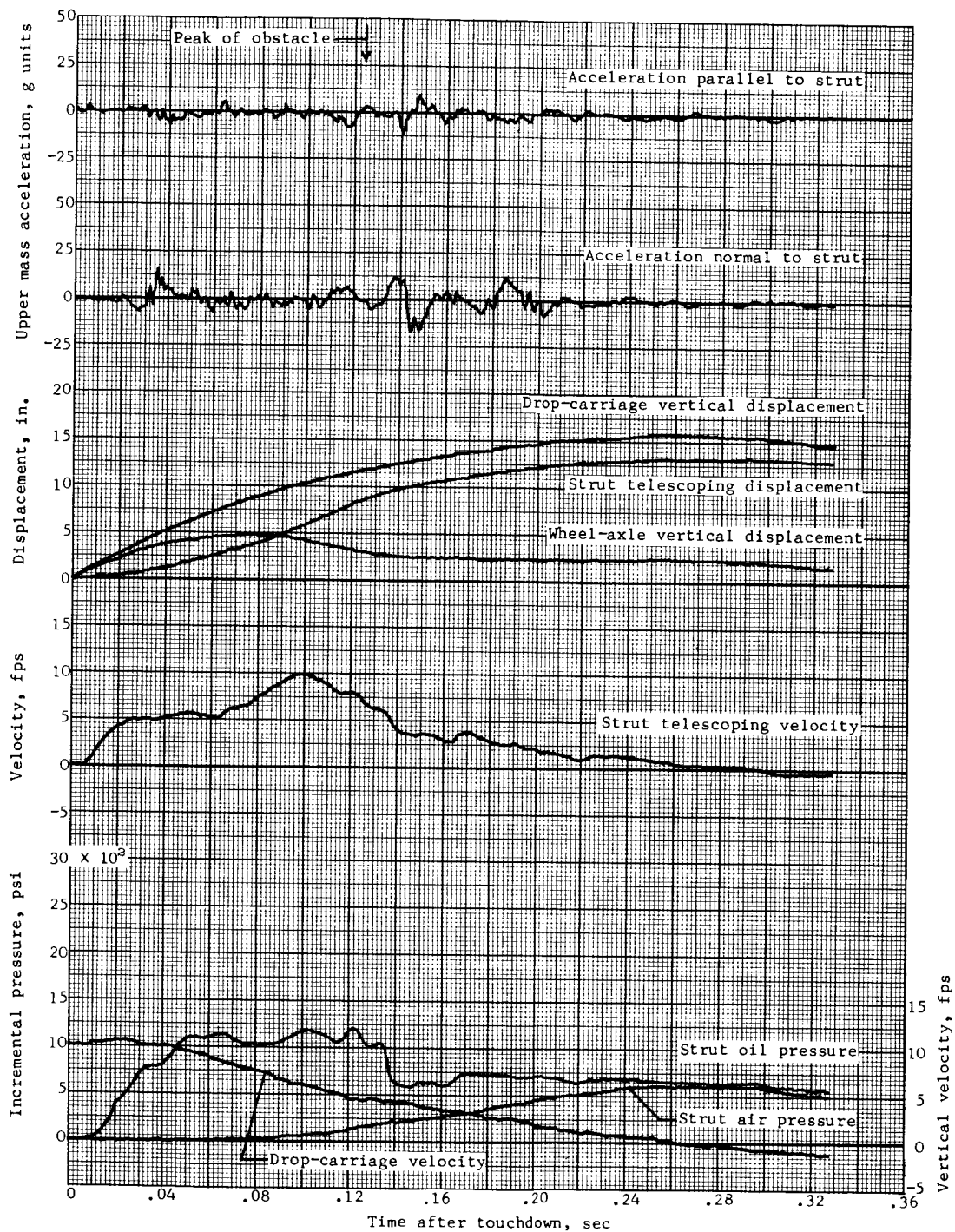
Figure 7.- Continued.





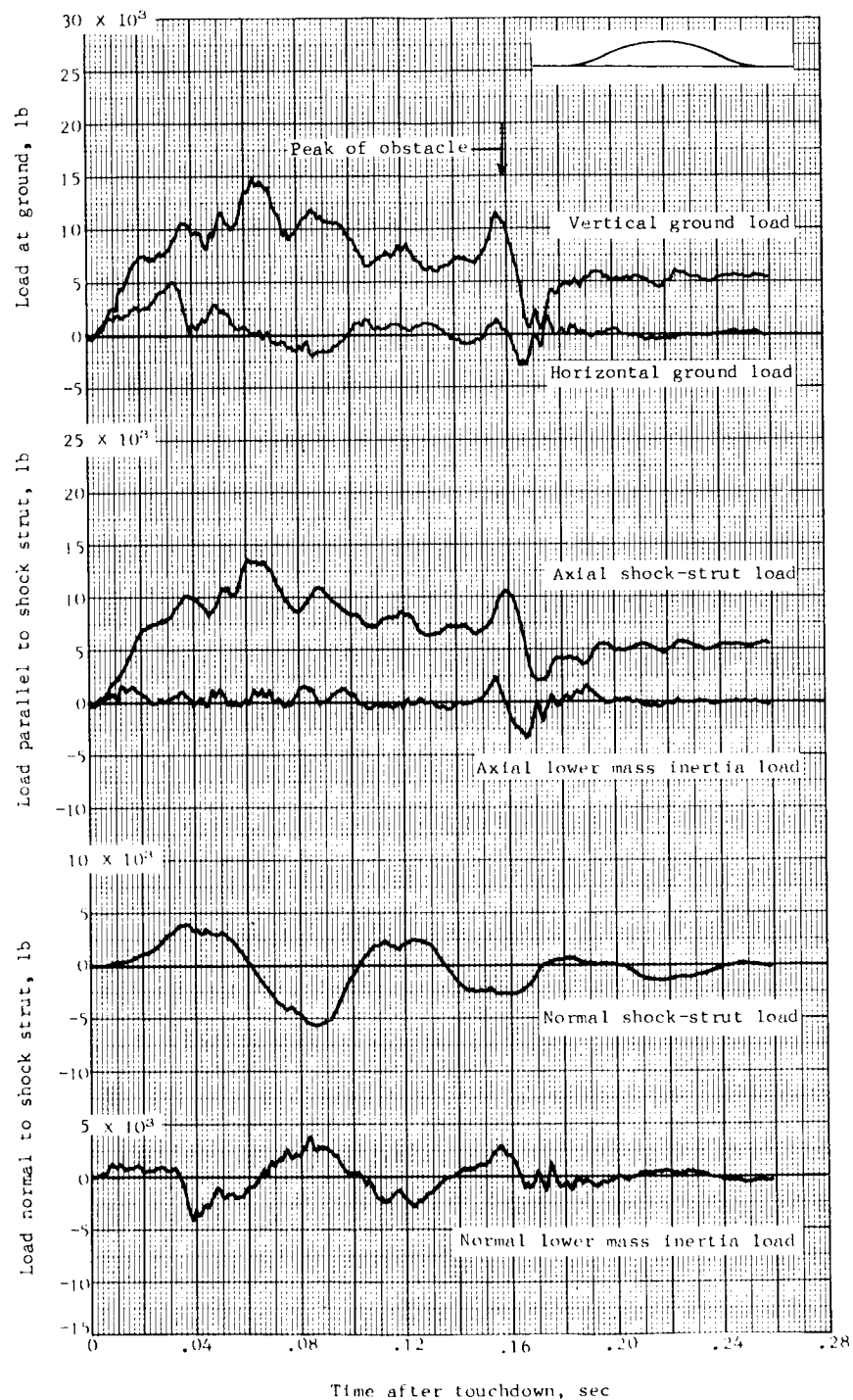
(b) Test 2.

Figure 7.- Continued.



(b) Concluded.

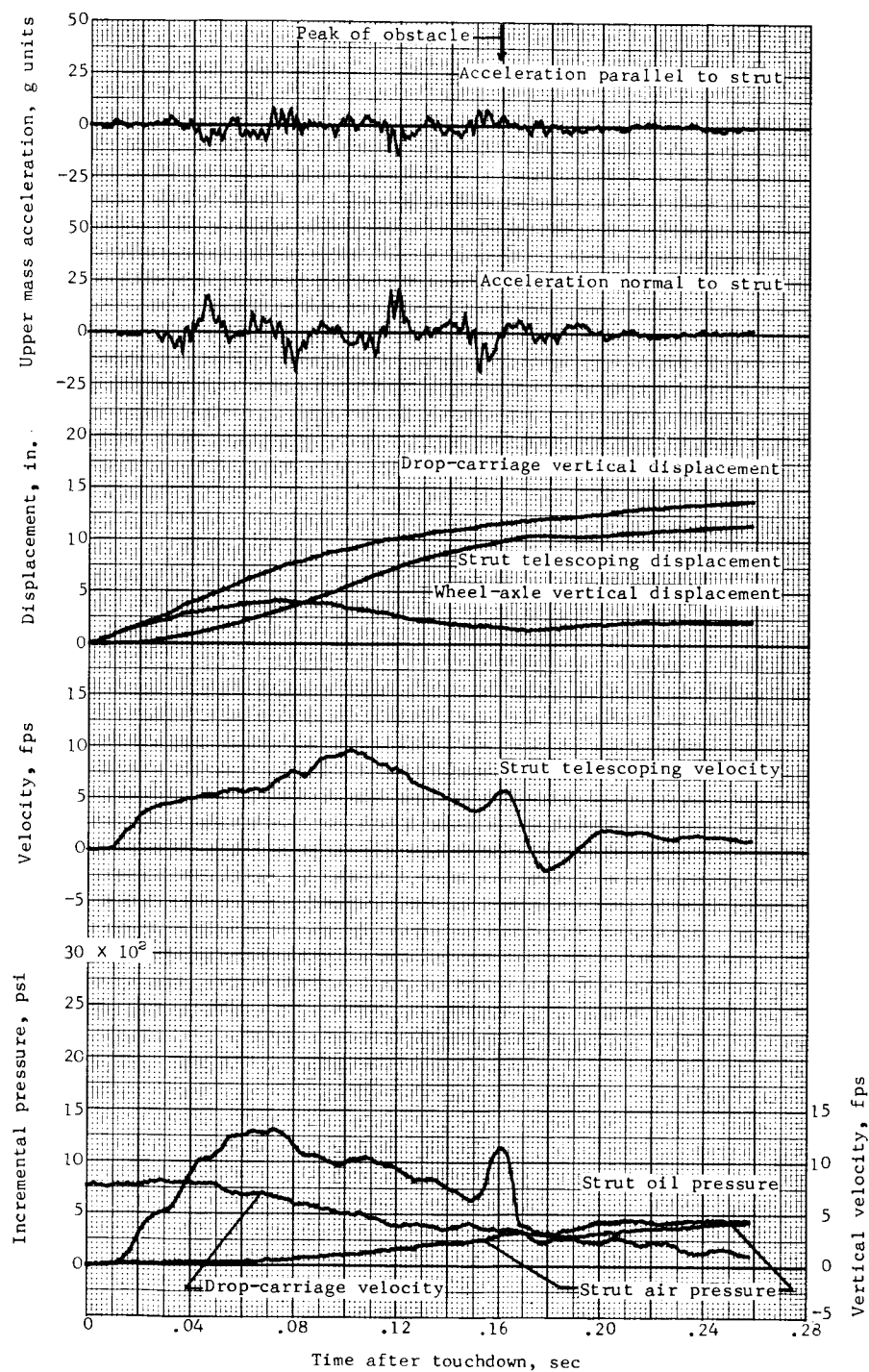
Figure 7.- Concluded.



(a) Test 3.

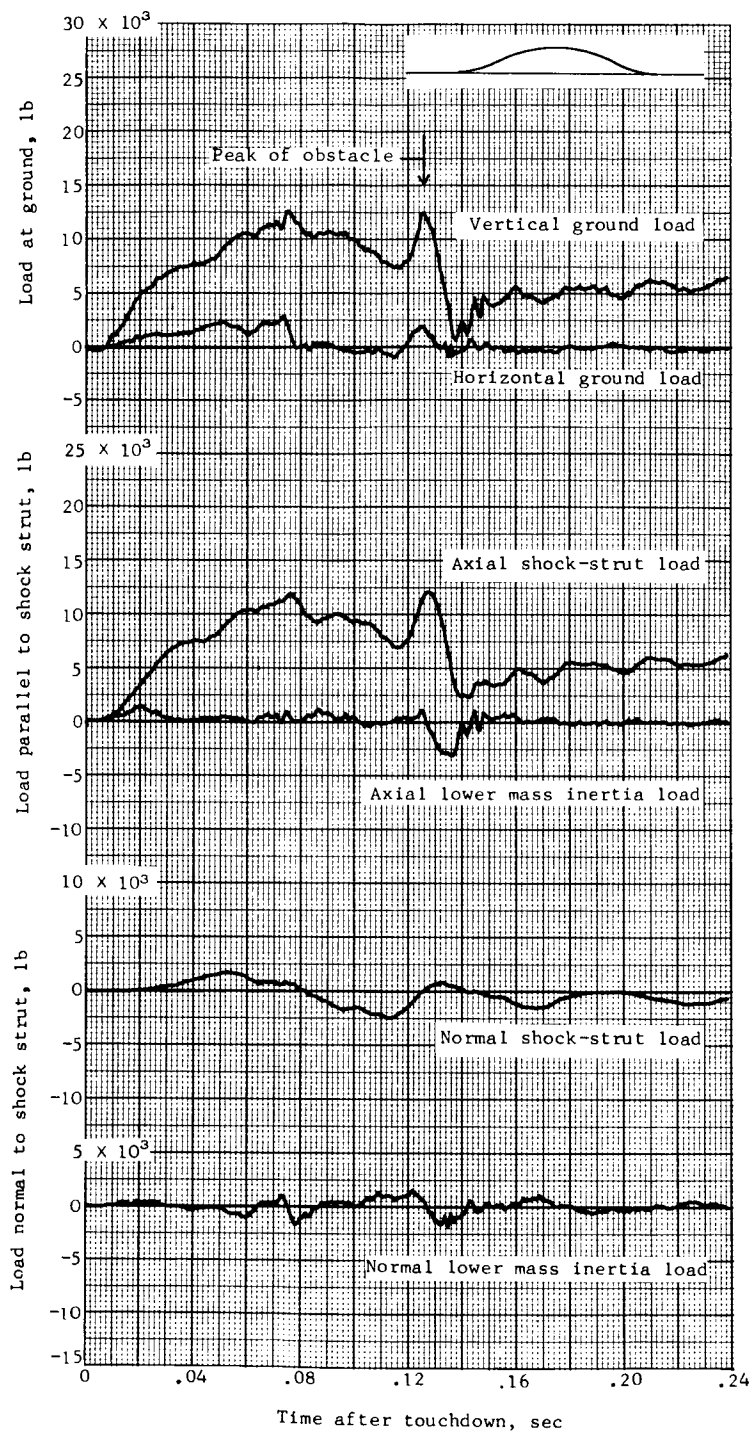
Figure 8.- Time histories of loads and other quantities obtained during landing impact over a 1 - cos, 2-inch-high, 30-inch-long obstacle.





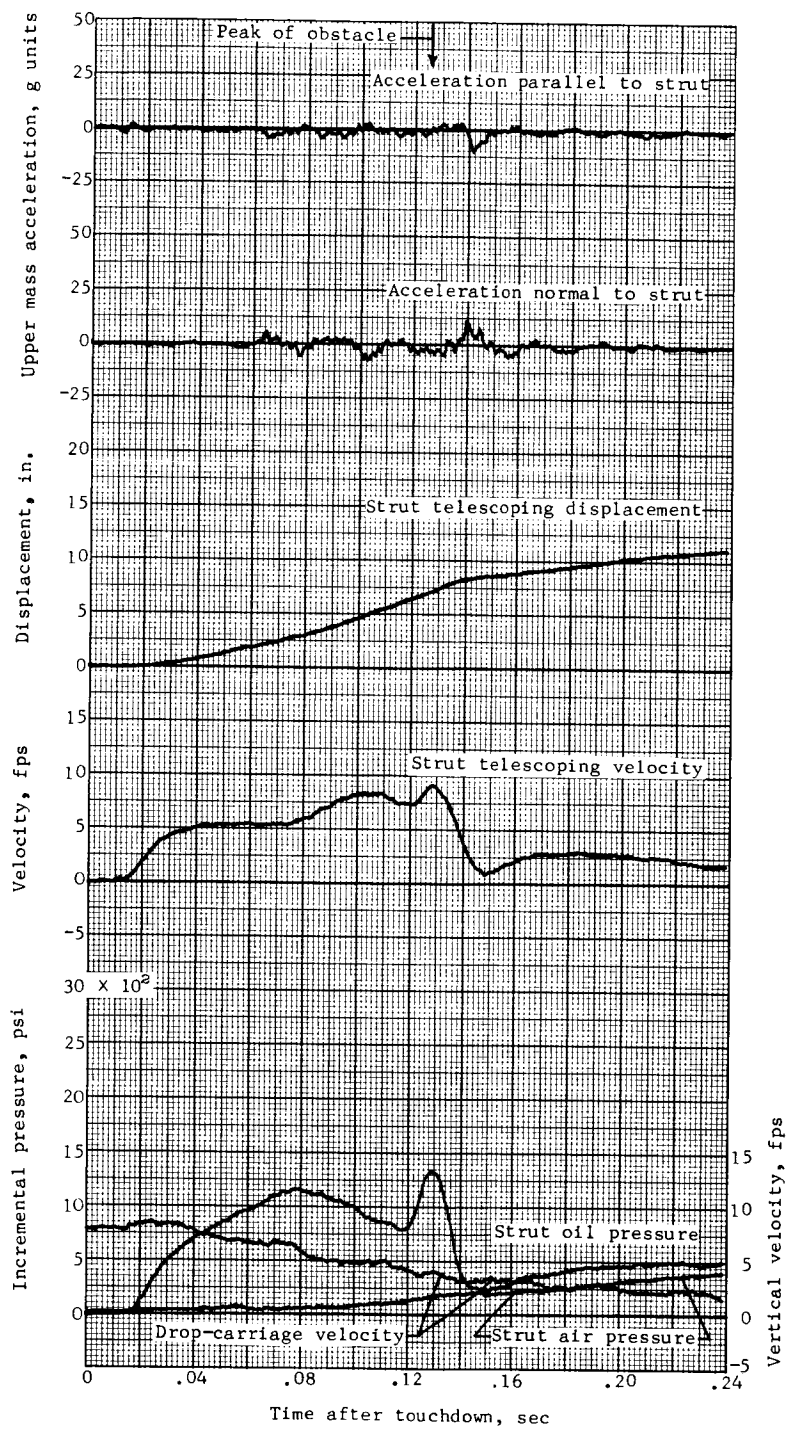
(a) Concluded.

Figure 8.- Continued.



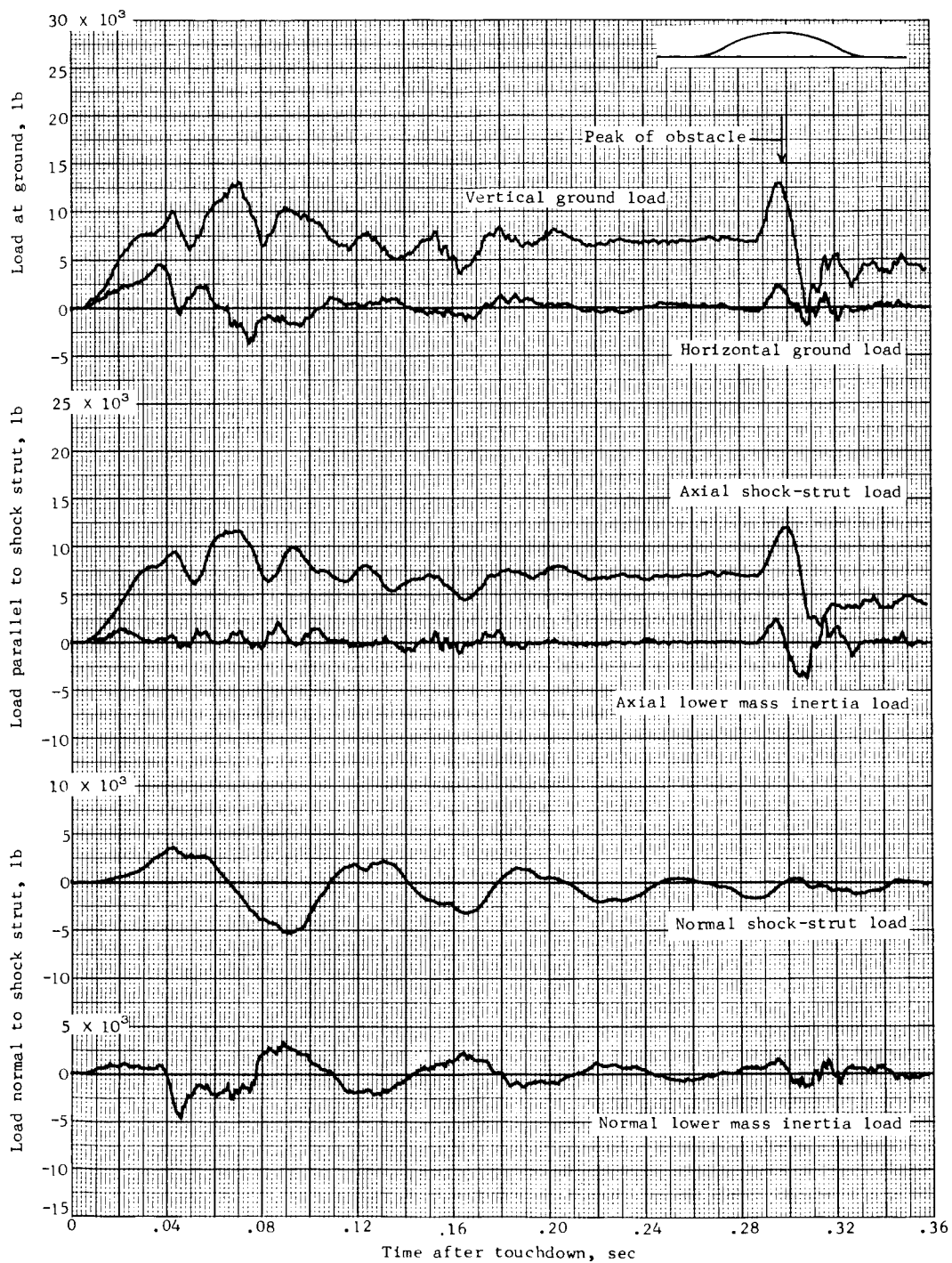
(b) Test 4.

Figure 8.- Continued.



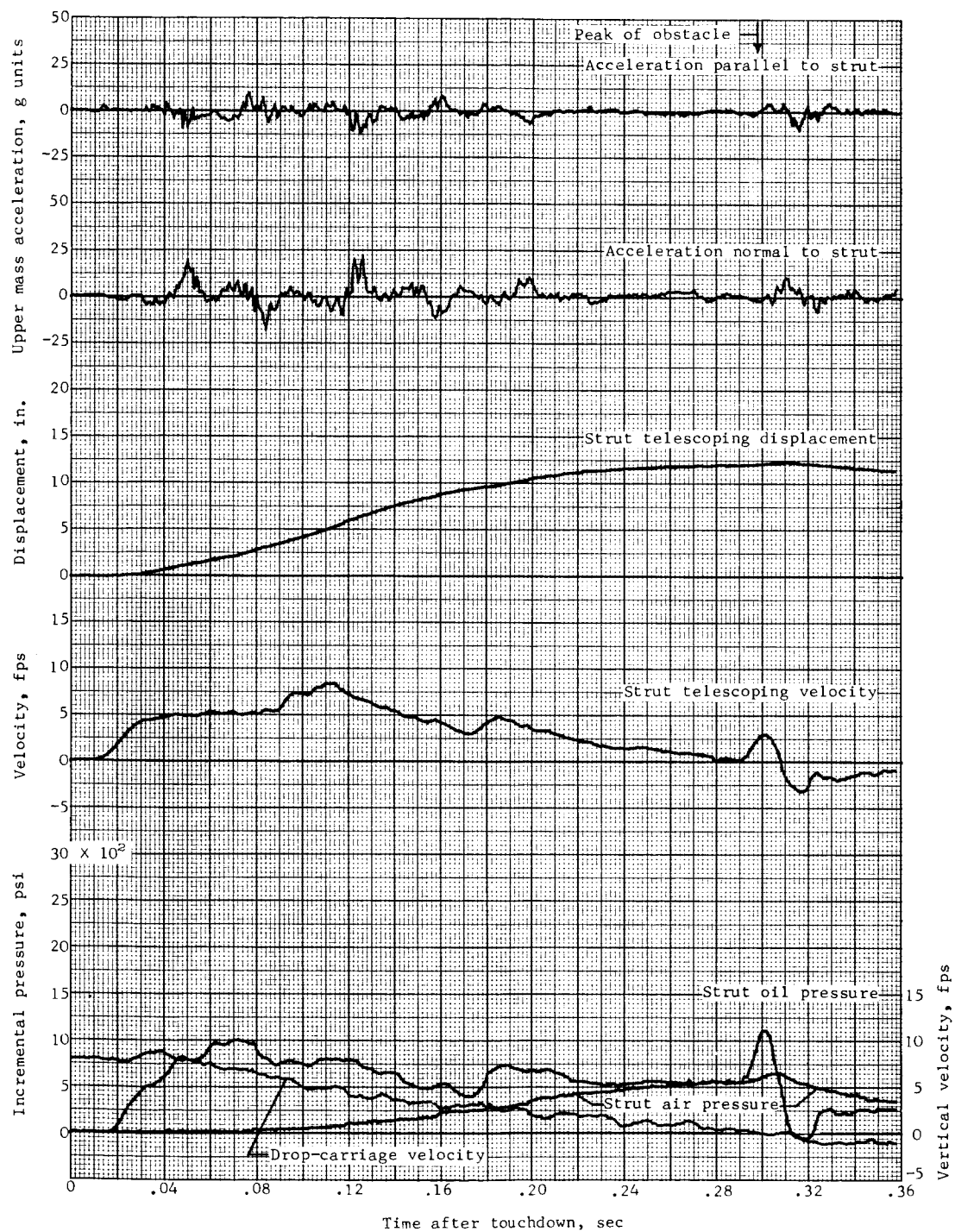
(b) Concluded.

Figure 8.- Continued.



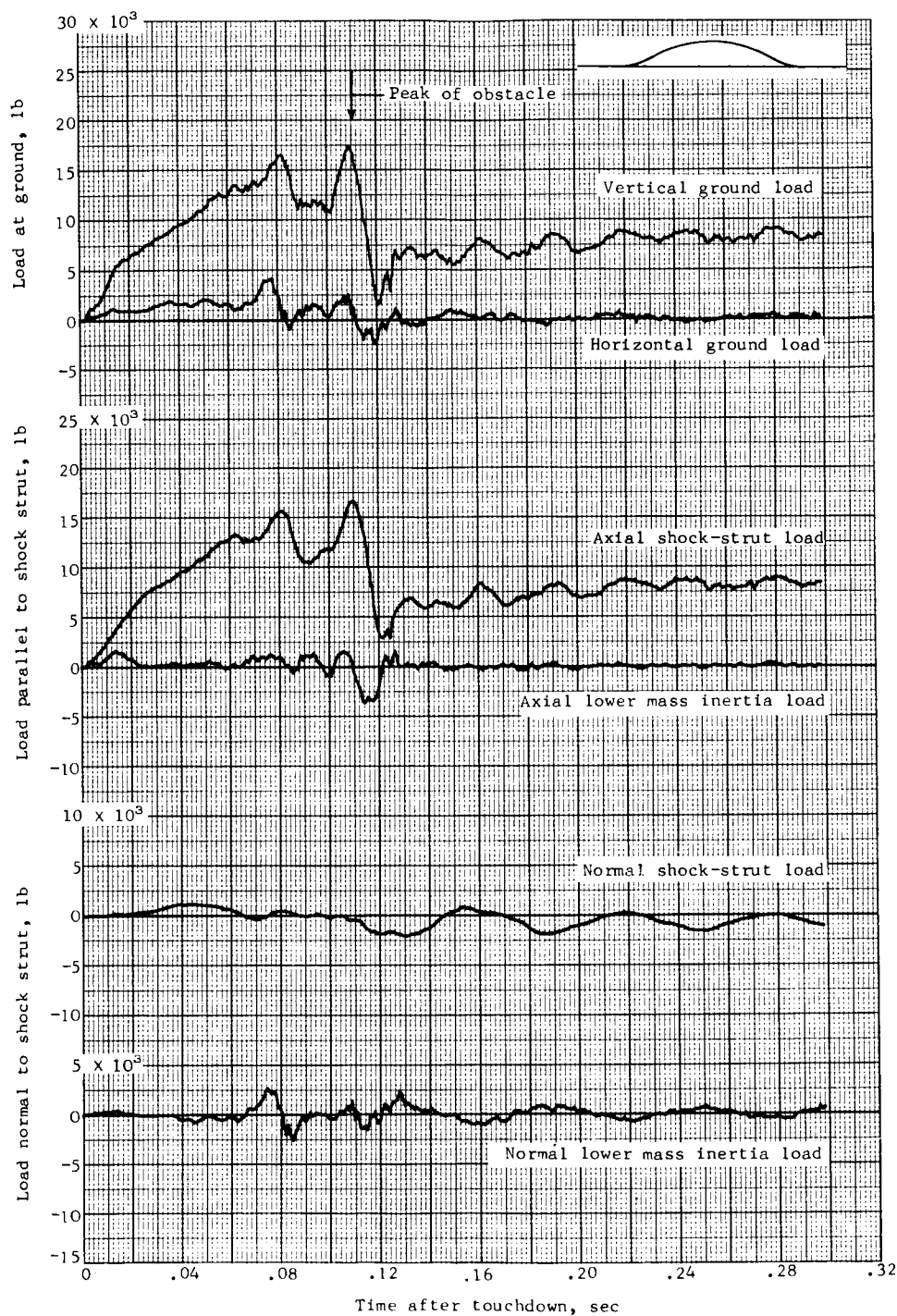
(c) Test 5.

Figure 8.- Continued.



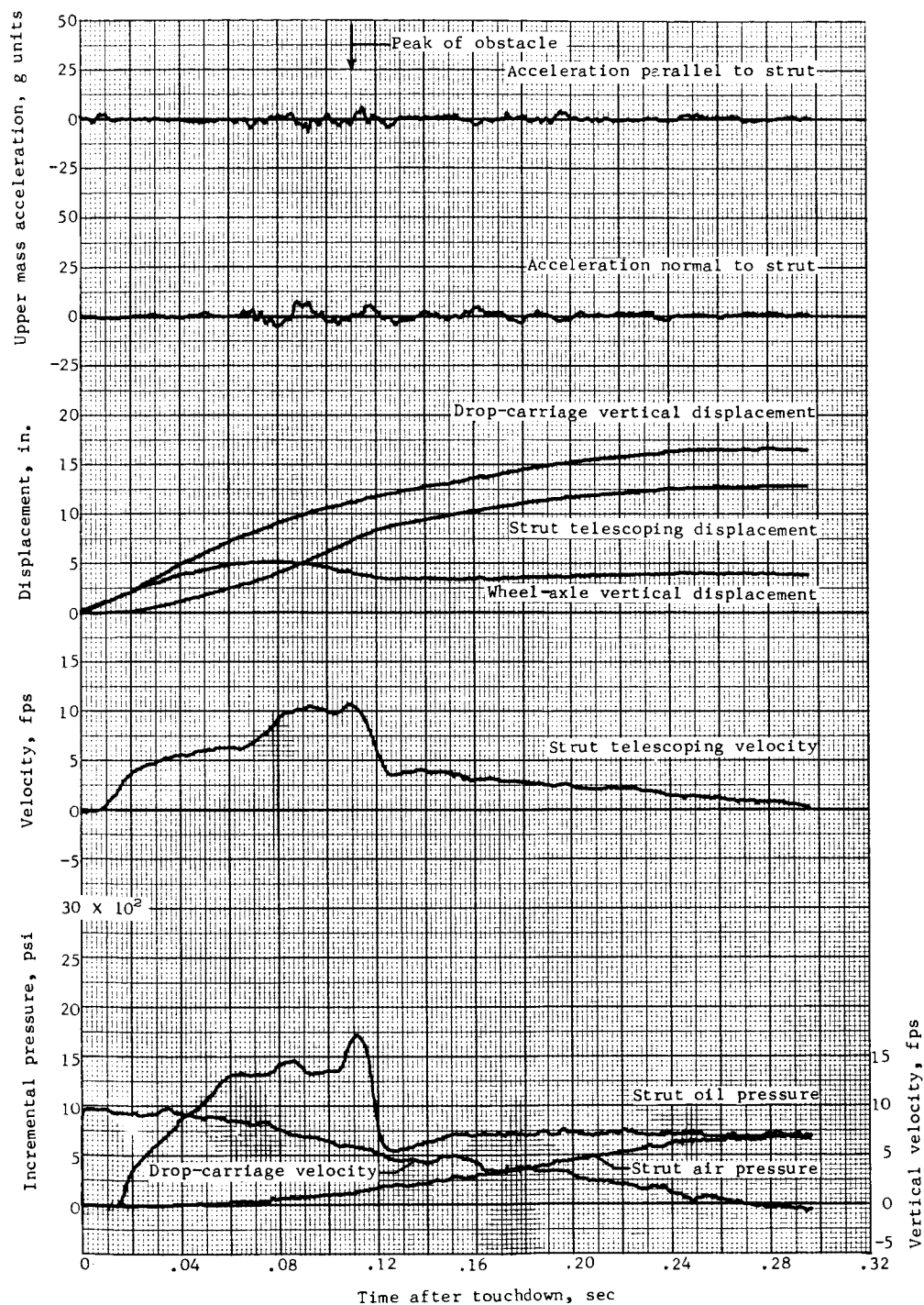
(c) Concluded.

Figure 8.- Continued.



(d) Test 6.

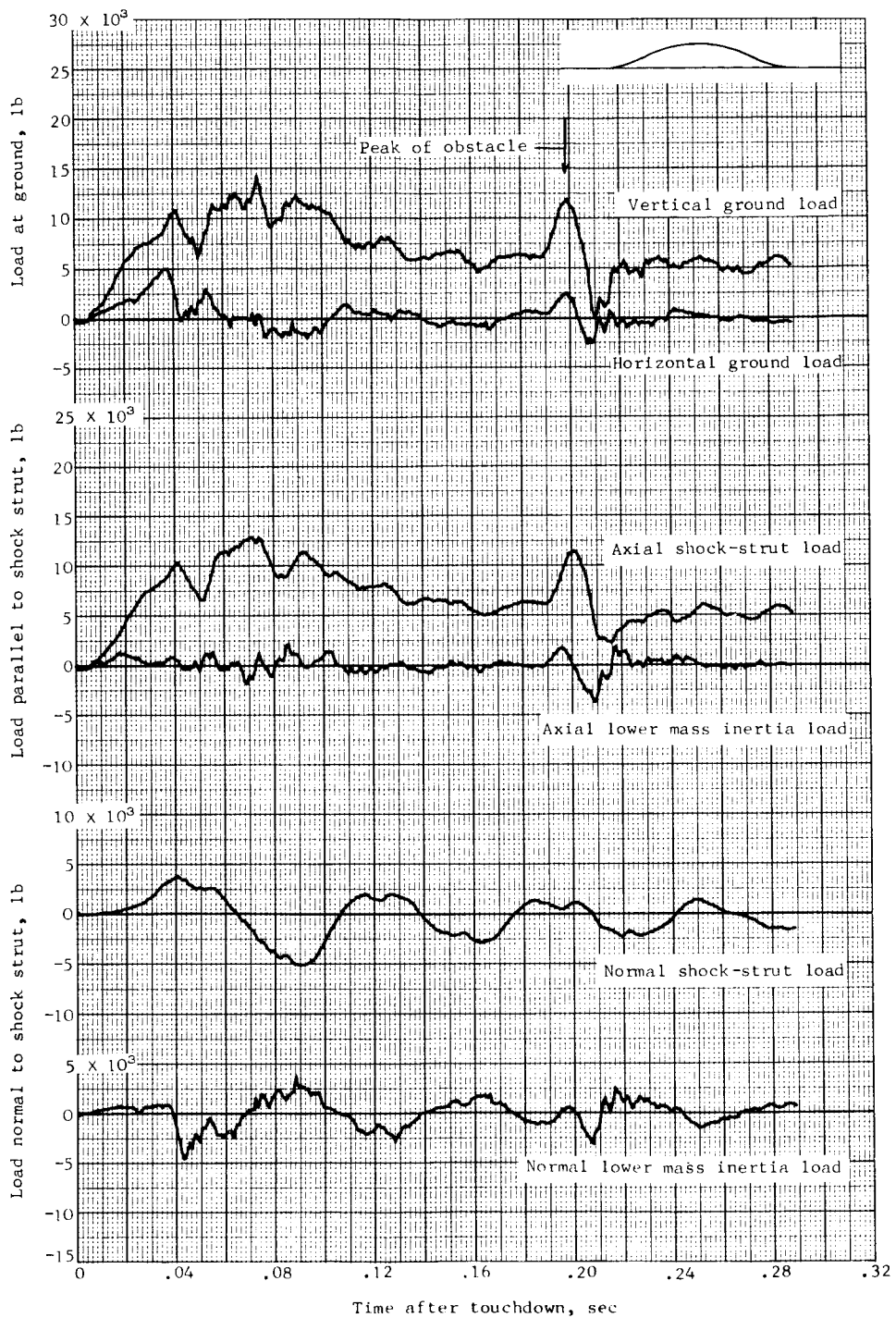
Figure 8.- Continued.



(d) Concluded.

Figure 8.- Continued.

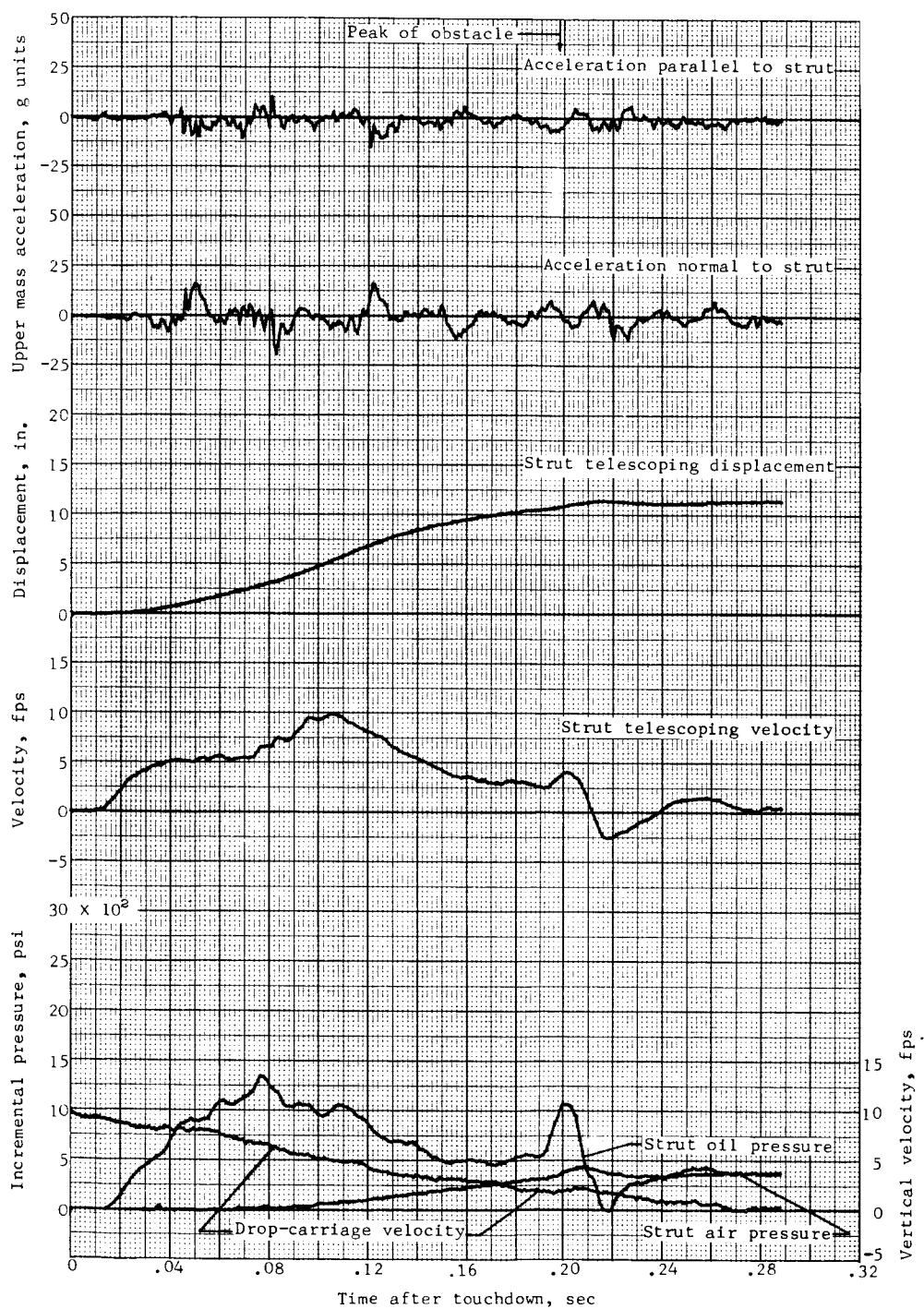




(e) Test 7.

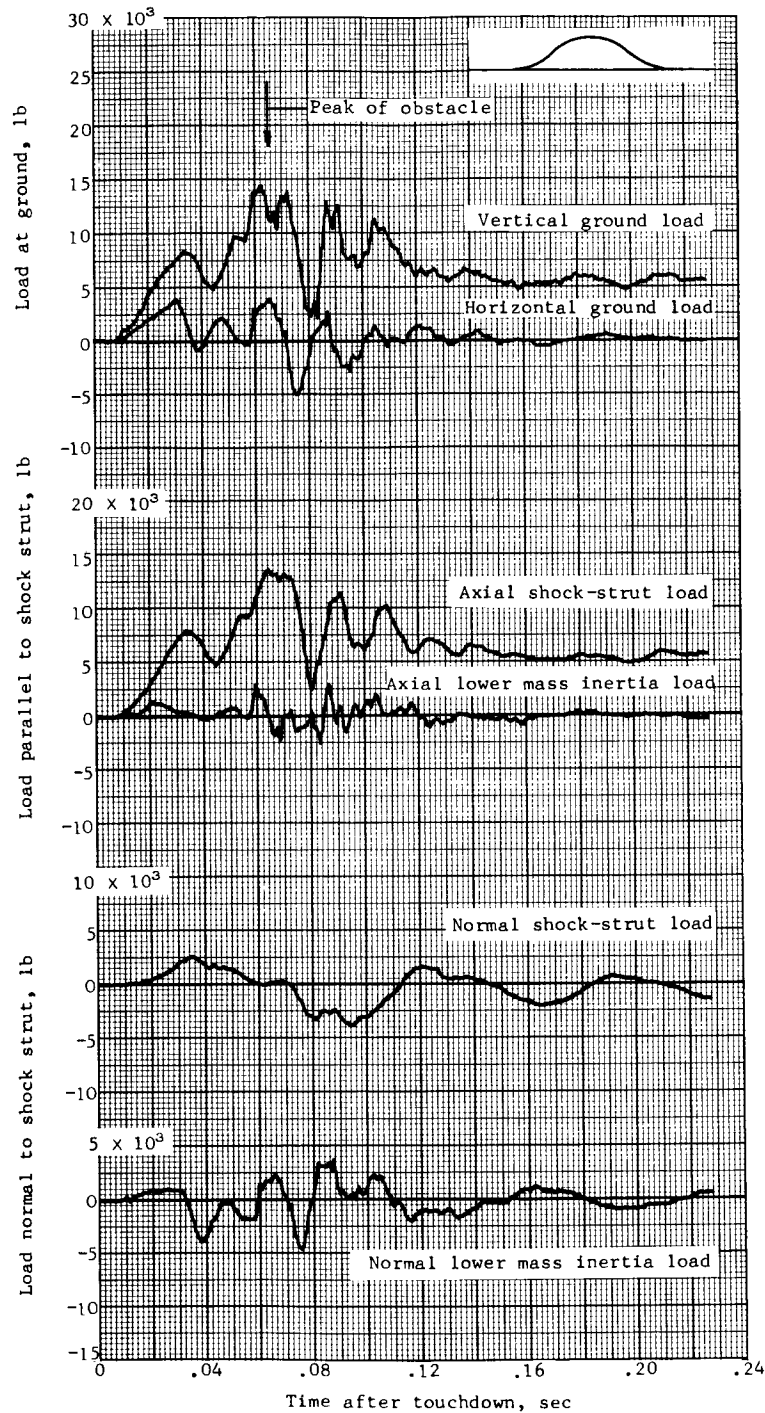
Figure 8.- Continued.





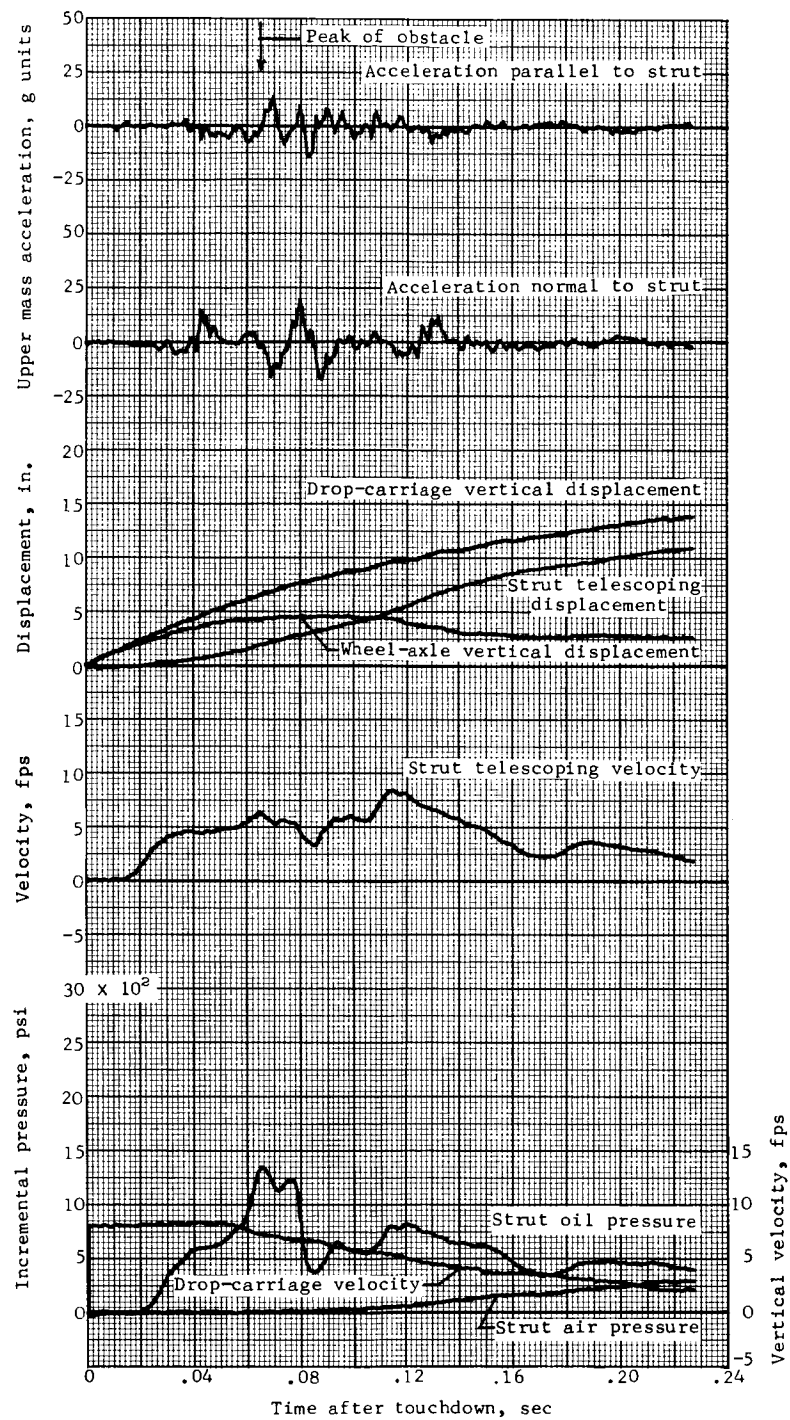
(e) Concluded.

Figure 8.- Concluded.



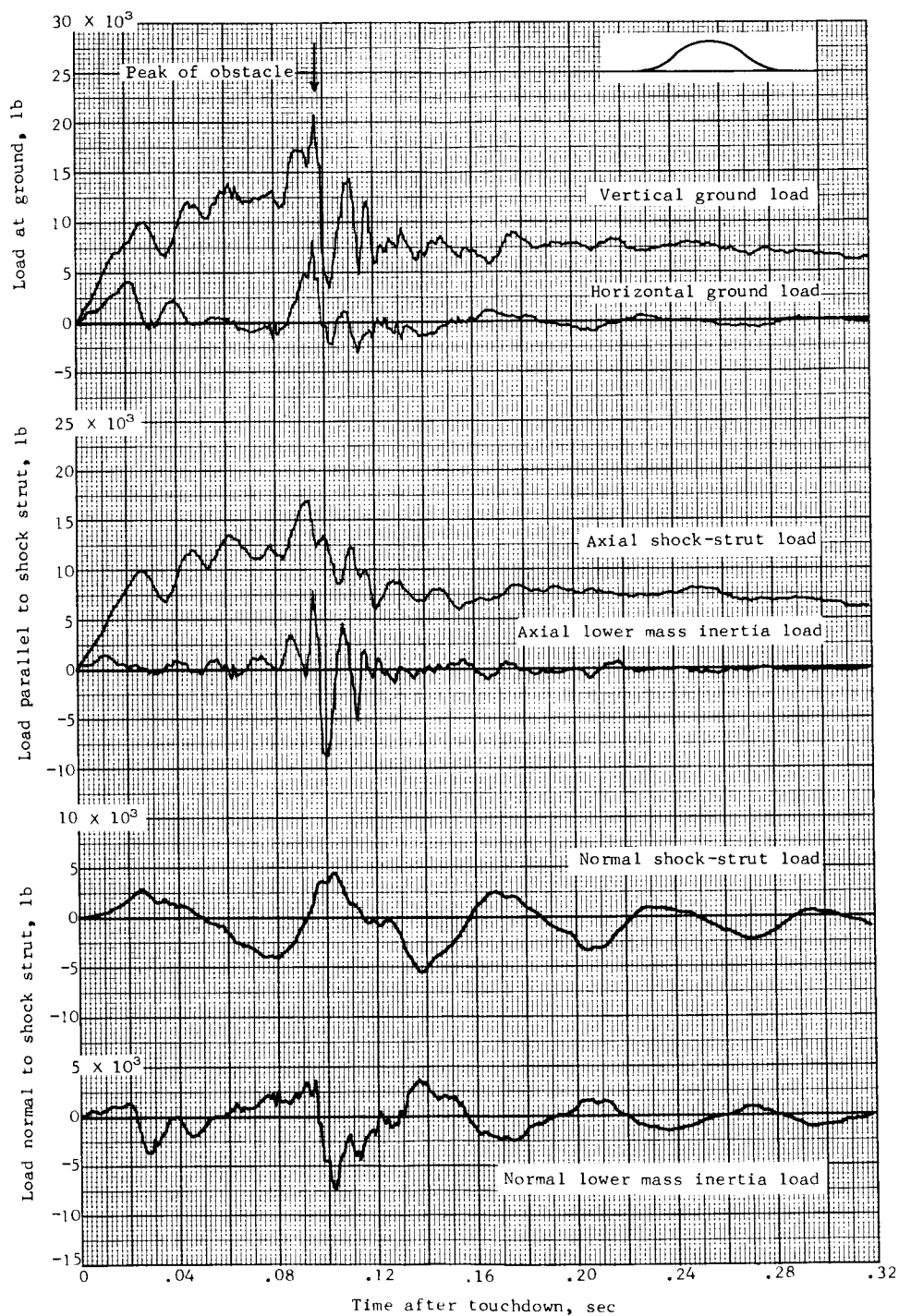
(a) Test 8.

Figure 9.- Time histories of loads and other quantities obtained during landing impact over a 1 - cos, 3-inch-high, 10-inch-long obstacle.



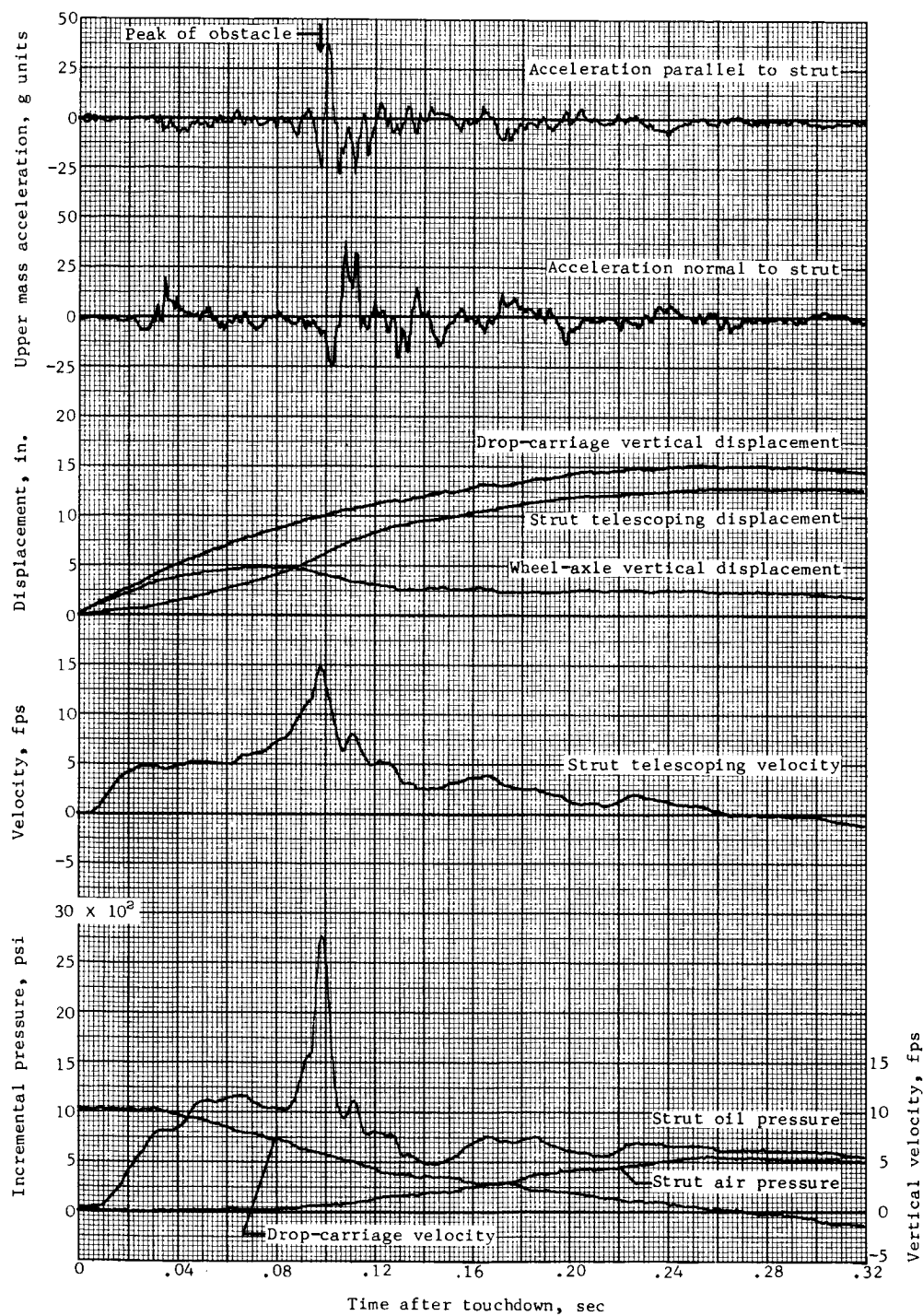
(a) Concluded.

Figure 9.- Continued.



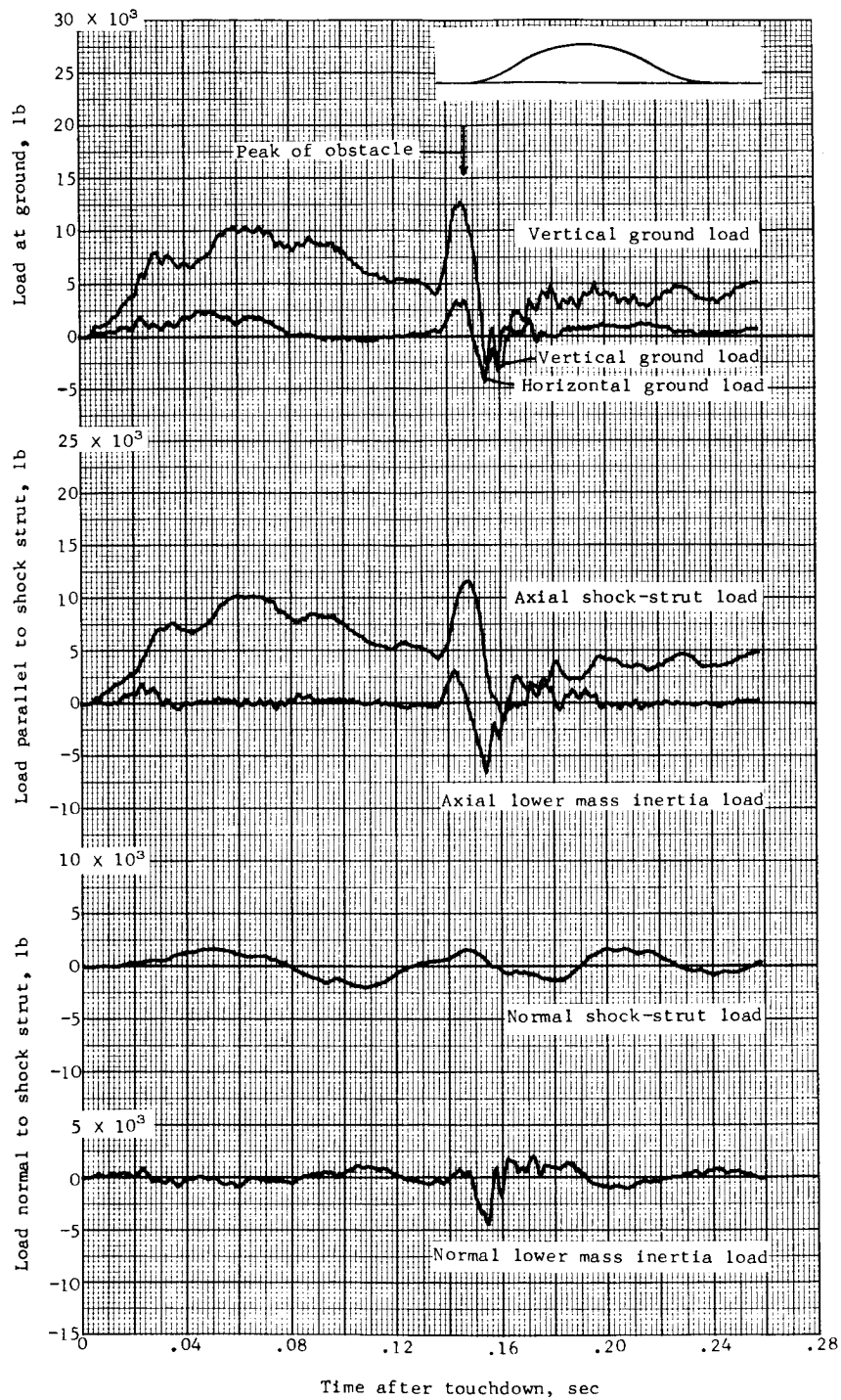
(b) Test 9.

Figure 9.- Continued.



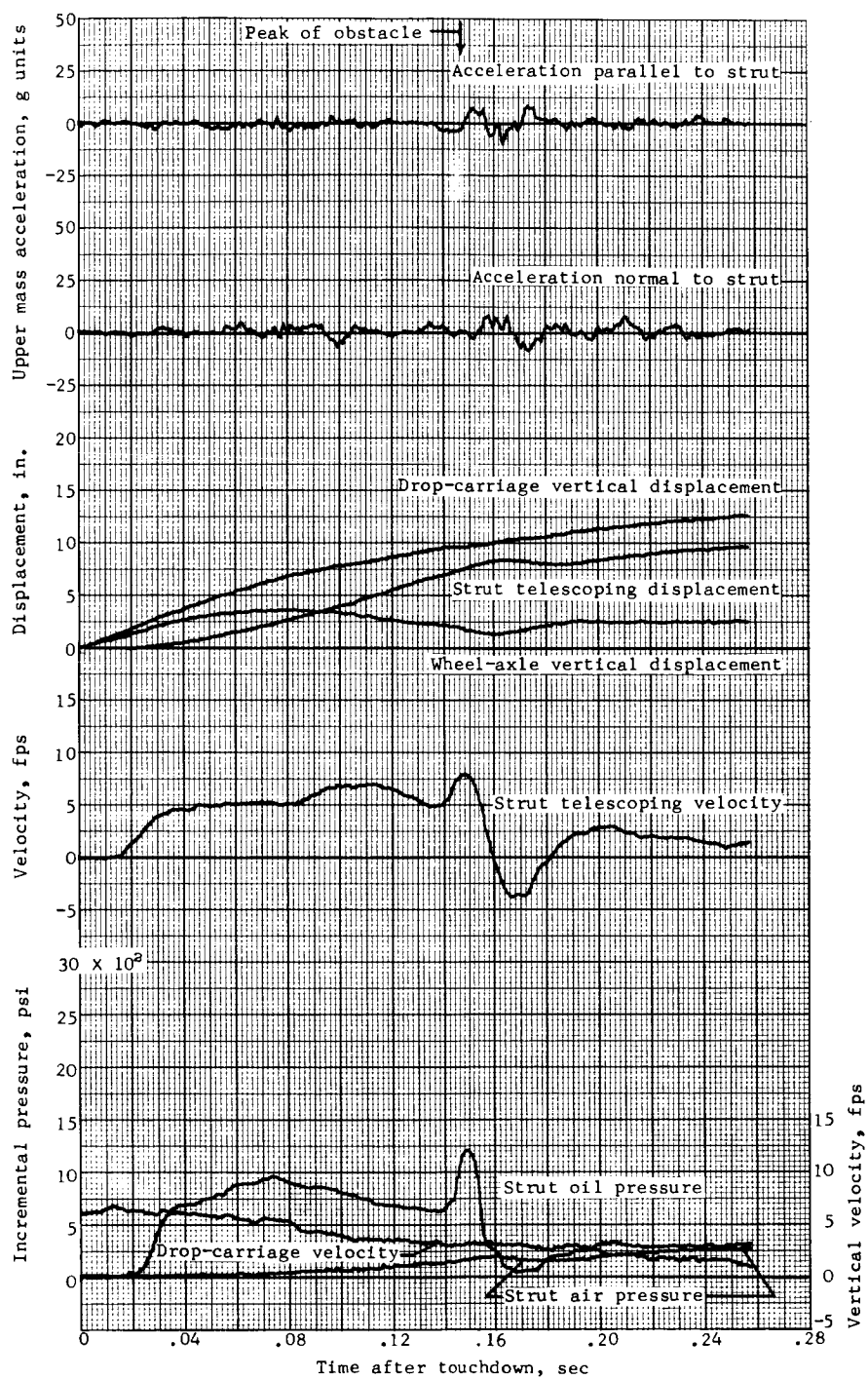
(b) Concluded.

Figure 9.- Concluded.



(a) Test 10.

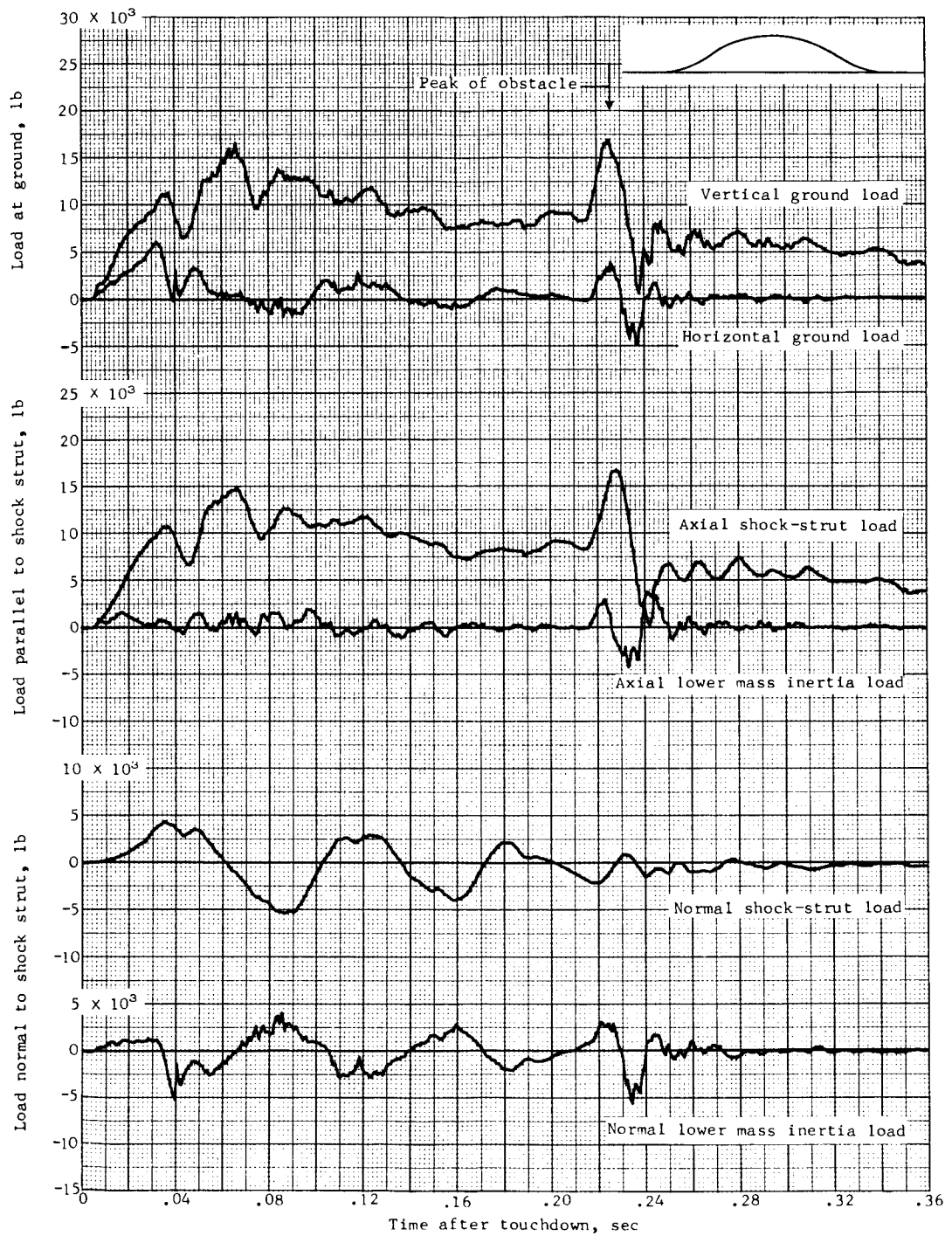
Figure 10.- Time histories of loads and other quantities obtained during landing impact over a 1 - cos, 3-inch-high, 30-inch-long obstacle.



(a) Concluded.

Figure 10.- Continued.

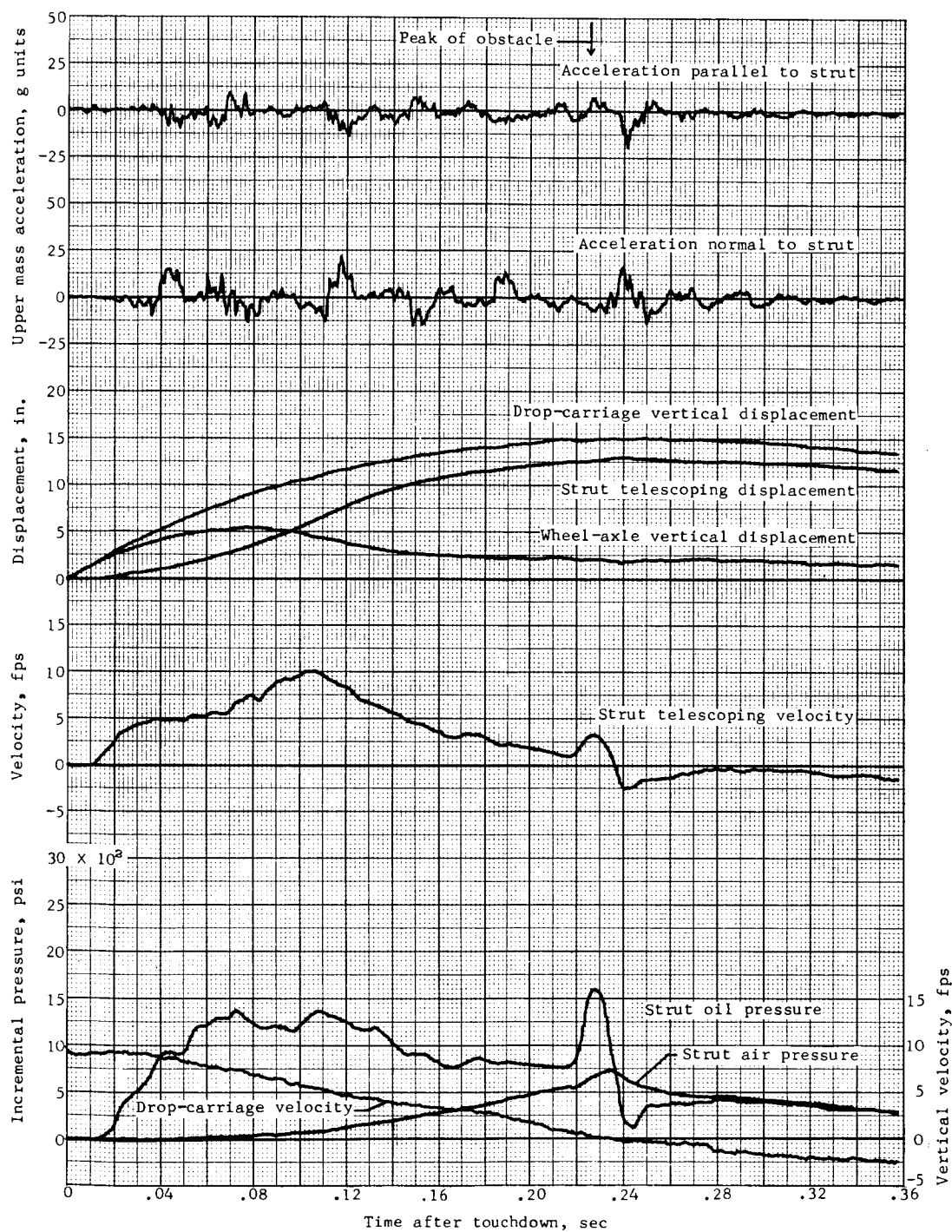




(b) Test 11.

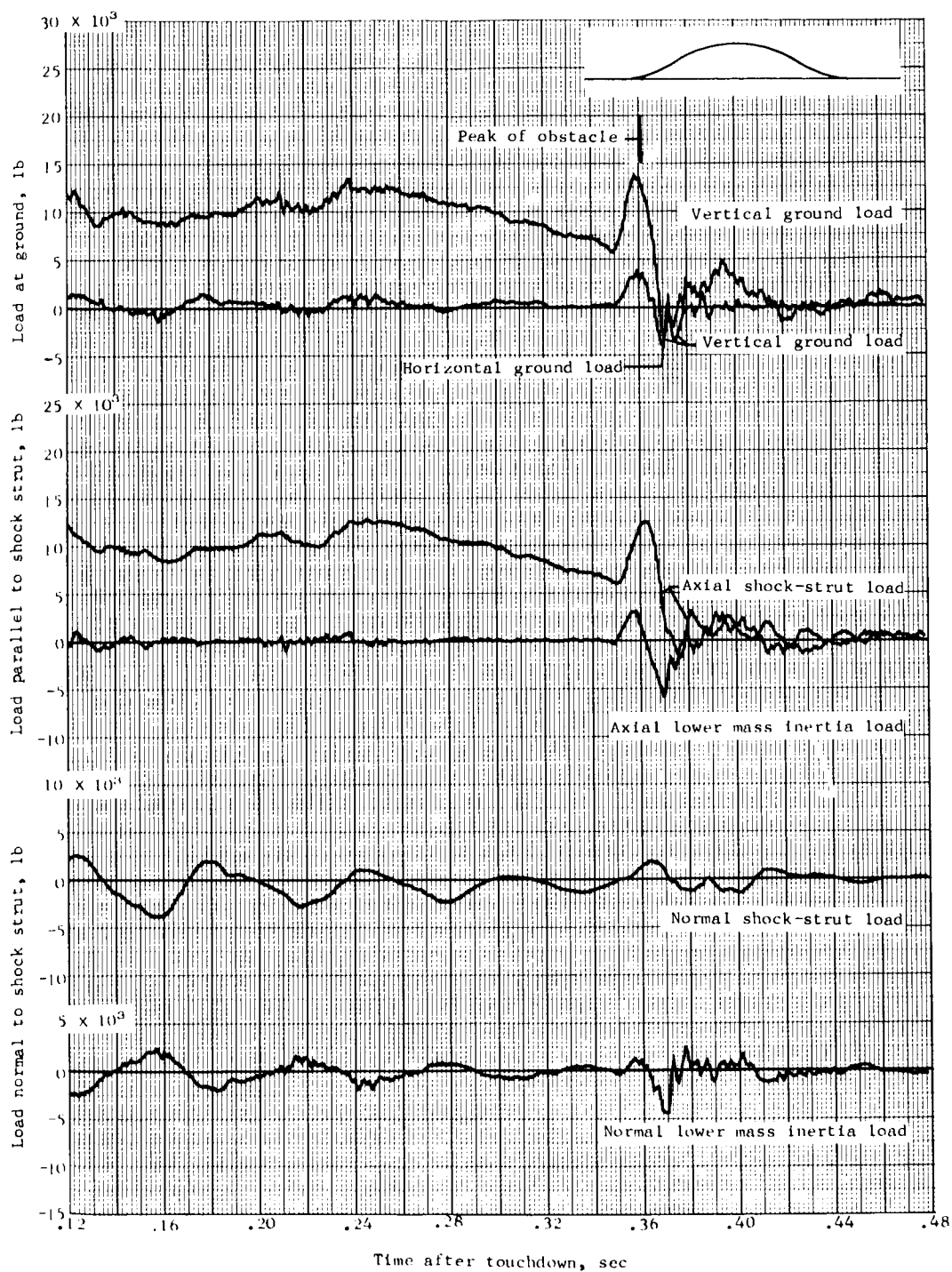
Figure 10.- Continued.





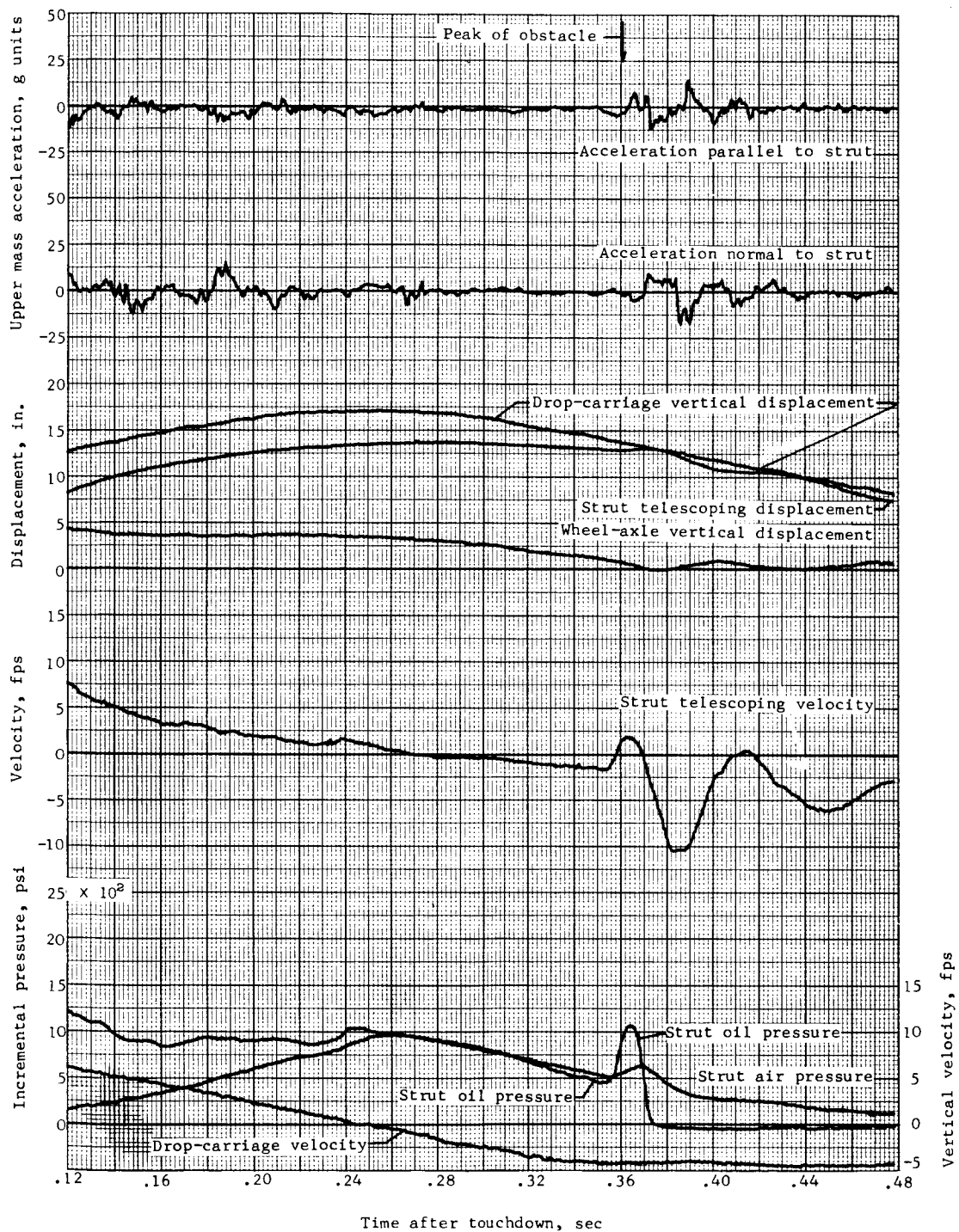
(b) Concluded.

Figure 10.- Continued.



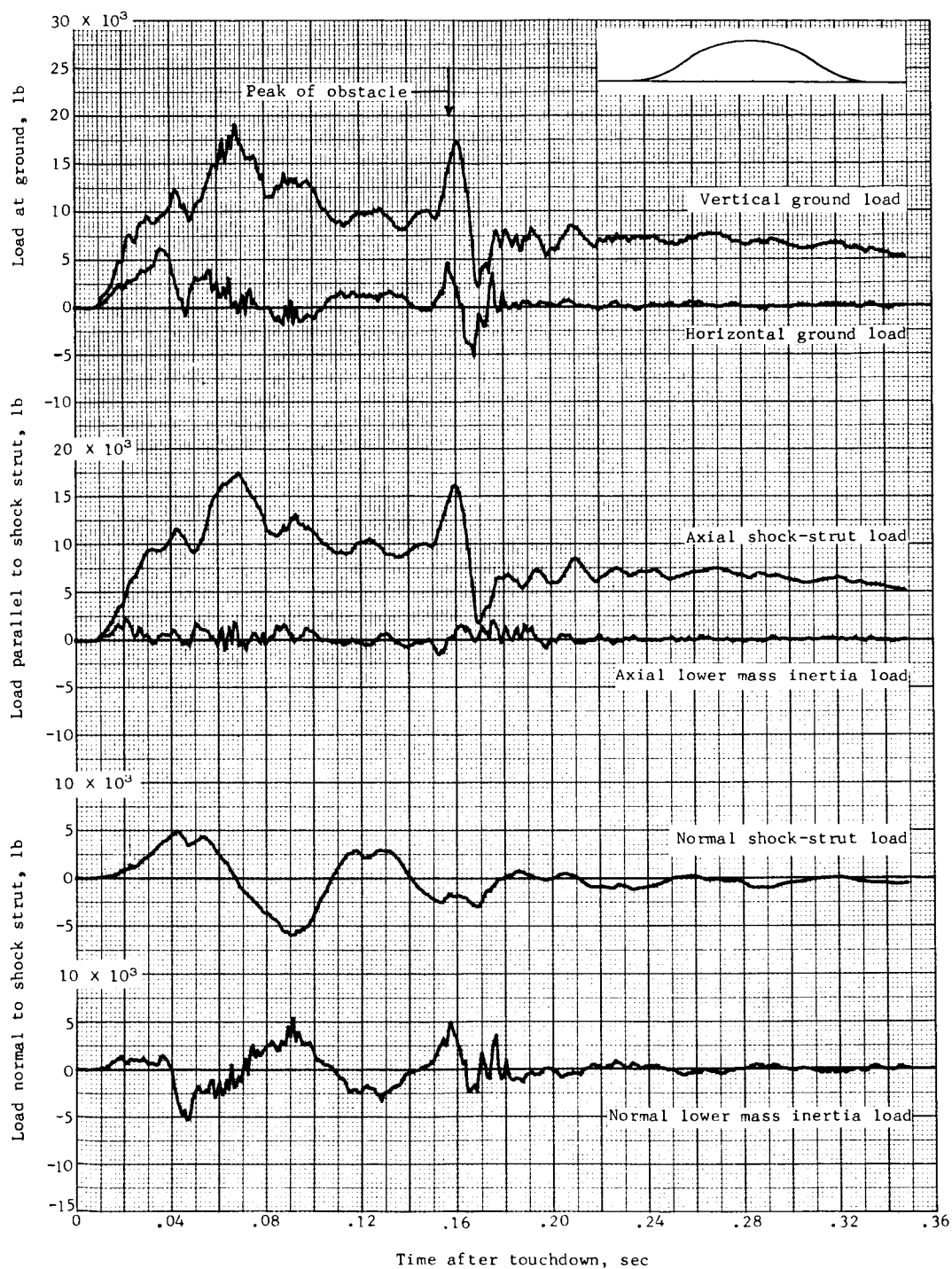
(c) Test 12.

Figure 10.- Continued.



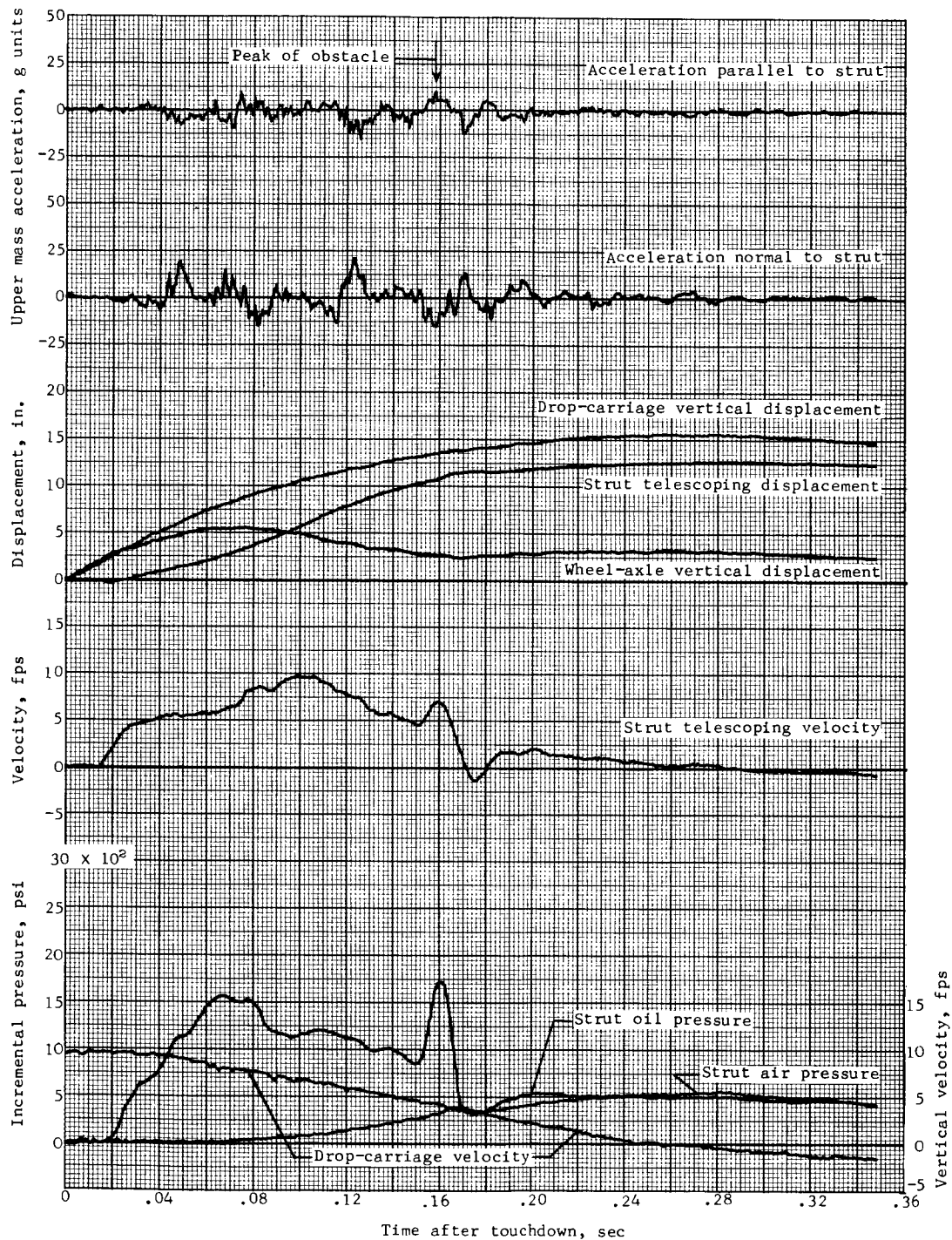
(c) Concluded.

Figure 10.- Continued.



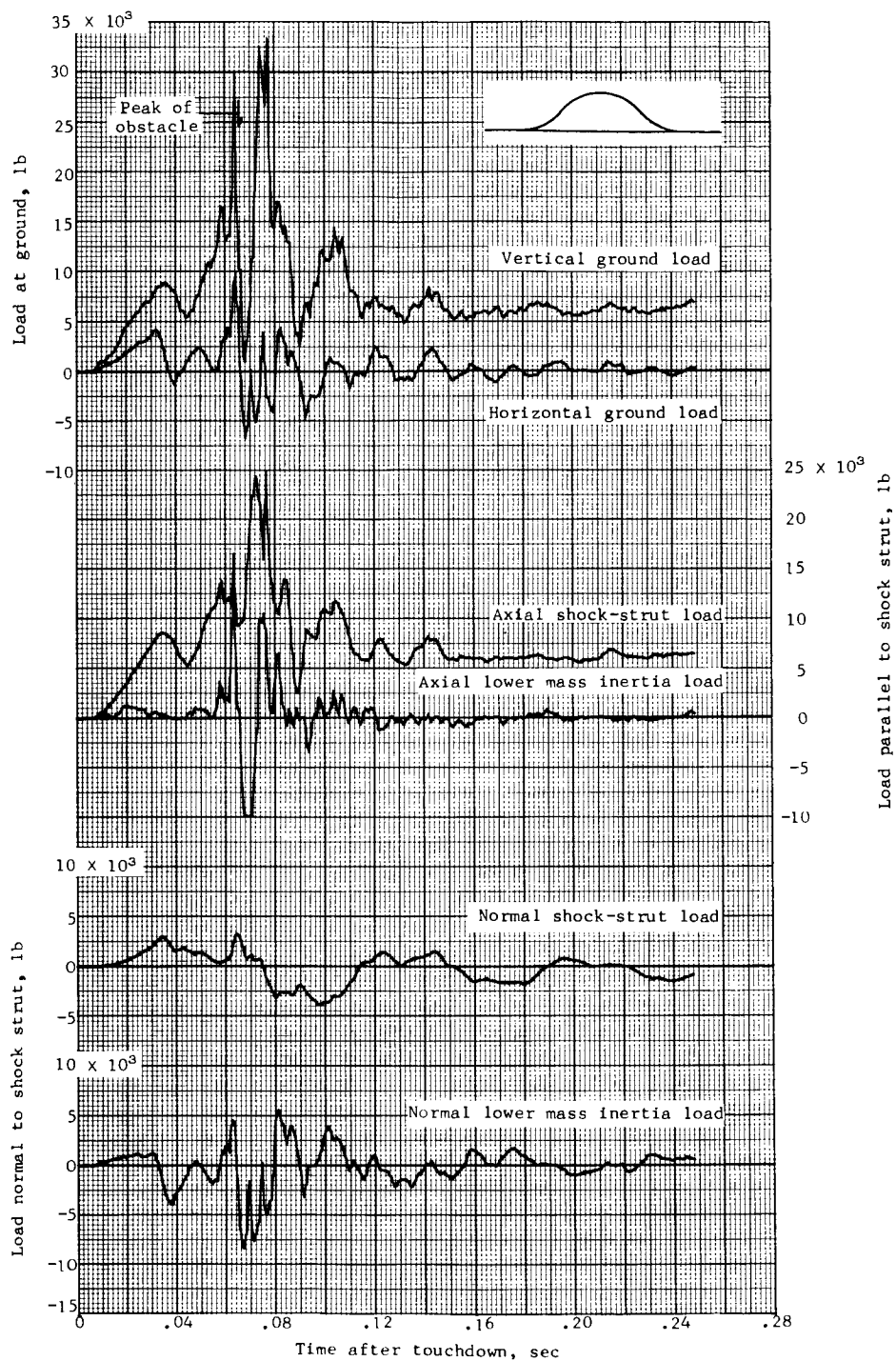
(d) Test 13.

Figure 10.- Continued.



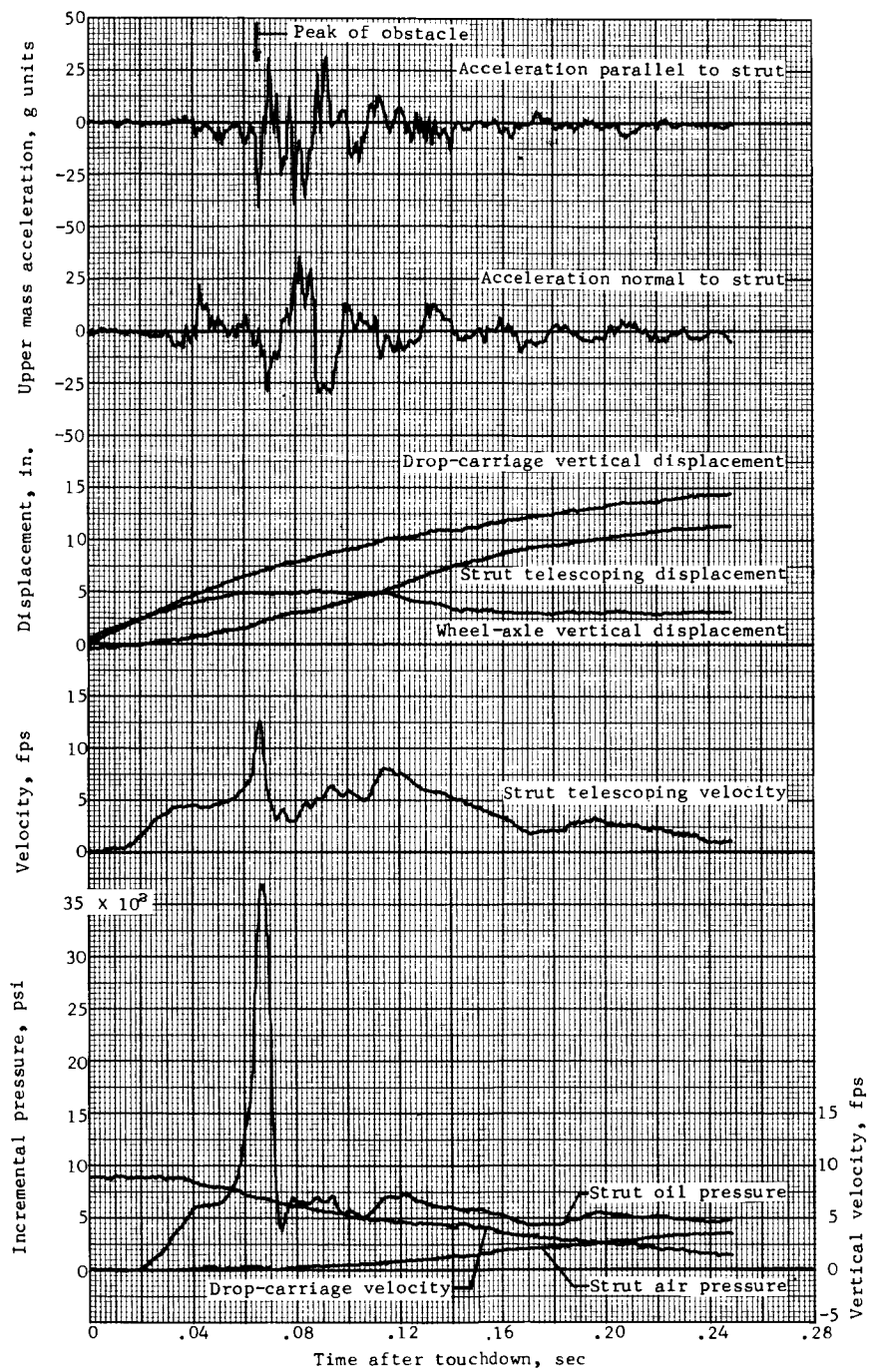
(d) Concluded.

Figure 10.- Concluded.



(a) Test 14.

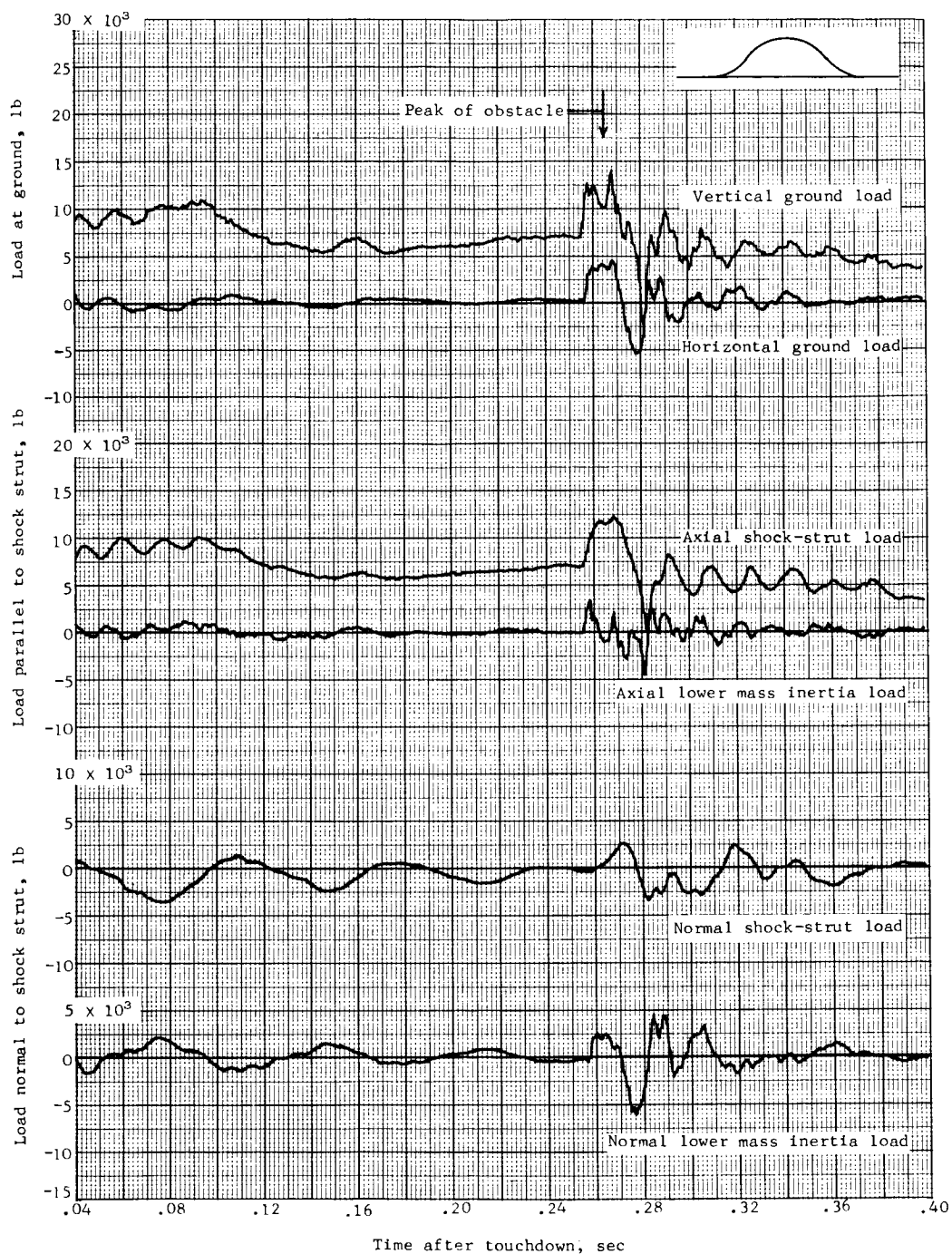
Figure 11.- Time histories of loads and other quantities obtained during landing impact over a 1 - cos, 4-inch-high, 10-inch-long obstacle.



(a) Concluded.

Figure 11.- Continued.

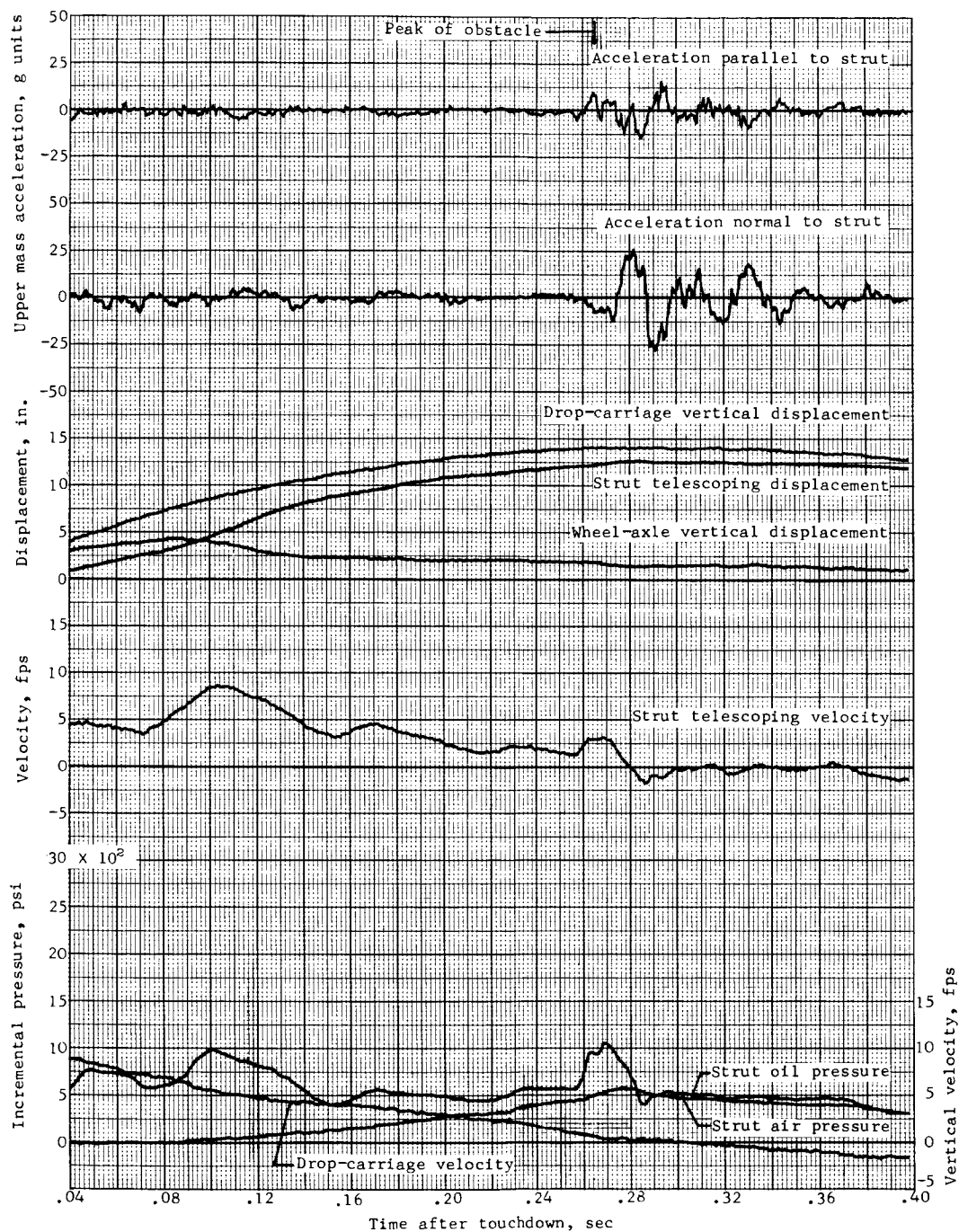




(b) Test 15.

Figure 11.- Continued.





(b) Concluded.

Figure 11.- Concluded.

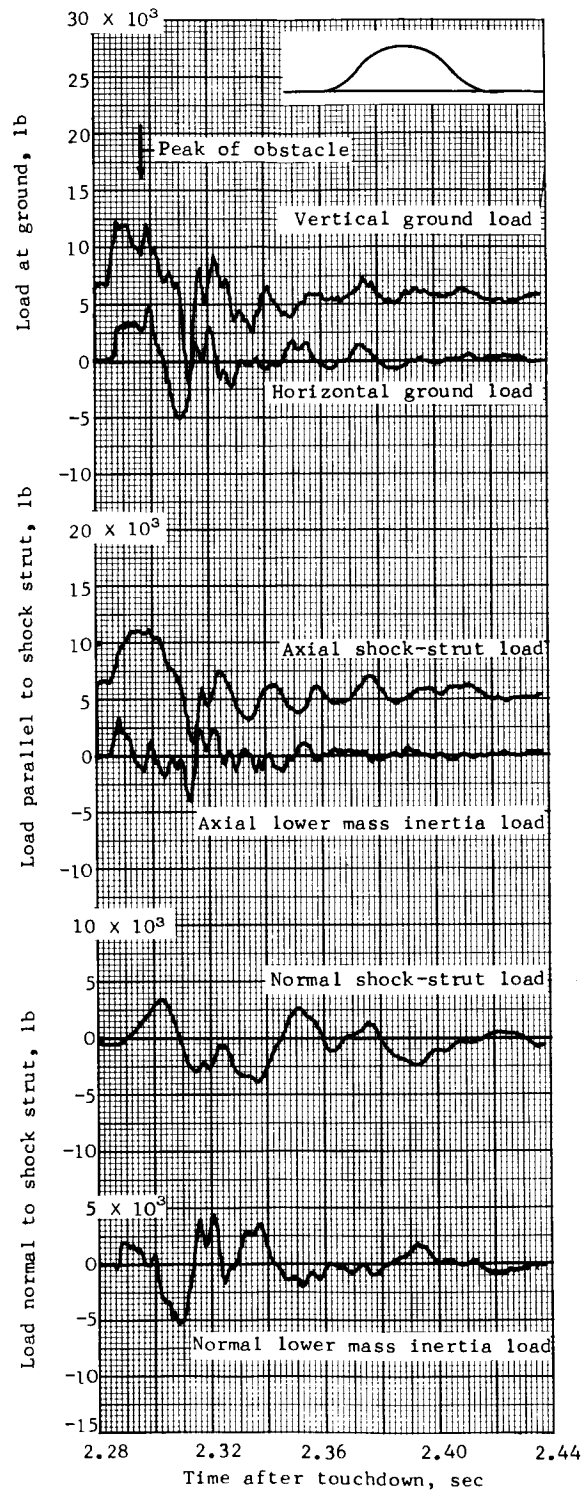


Figure 12.- Time histories of loads and other quantities obtained during taxiing over a 1 - cos, 4-inch-high, 10-inch-long obstacle. Test 16.

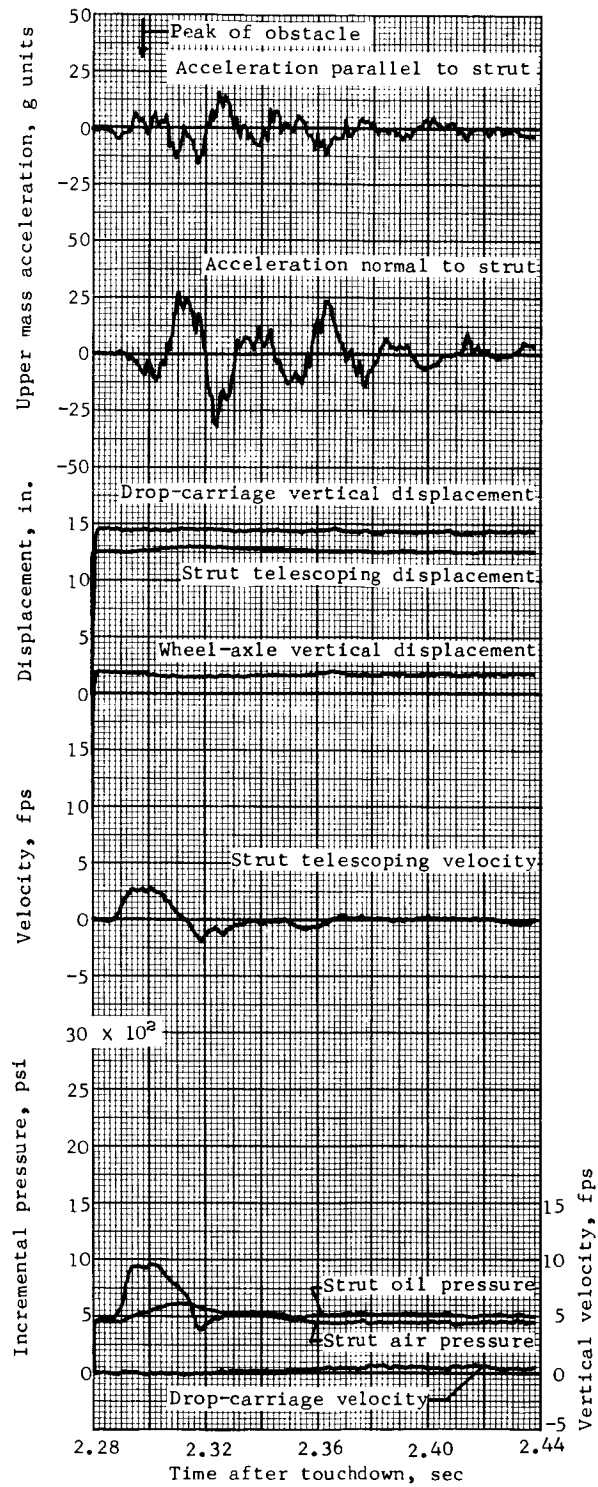


Figure 12.- Concluded.

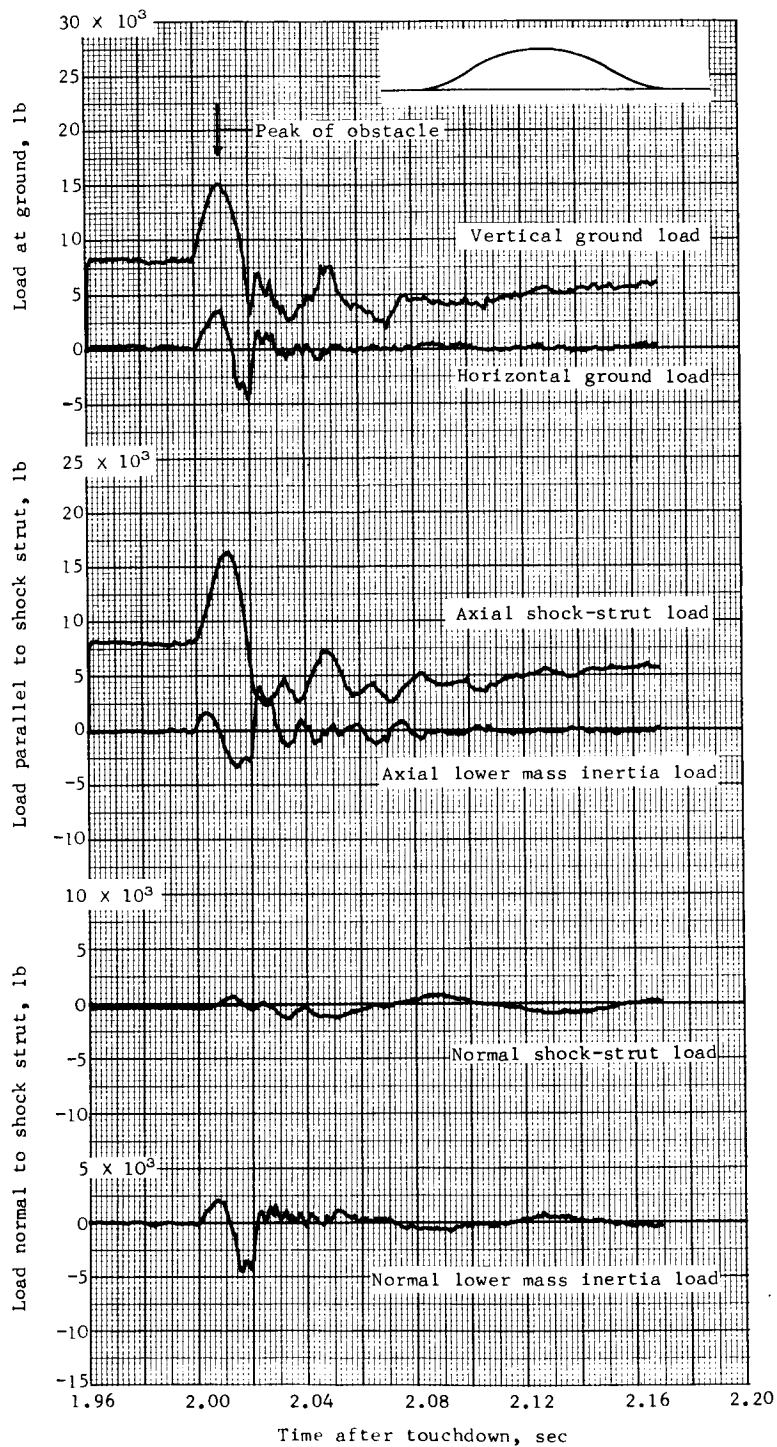


Figure 13.- Time histories of loads and other quantities obtained during taxiing over a 1 - cos, 3-inch-high, 30-inch-long obstacle. Strut is locked in fully extended position. Test 17.

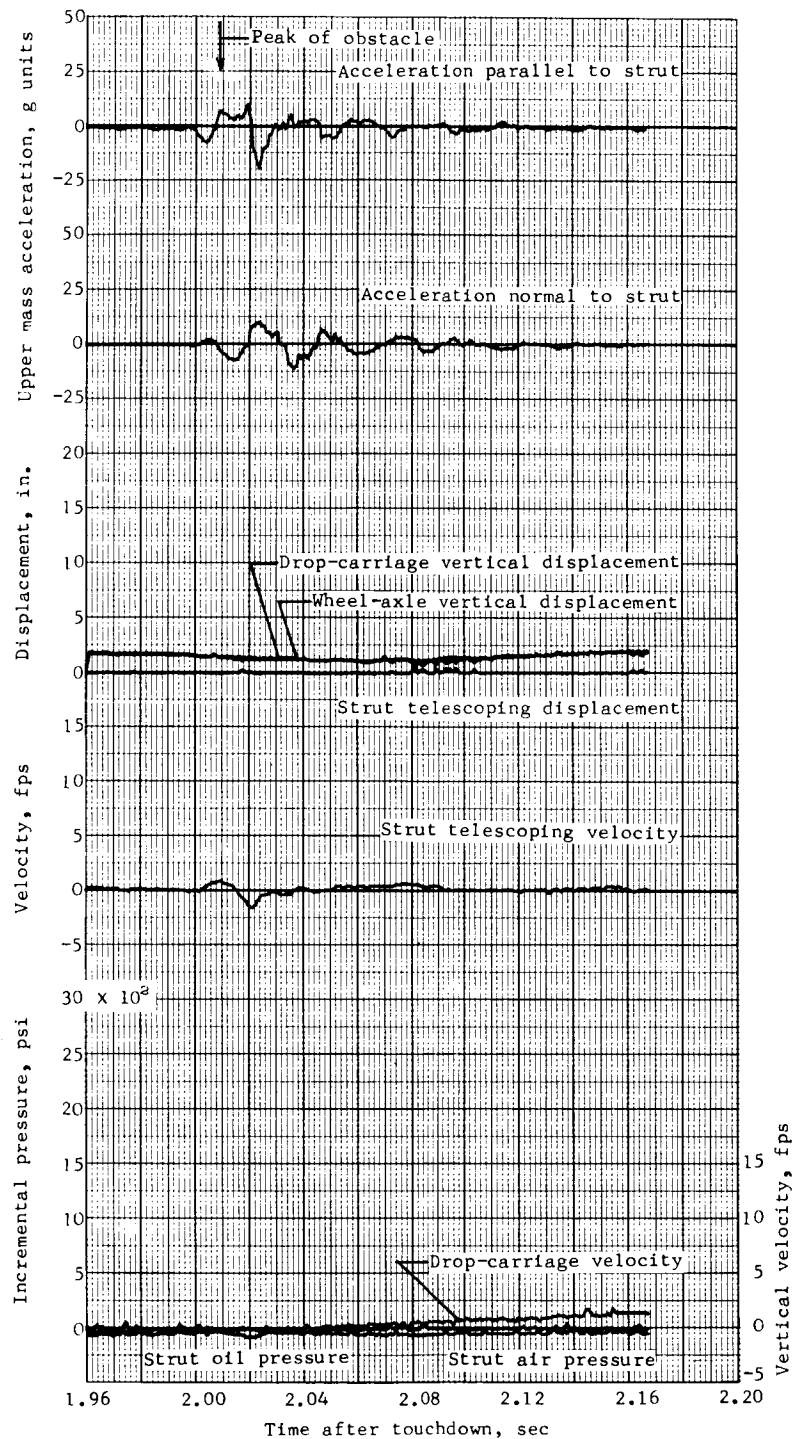


Figure 13.- Concluded.

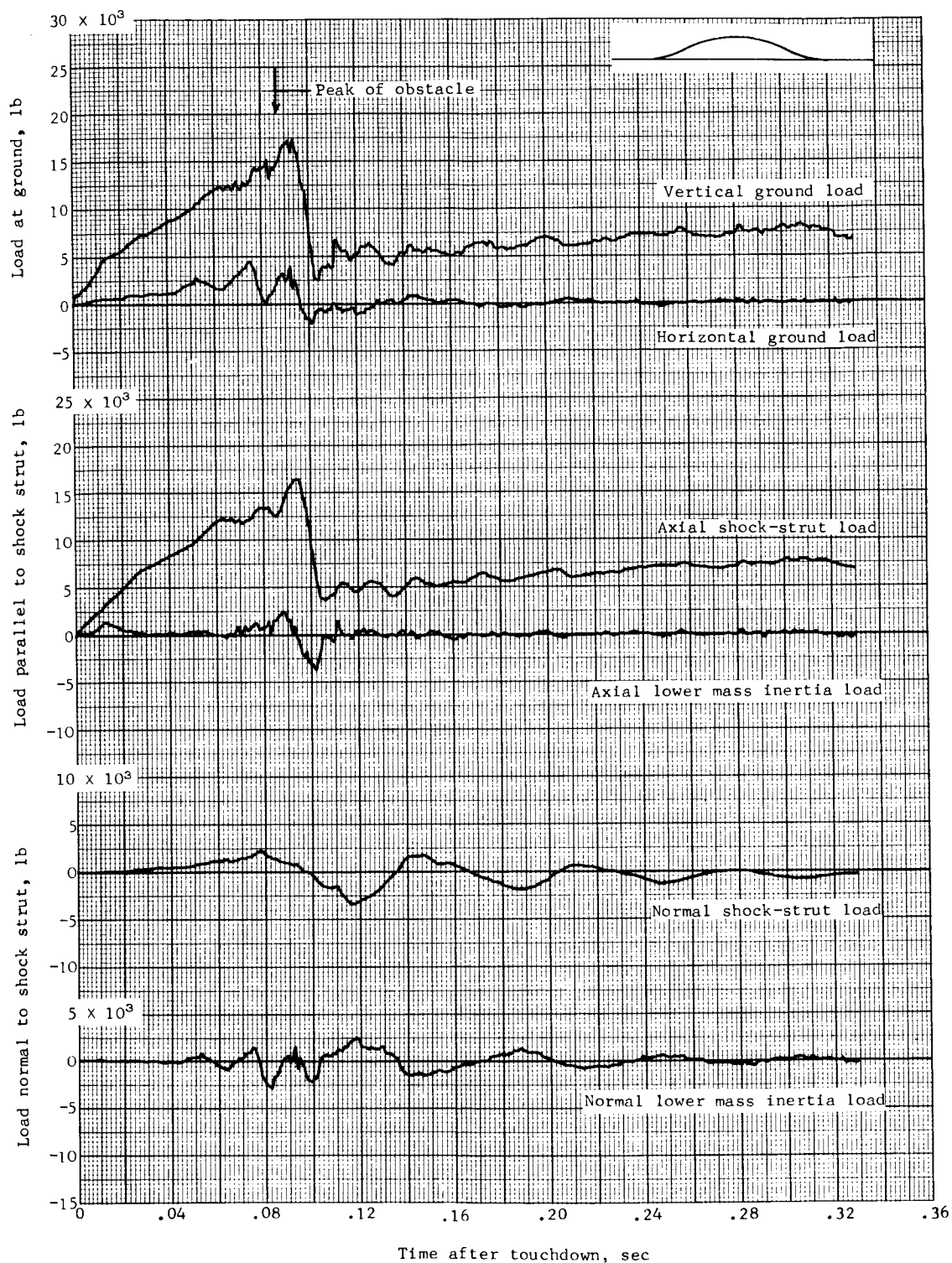


Figure 14.- Time histories of loads and other quantities obtained during landing impact over a 1 - cos, 2-inch-high, 30-inch-long obstacle oriented  $45^\circ$  to runway. Test 18.

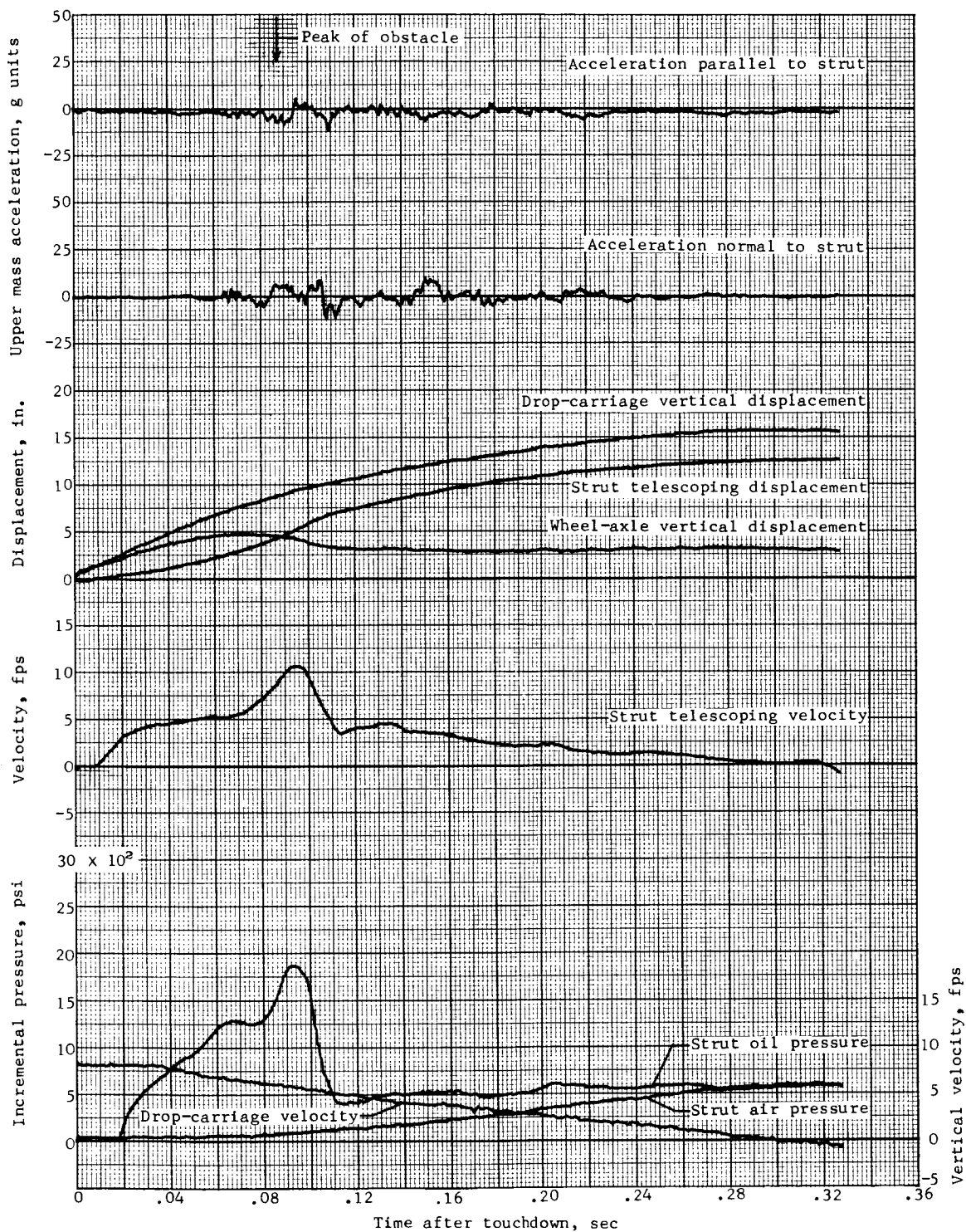


Figure 14.- Concluded.



Figure 15.- Time histories of loads and other quantities obtained during landing impact over a 1 - cos, 3-inch-high, 30-inch-long obstacle oriented 45° to runway. Test 19.



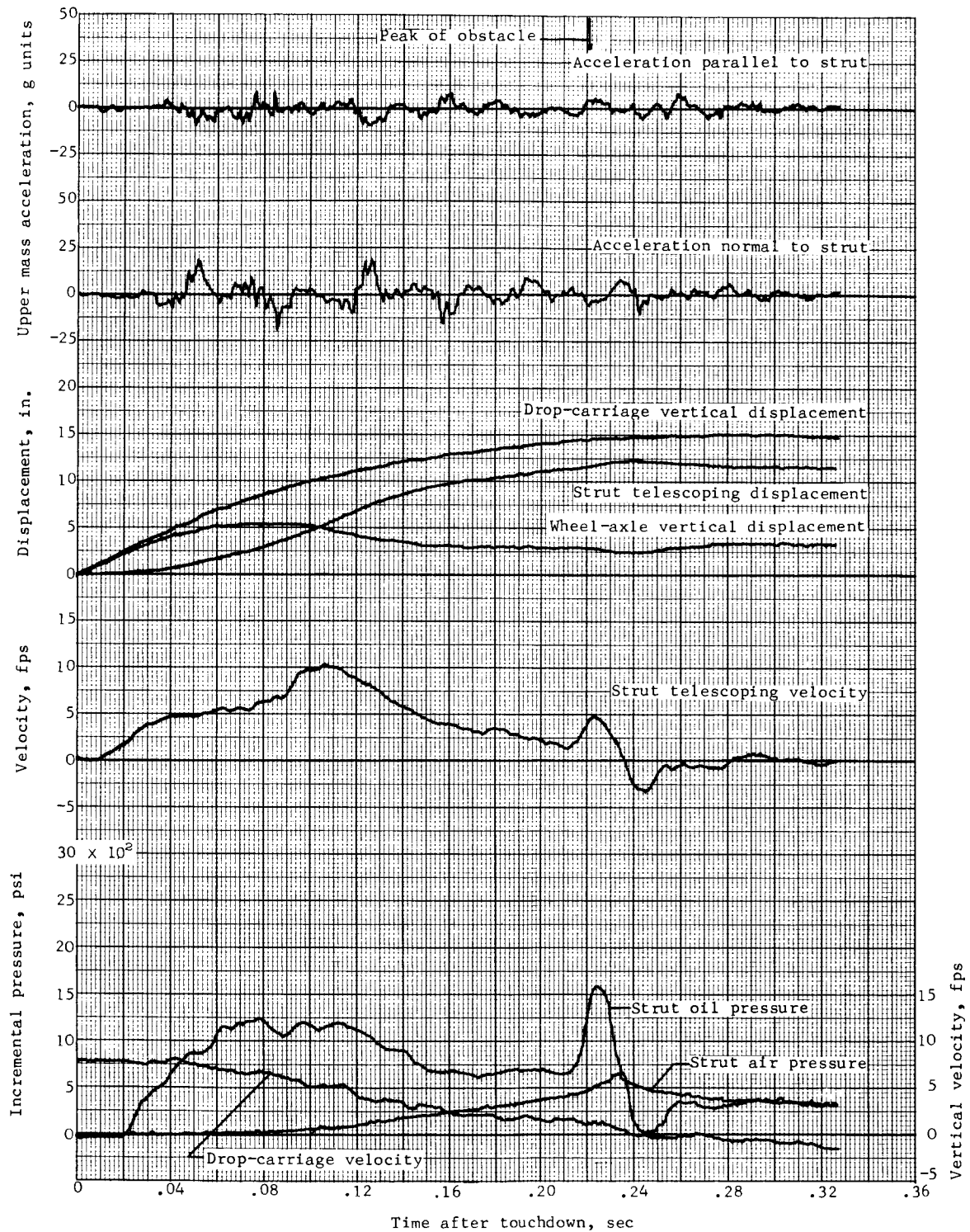
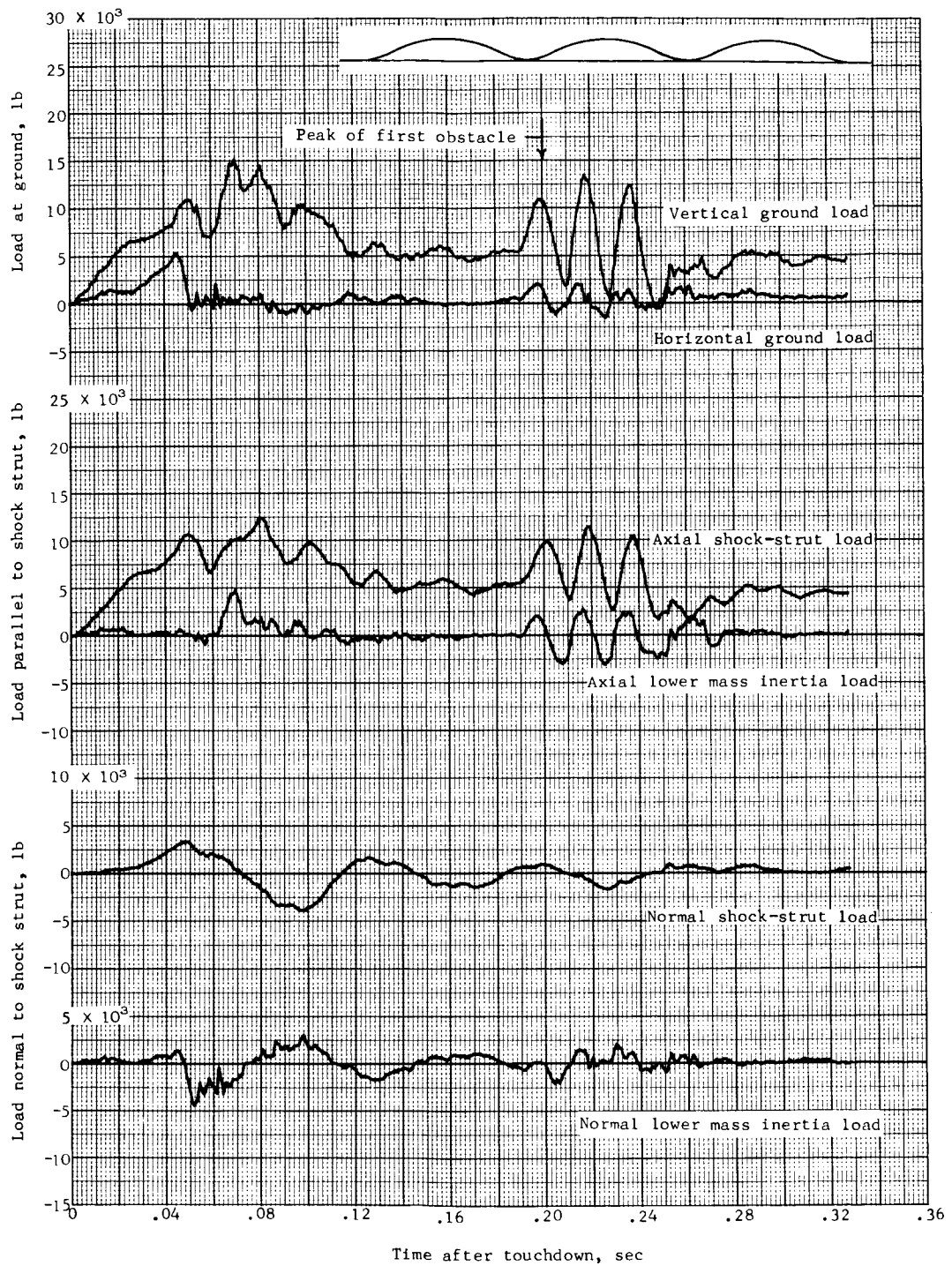
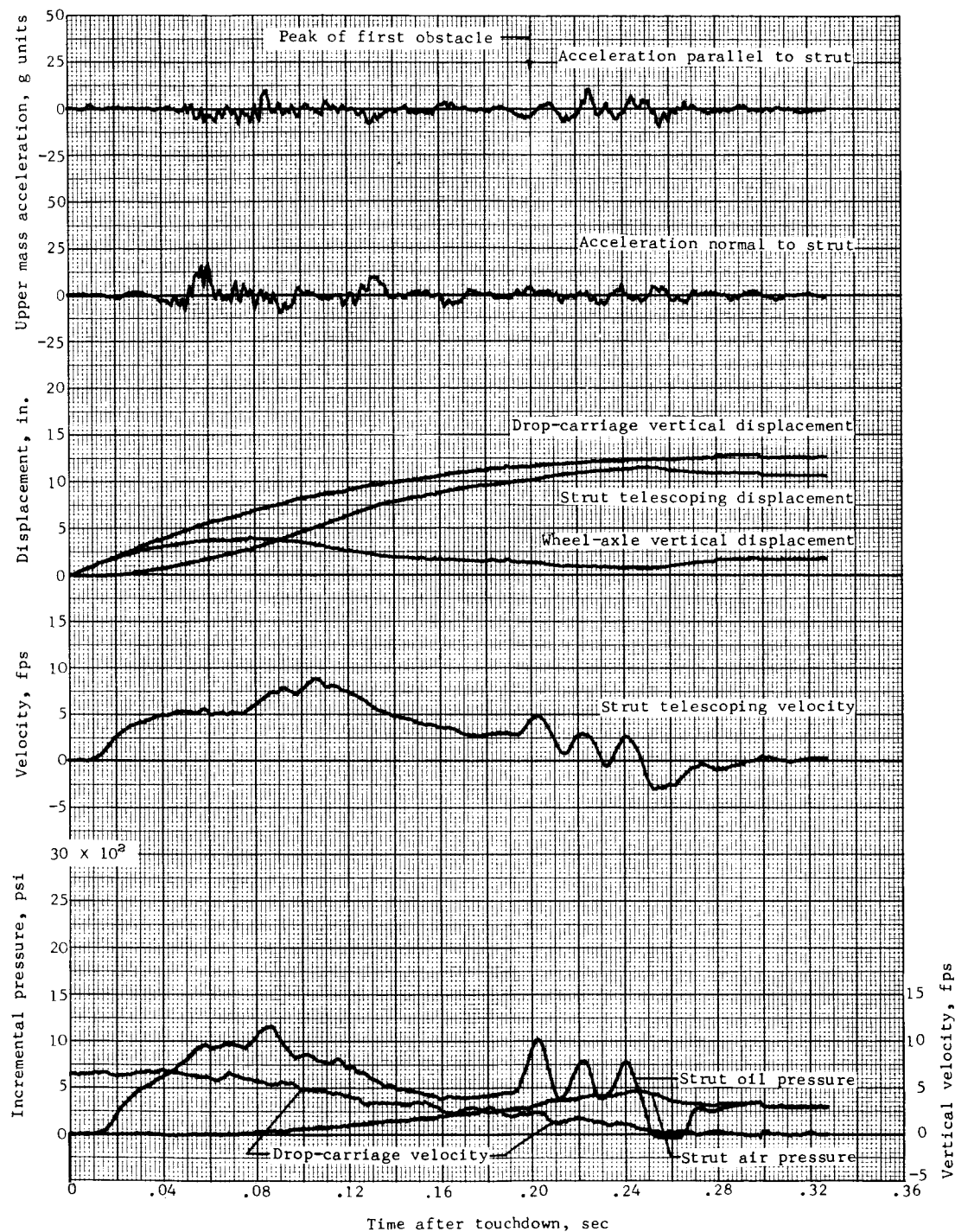


Figure 15.- Concluded.



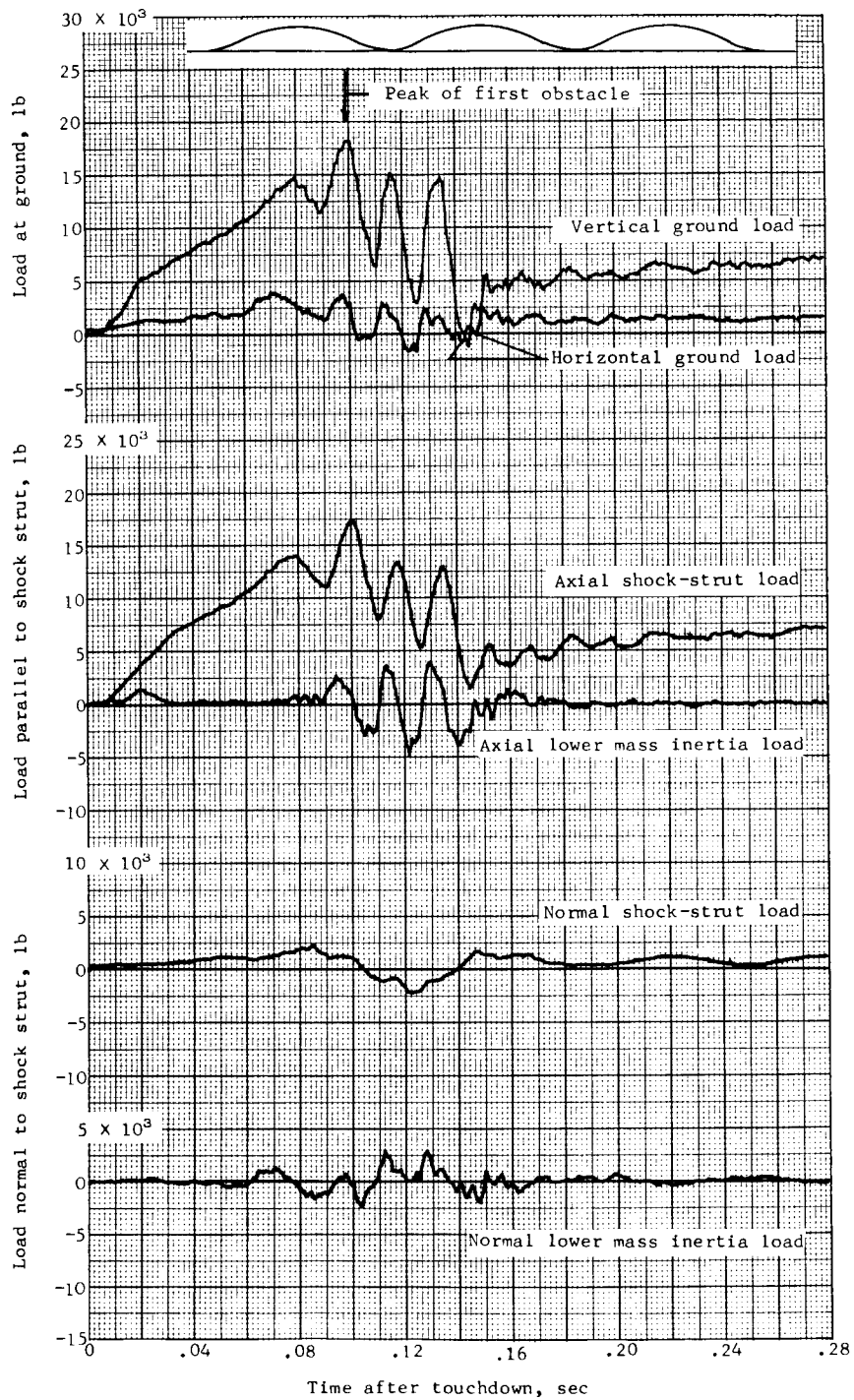
(a) Test 20.

Figure 16.- Time histories of loads and other quantities obtained during landing impact over 1 - cos undulations, 2 inches high and 30 inches long.



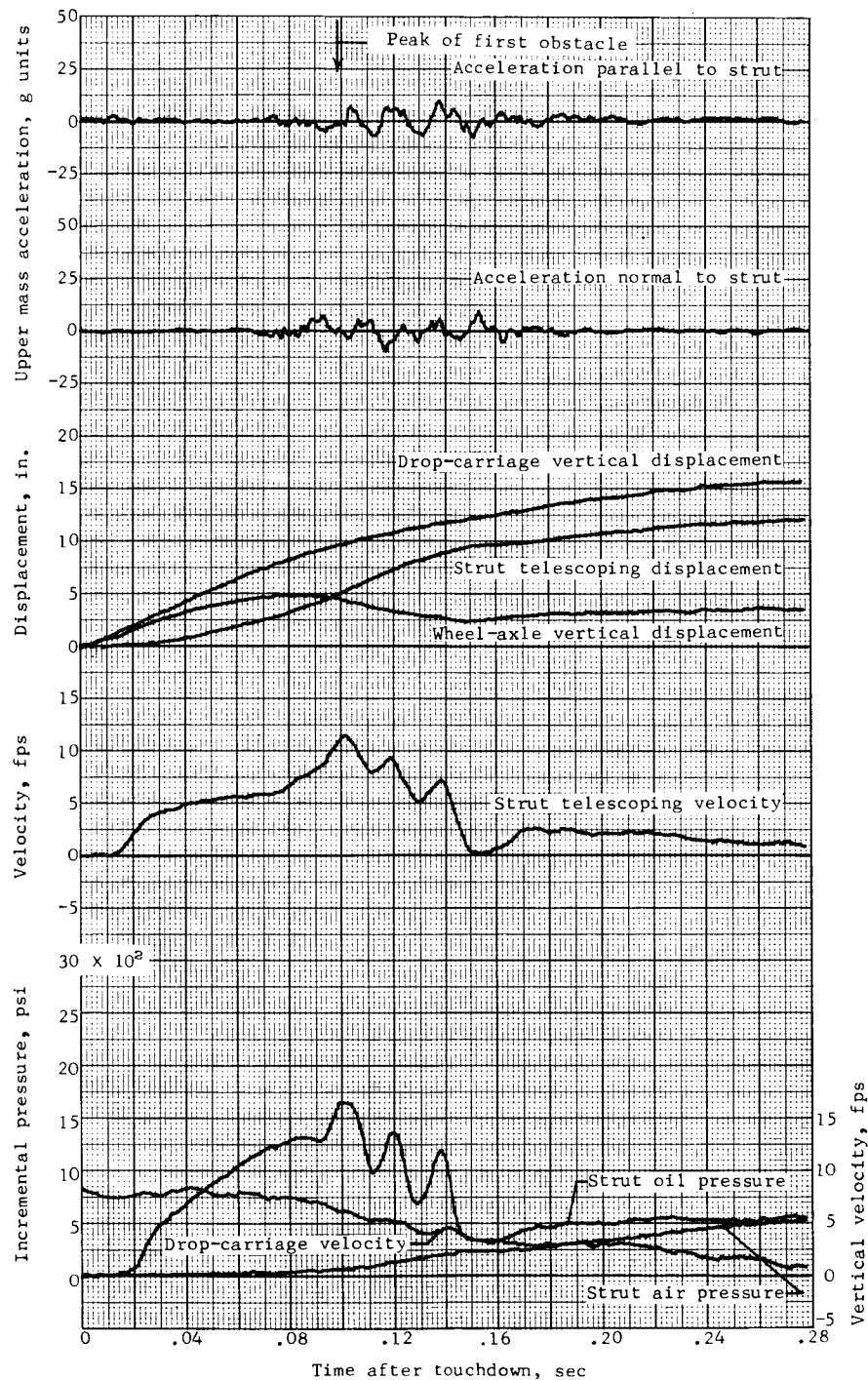
(a) Concluded.

Figure 16.- Continued.



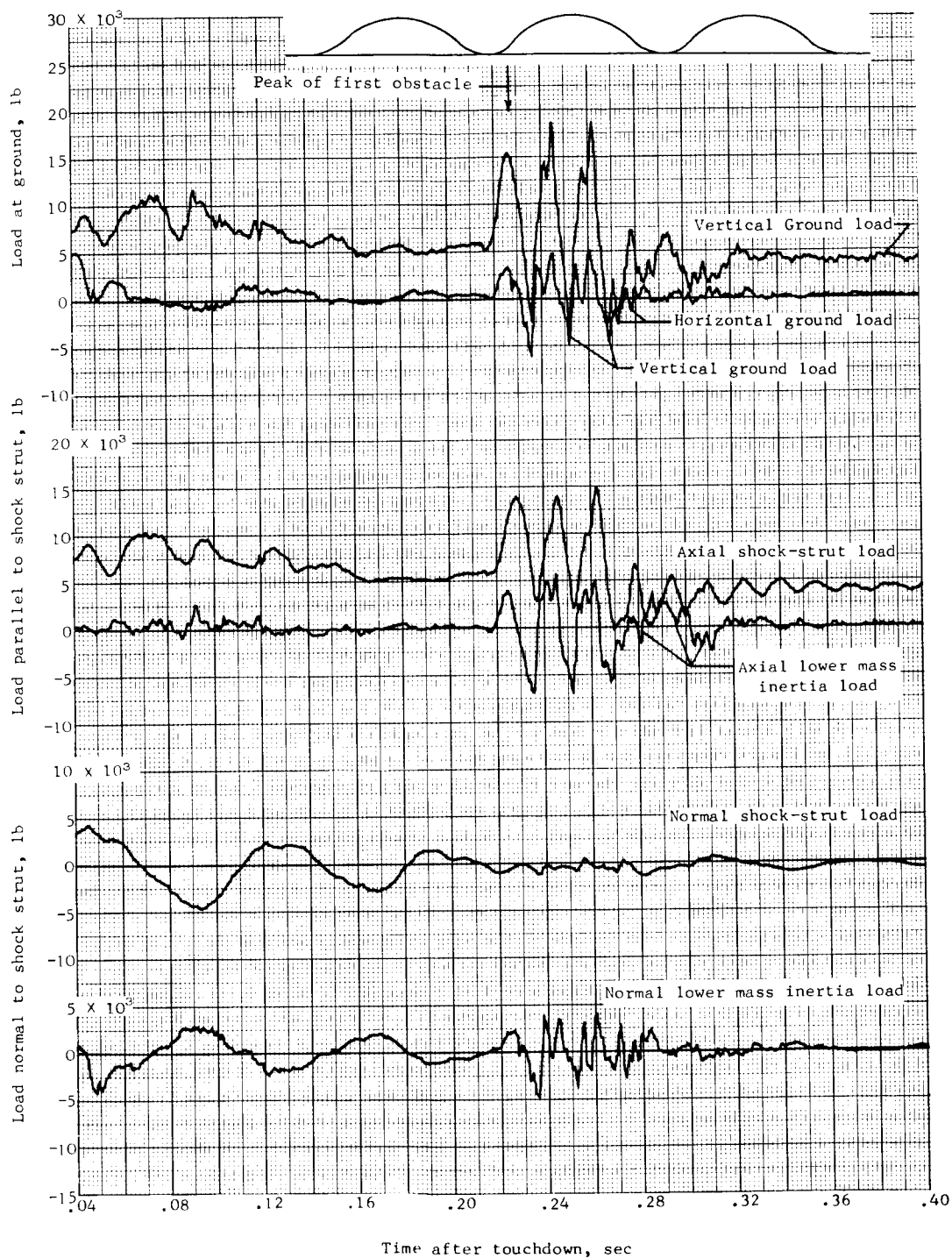
(b) Test 21.

Figure 16.- Continued.



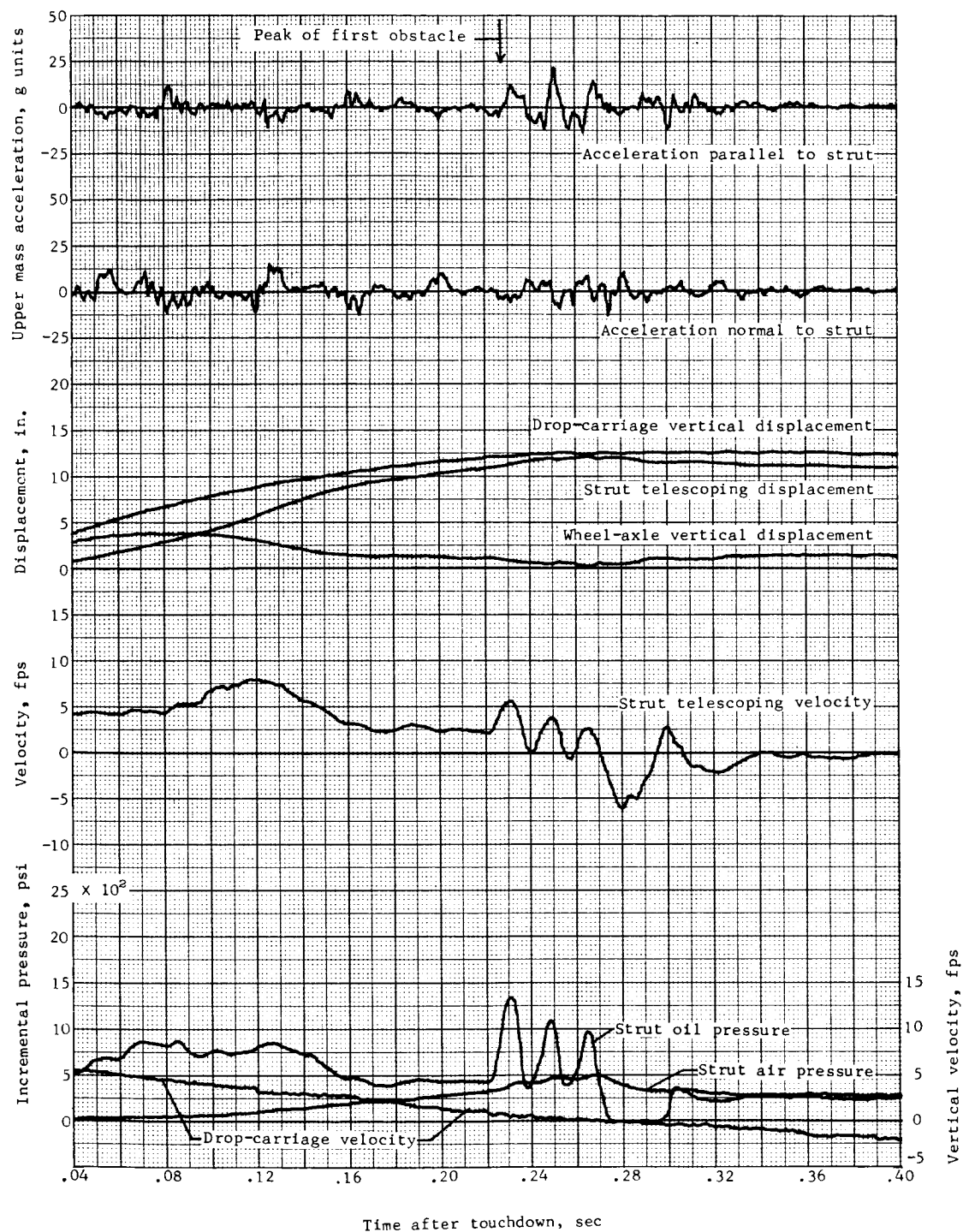
(b) Concluded.

Figure 16.- Concluded.



(a) Test 22.

Figure 17.- Time histories of loads and other quantities obtained during landing impact over 1 - cos undulations, 3 inches high and 30 inches long.



(a) Concluded.

Figure 17.- Continued.

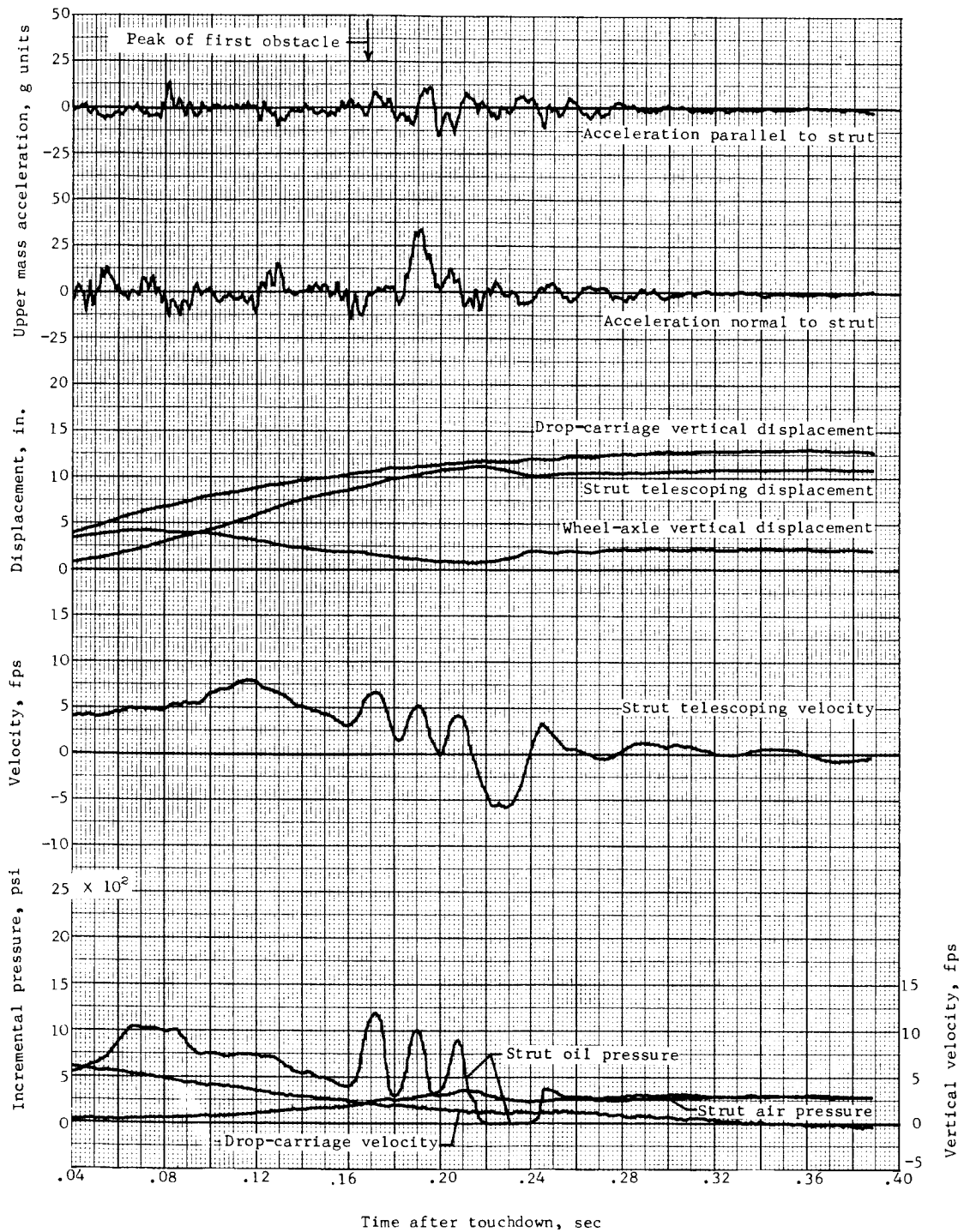




(b) Test 23.

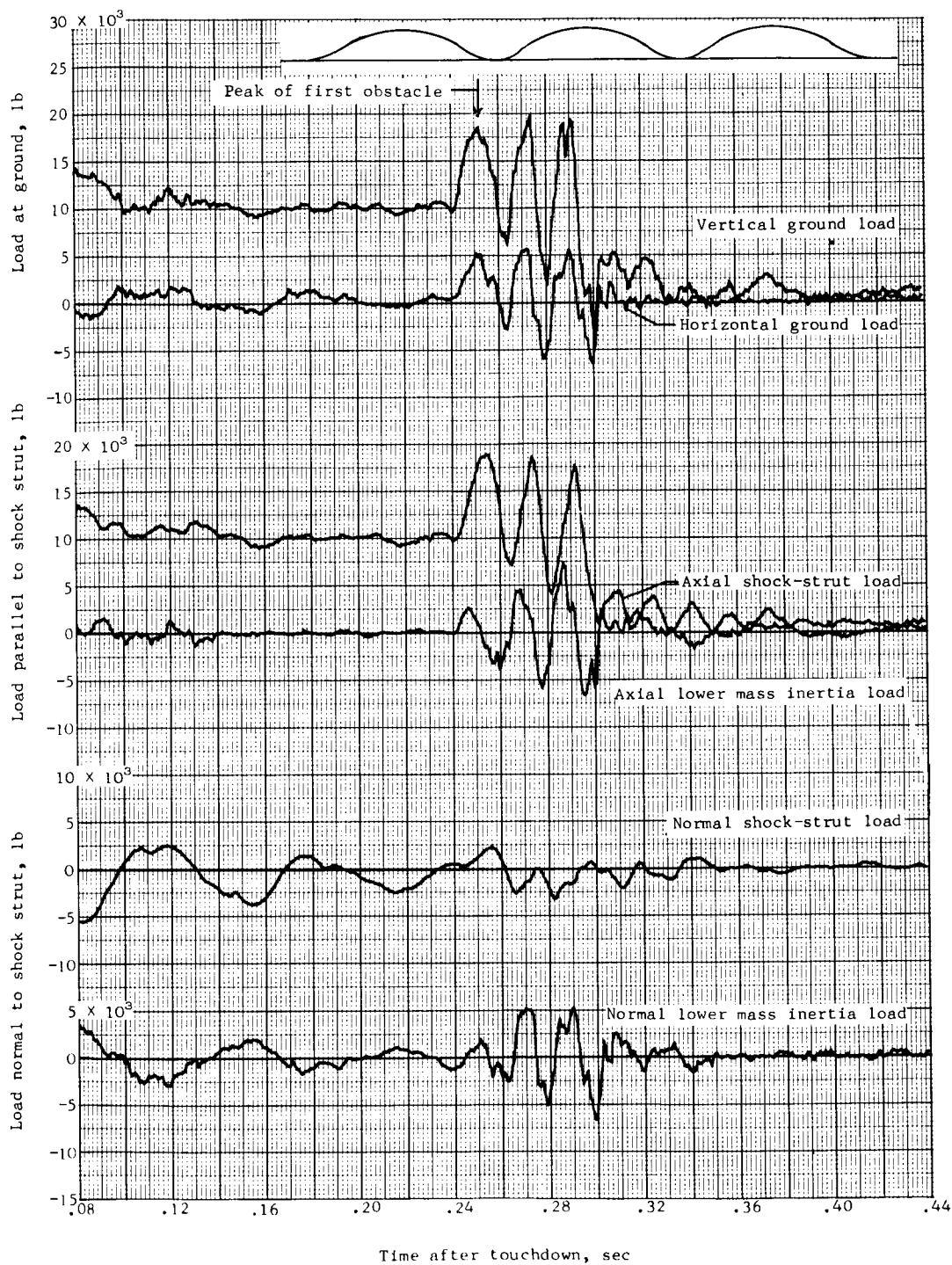
Figure 17.- Continued.





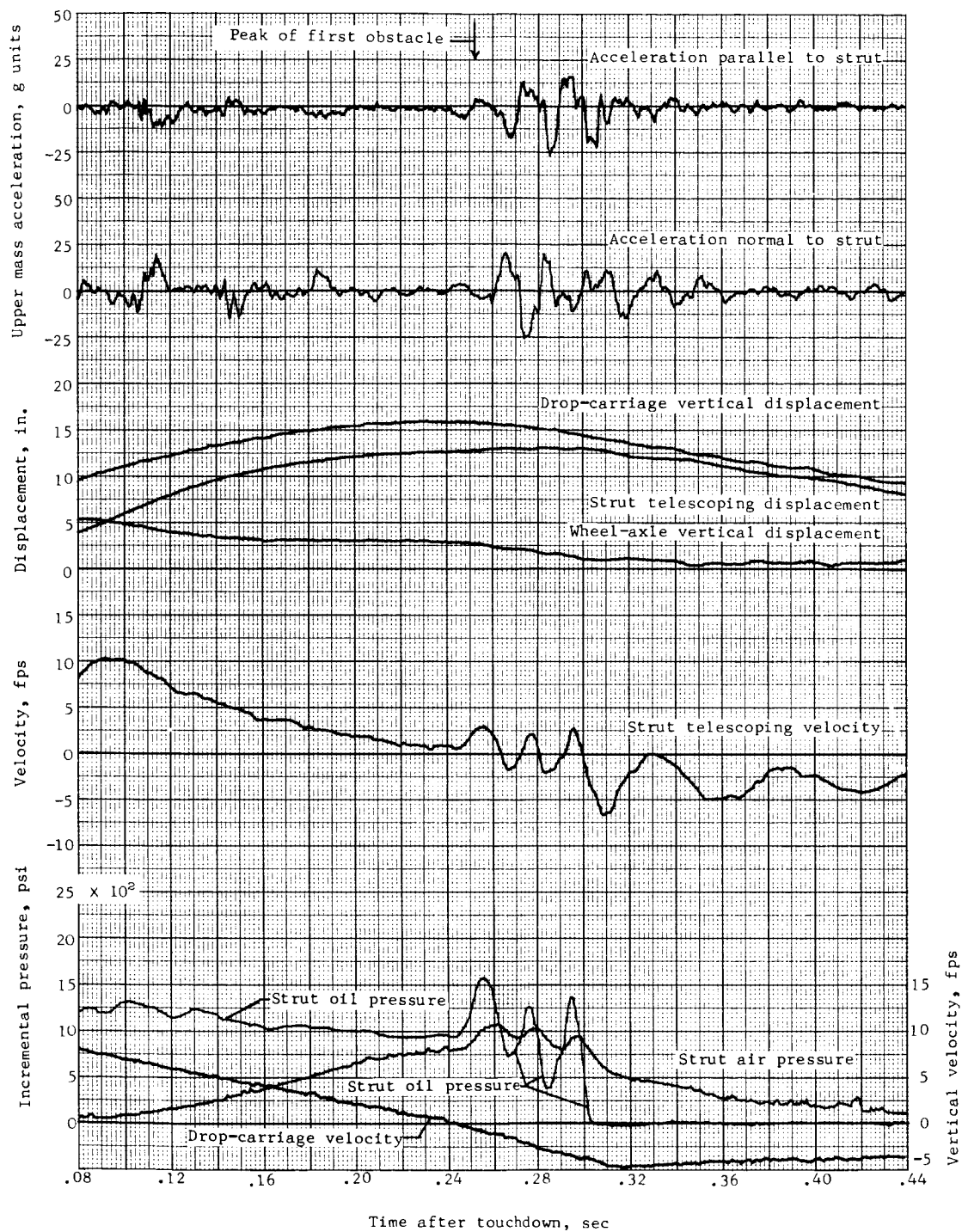
(b) Concluded.

Figure 17.- Continued.



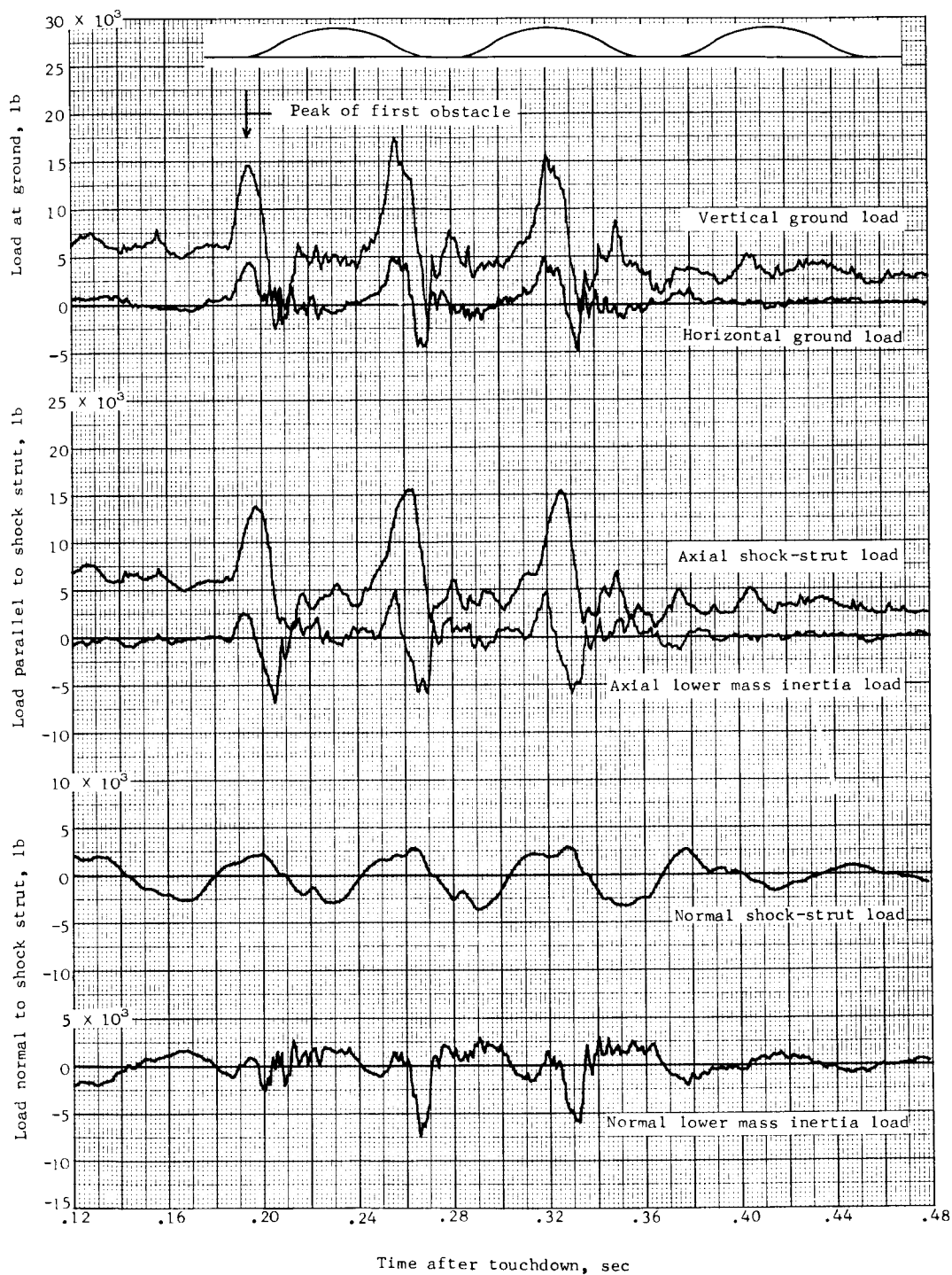
(c) Test 24.

Figure 17.- Continued.



(c) Concluded.

Figure 17.- Concluded.



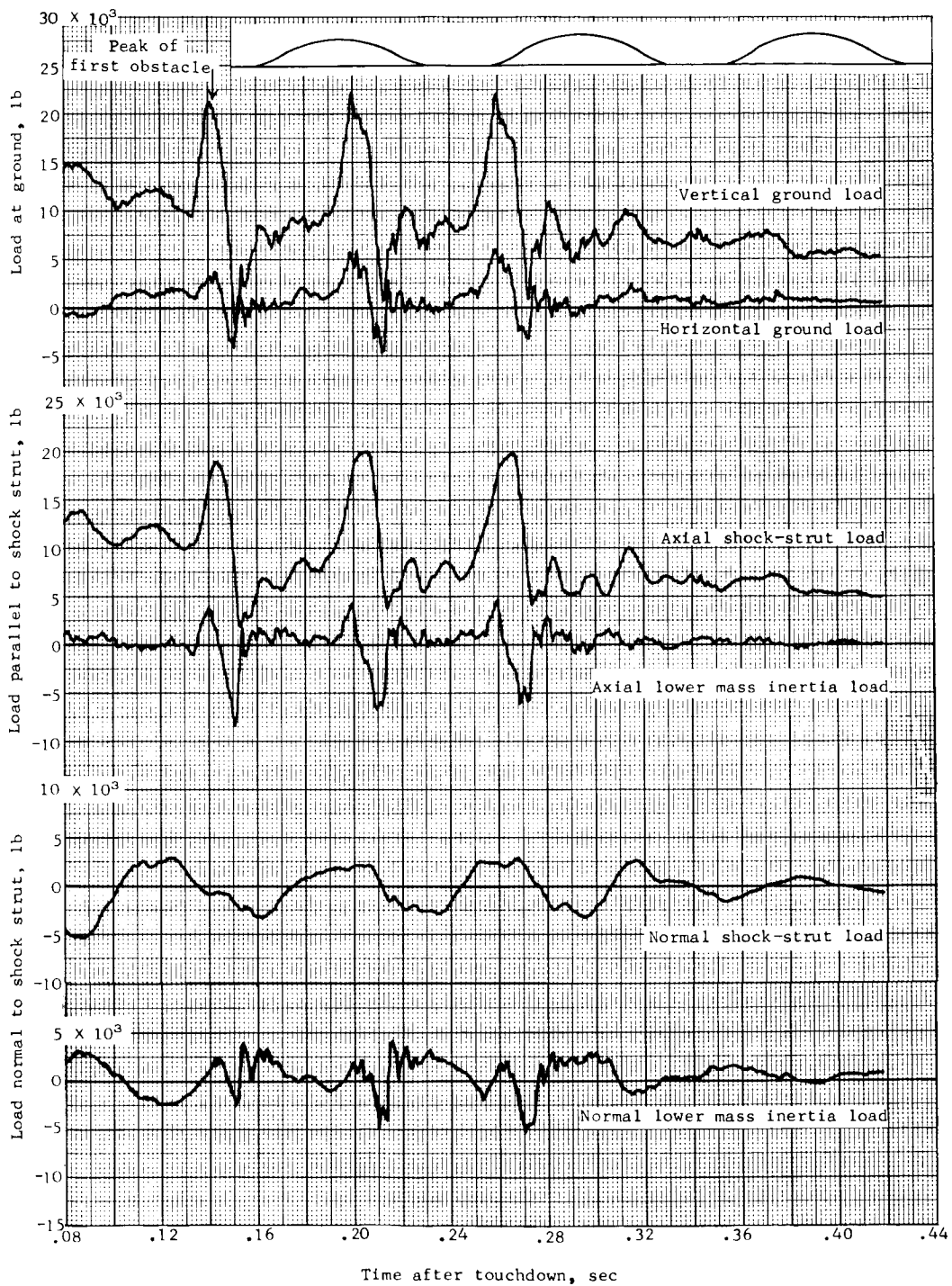
(a) Test 25.

Figure 18.- Time histories of loads and other quantities obtained during landing impact over three 1 - cos, 3-inch-high, 30-inch-long obstacles, spaced 9 feet apart.



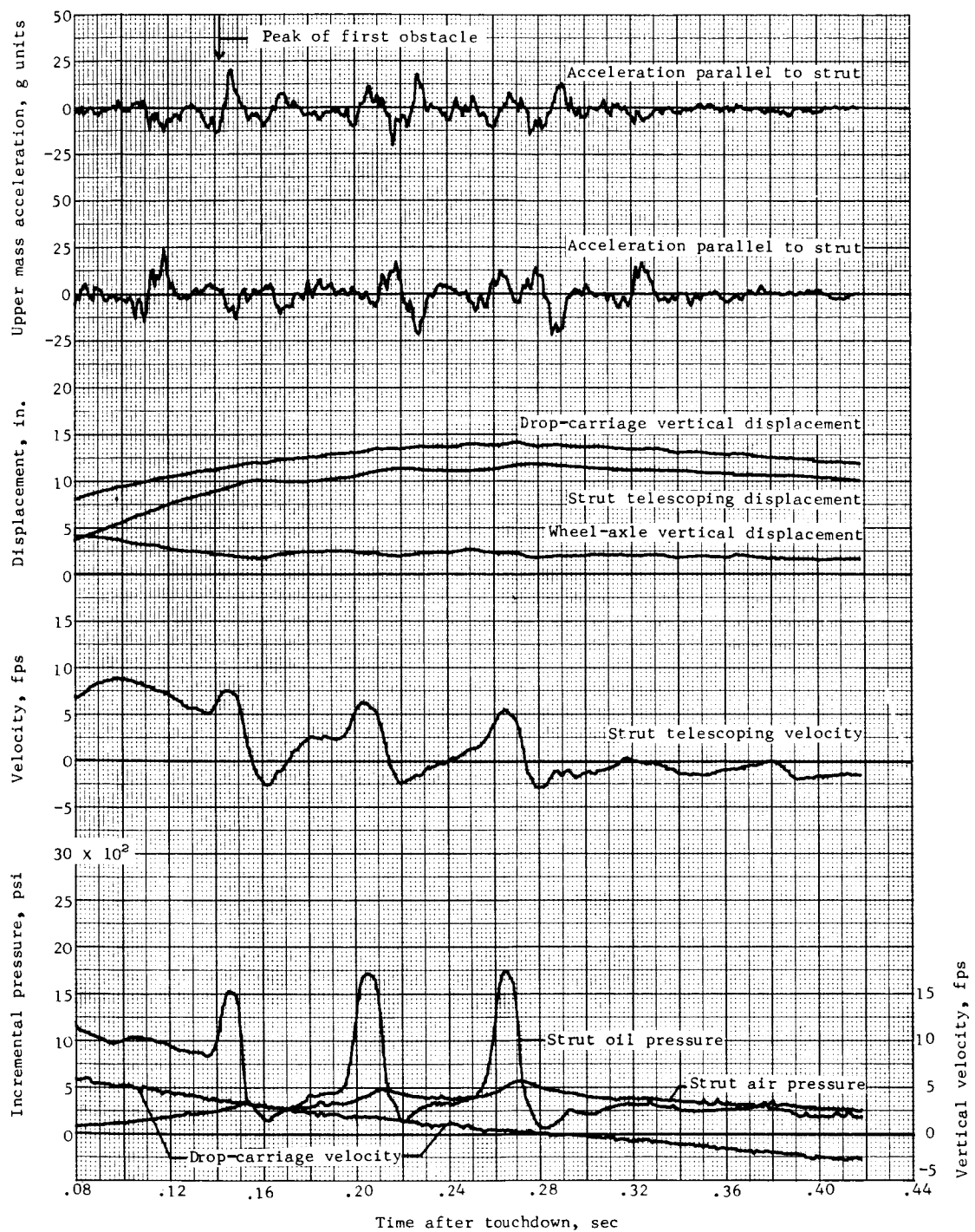
(a) Concluded.

Figure 18.- Continued.



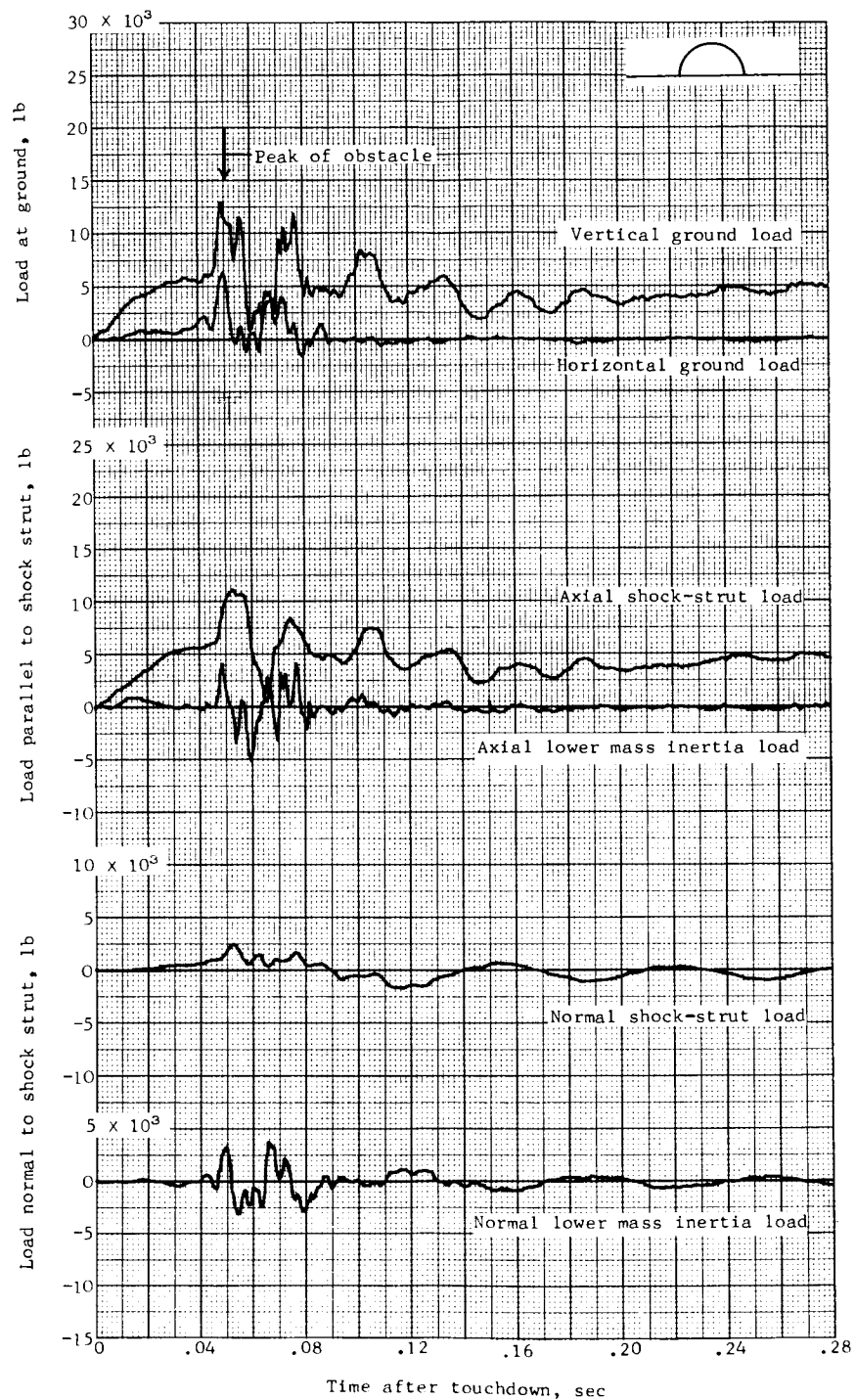
(b) Test 26.

Figure 18.- Continued.



(b) Concluded.

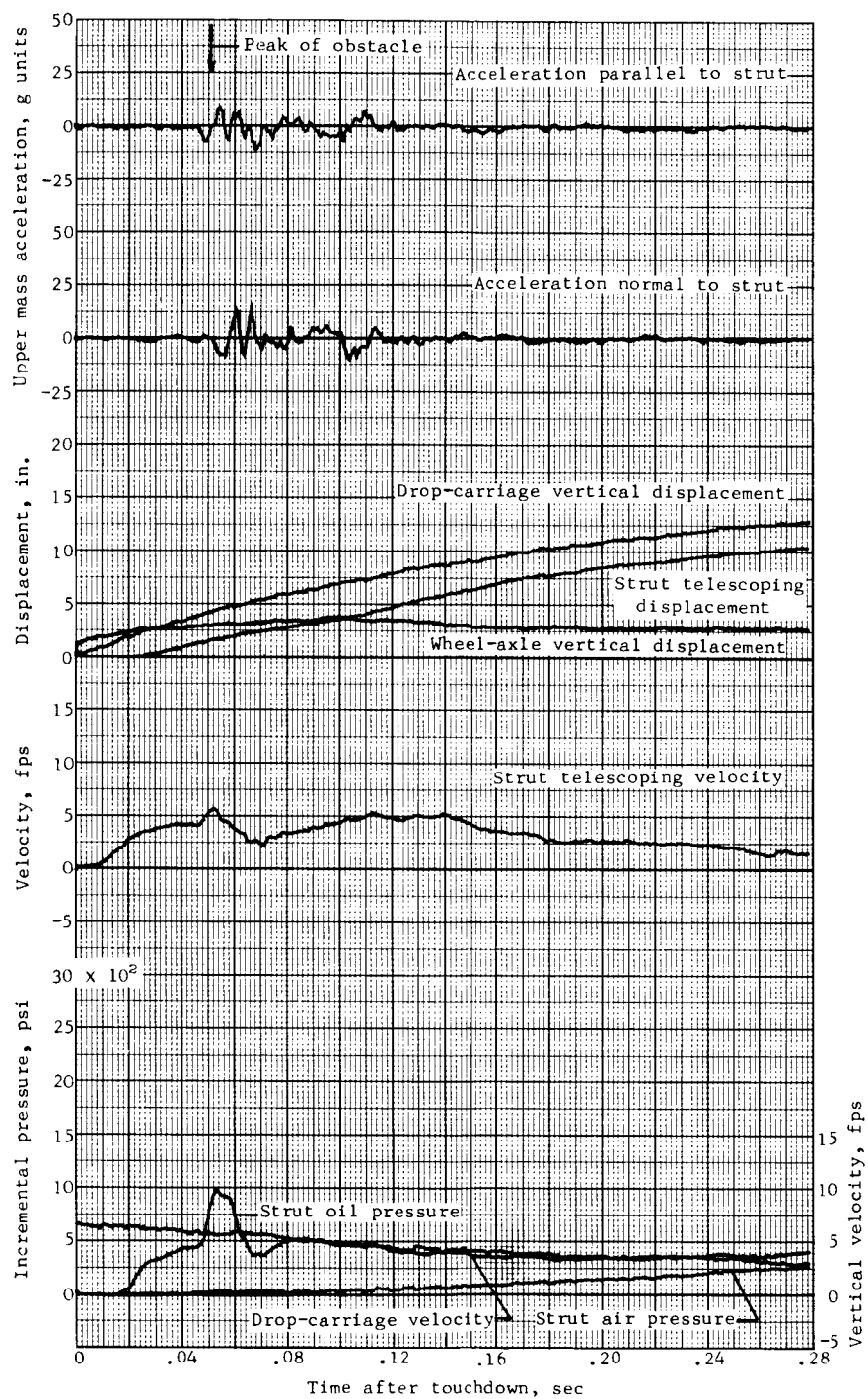
Figure 18.- Concluded.



(a) Test 27.

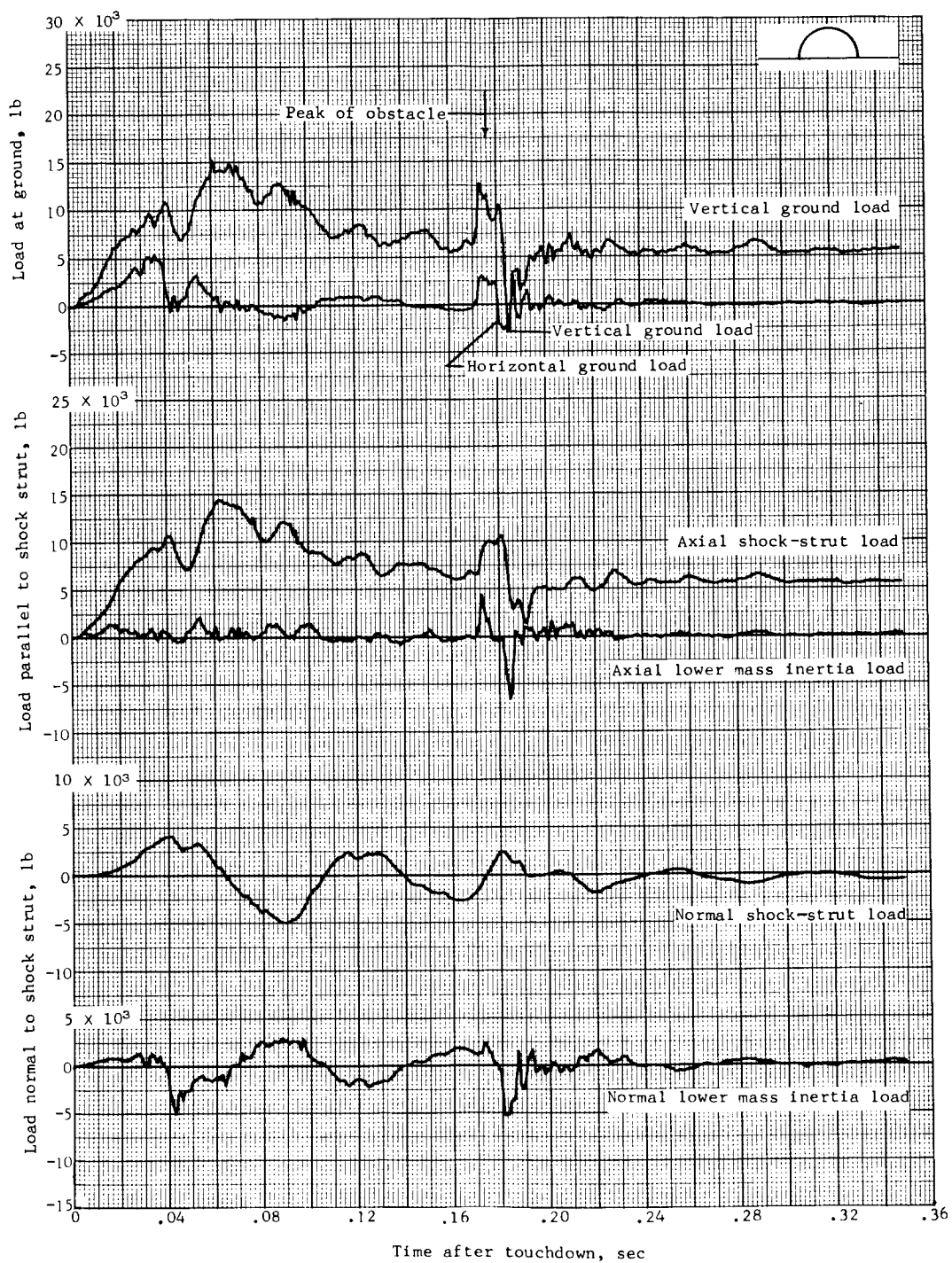
Figure 19.- Time histories of loads and other quantities obtained during landing impact over a semicylinder, 3 inches high and 6 inches long.





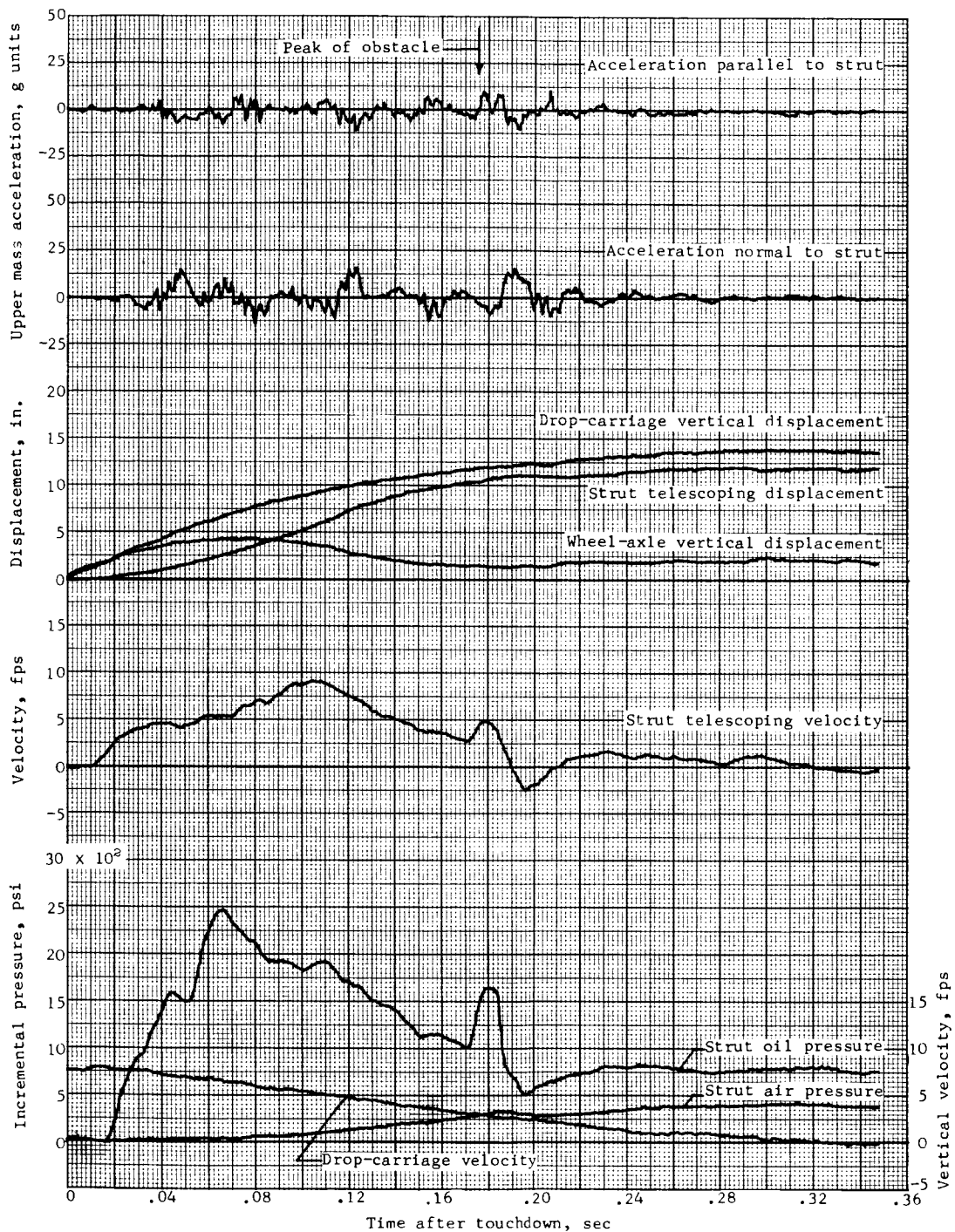
(a) Concluded.

Figure 19.- Continued.



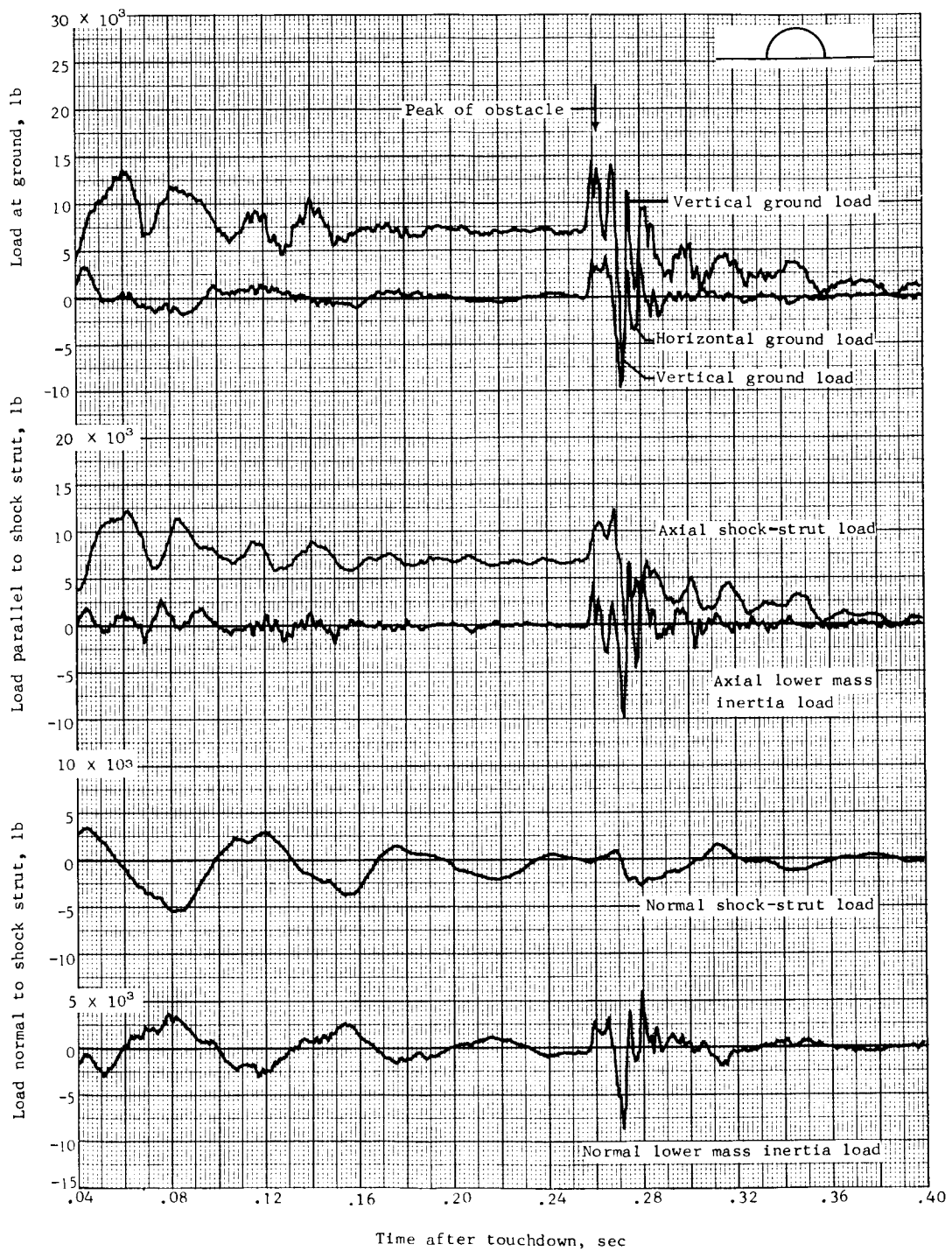
(b) Test 28.

Figure 19.- Continued.



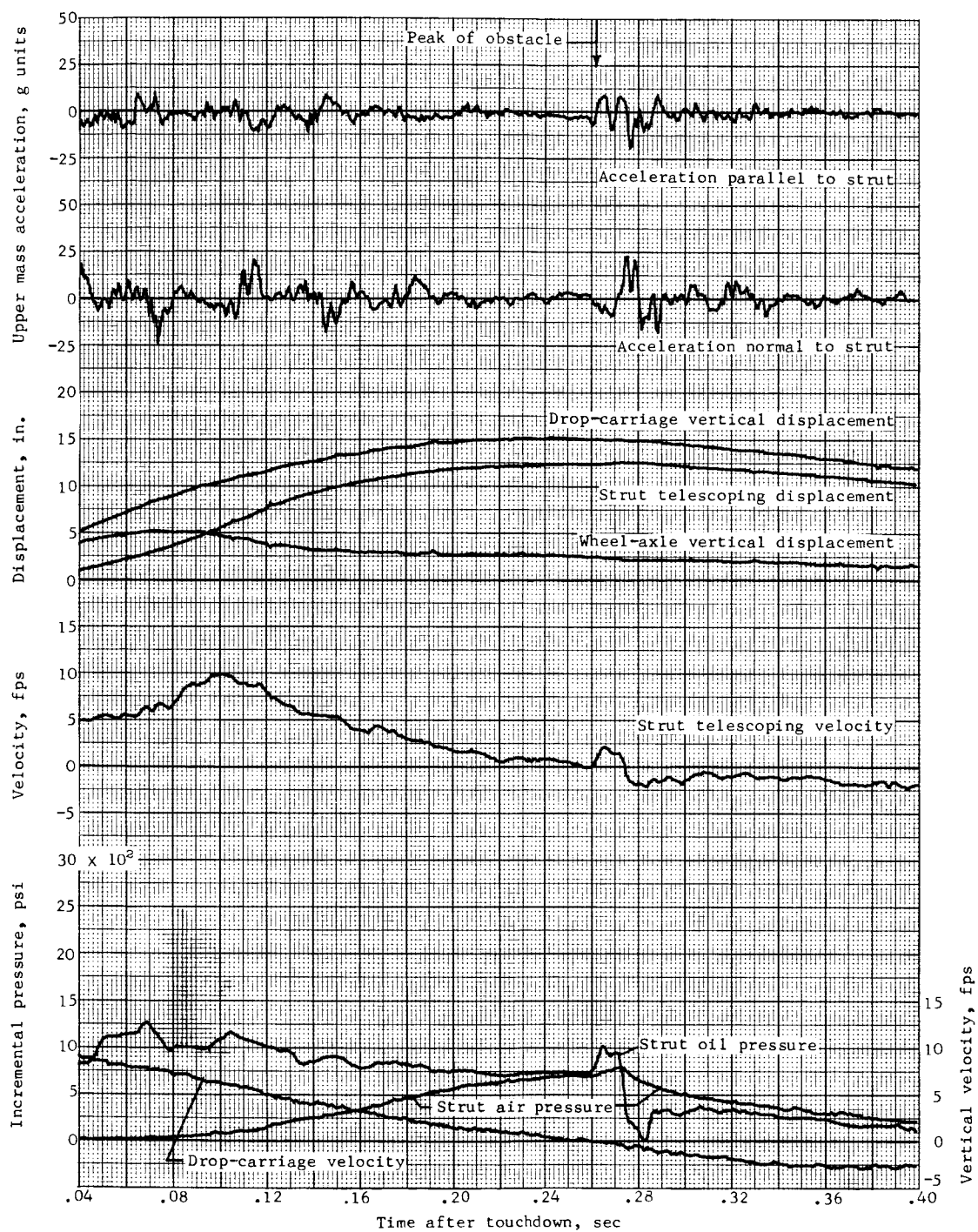
(b) Concluded.

Figure 19.- Continued.



(c) Test 29.

Figure 19.- Continued.



(c) Concluded.

Figure 19.- Concluded.

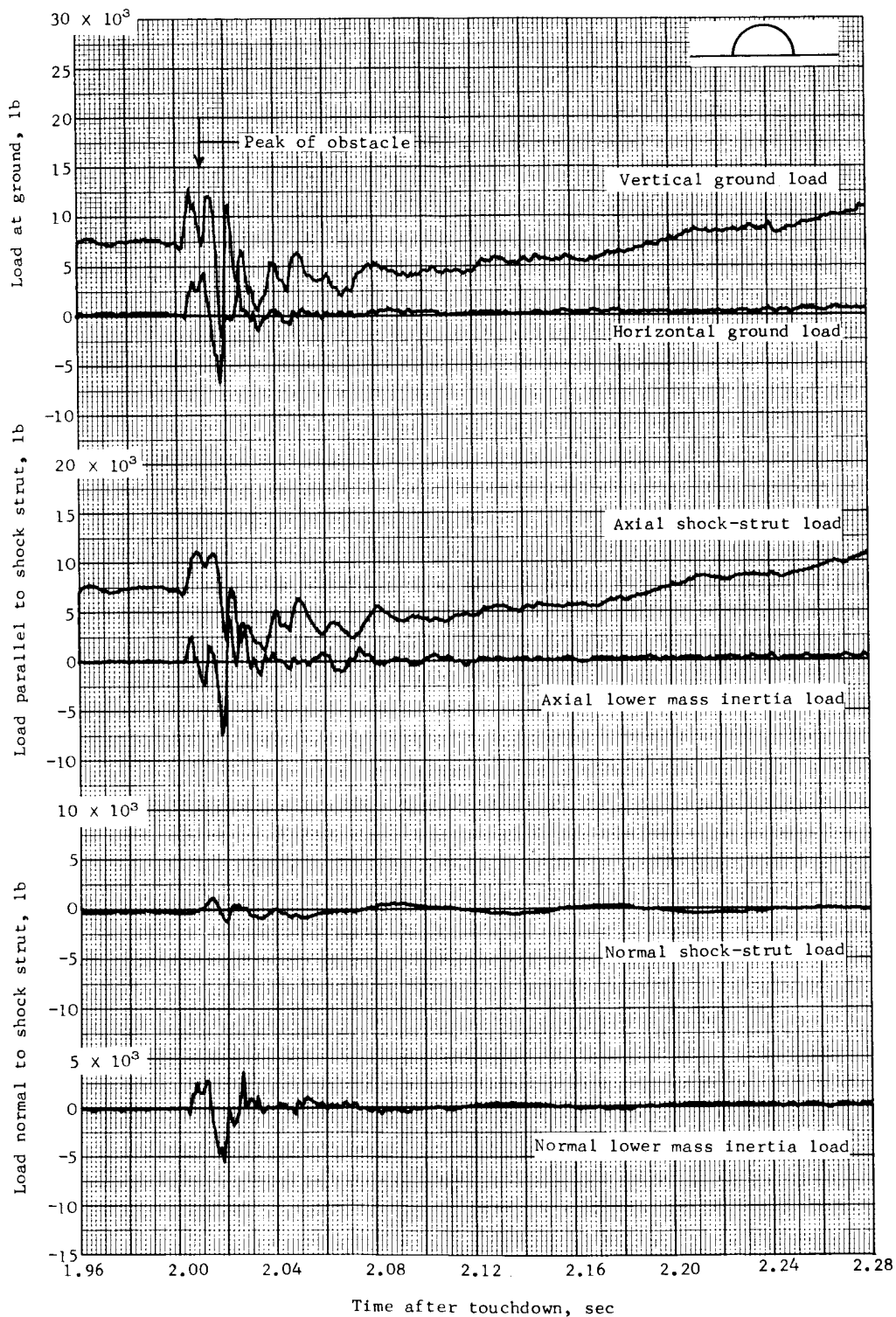


Figure 20.- Time histories of loads and other quantities obtained during taxiing over a semicylinder, 3 inches high and 6 inches long. Strut is locked in fully extended position. Test 30.

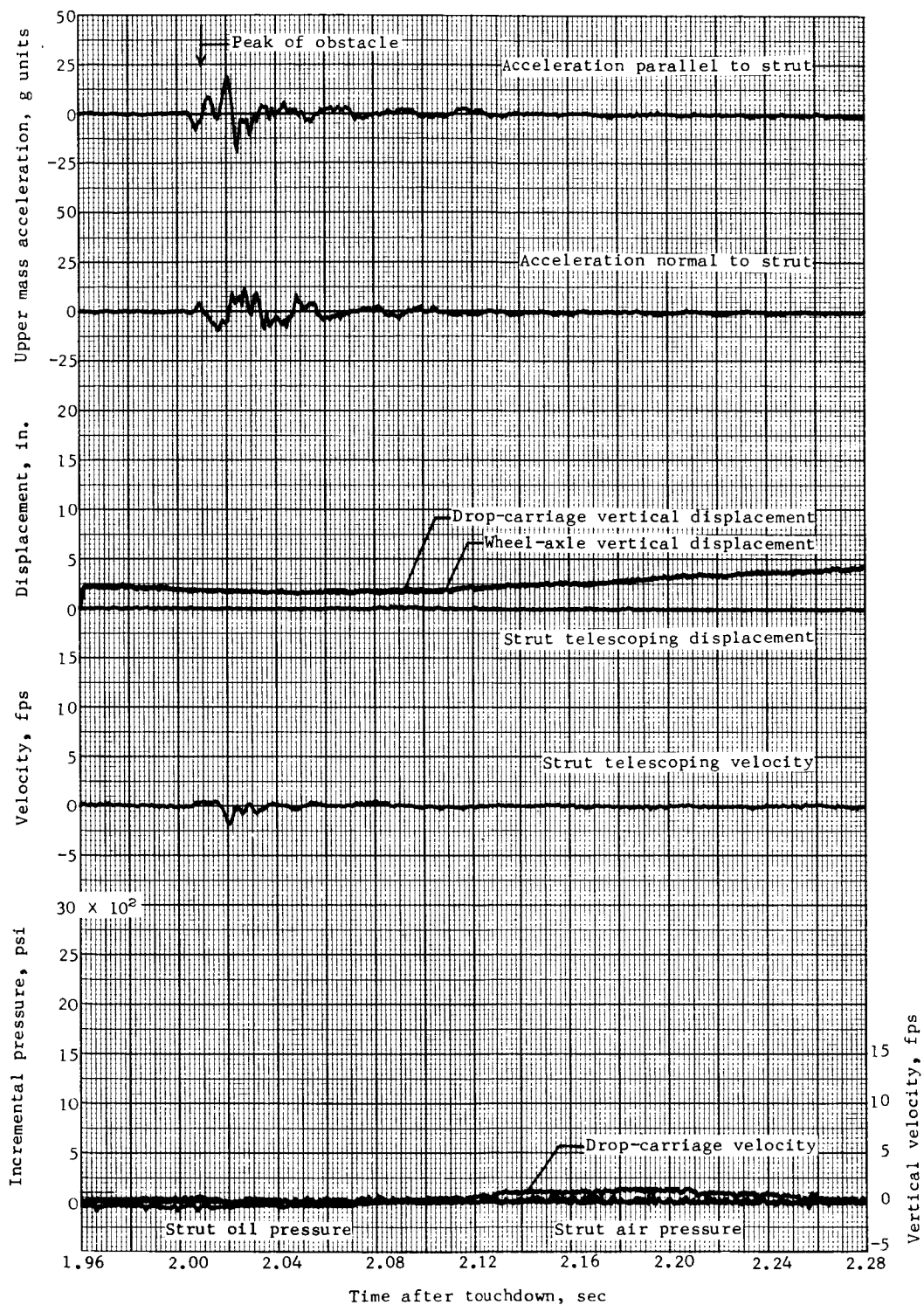
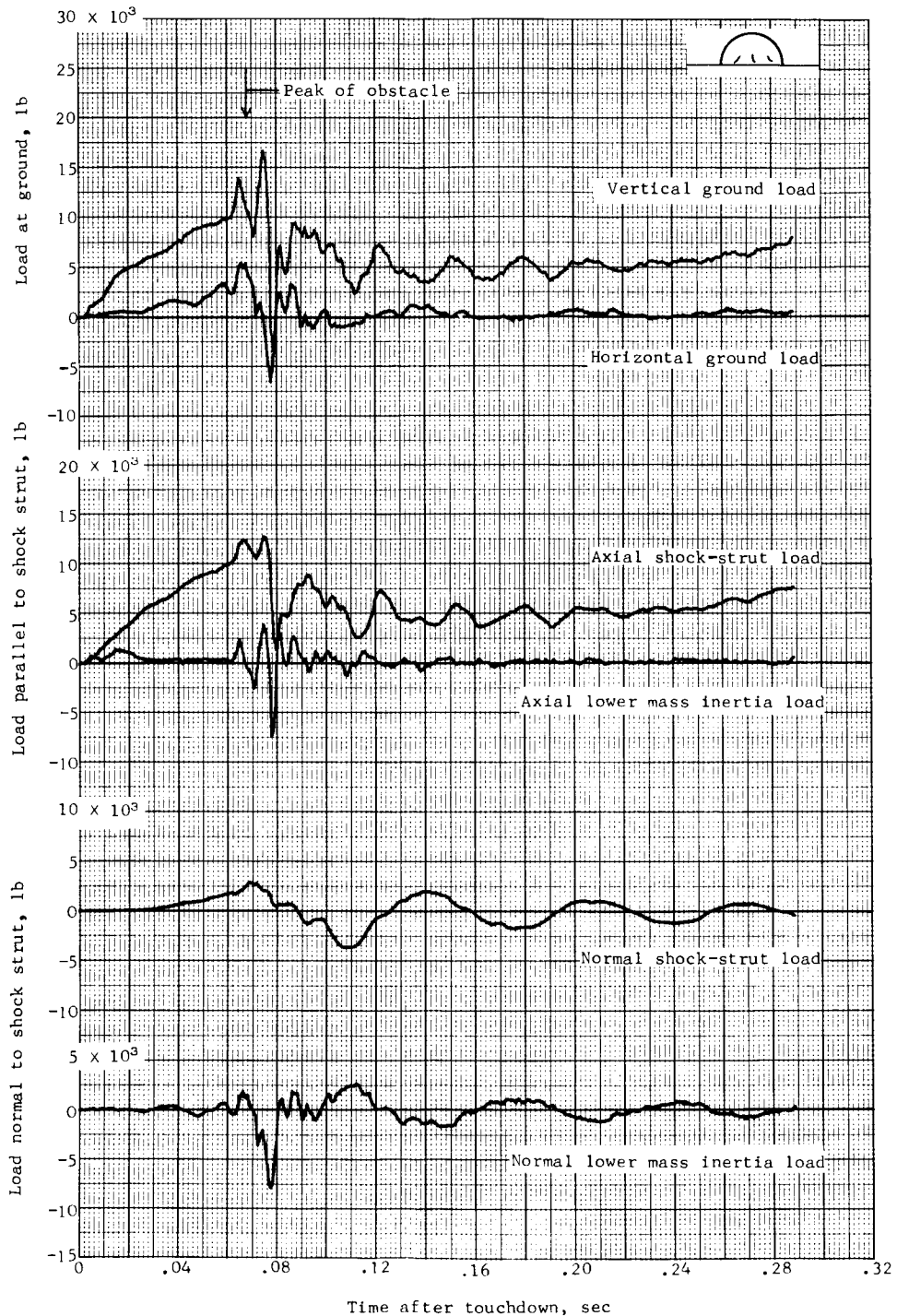


Figure 20.- Concluded.

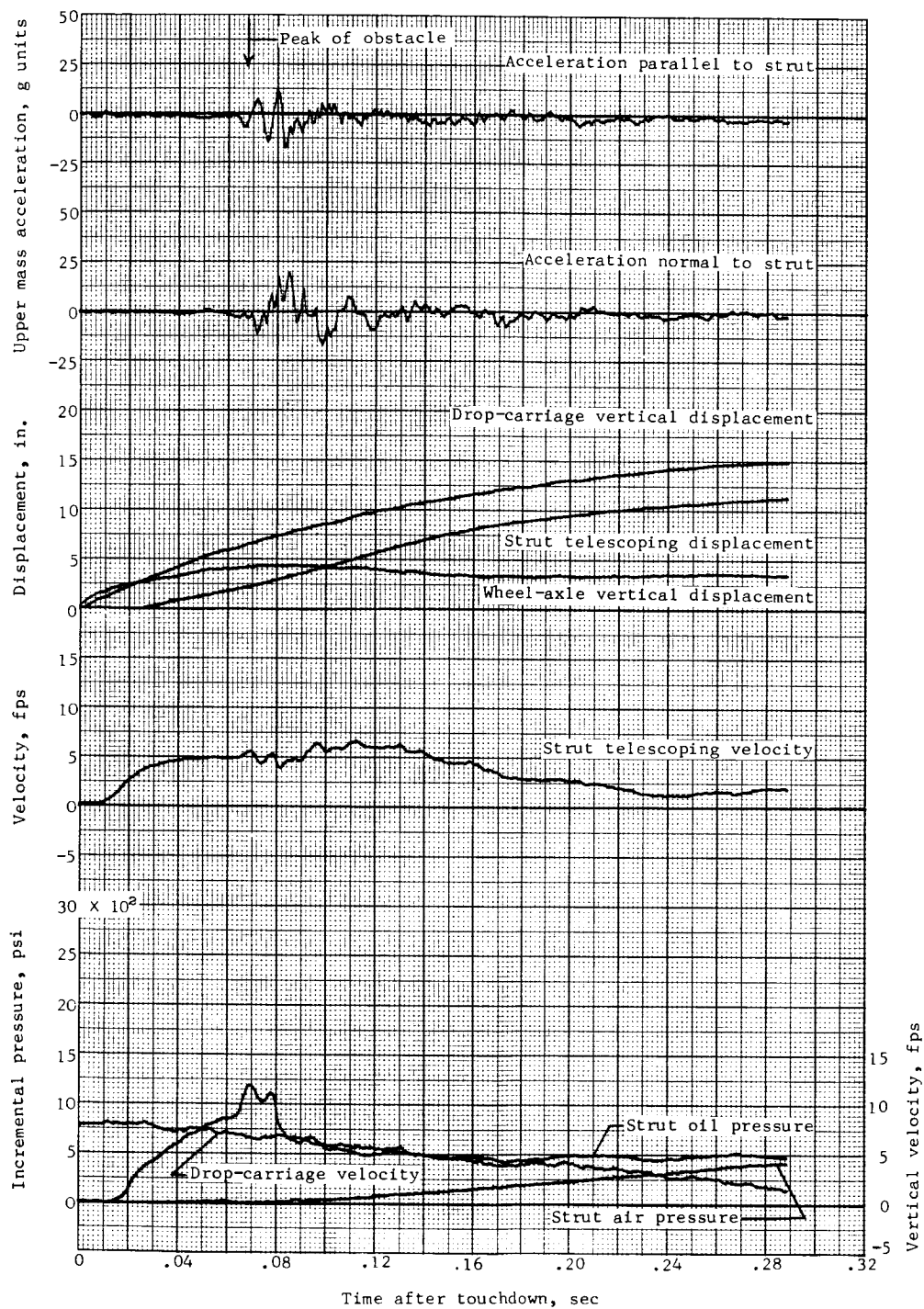




(a) Test 31.

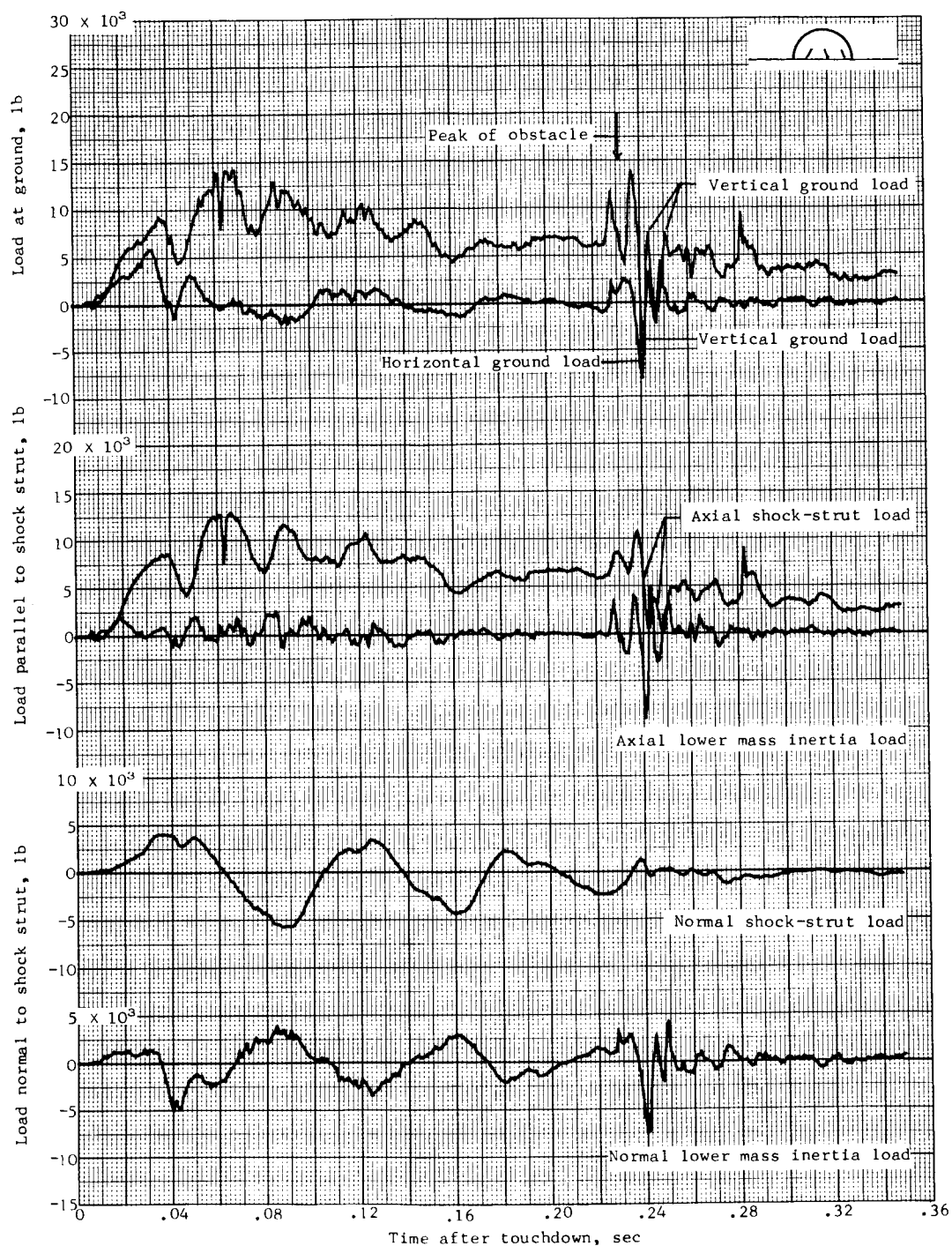
Figure 21.- Time histories of loads and other quantities obtained during landing impact over a hemisphere, 3 inches high and 6 inches long.





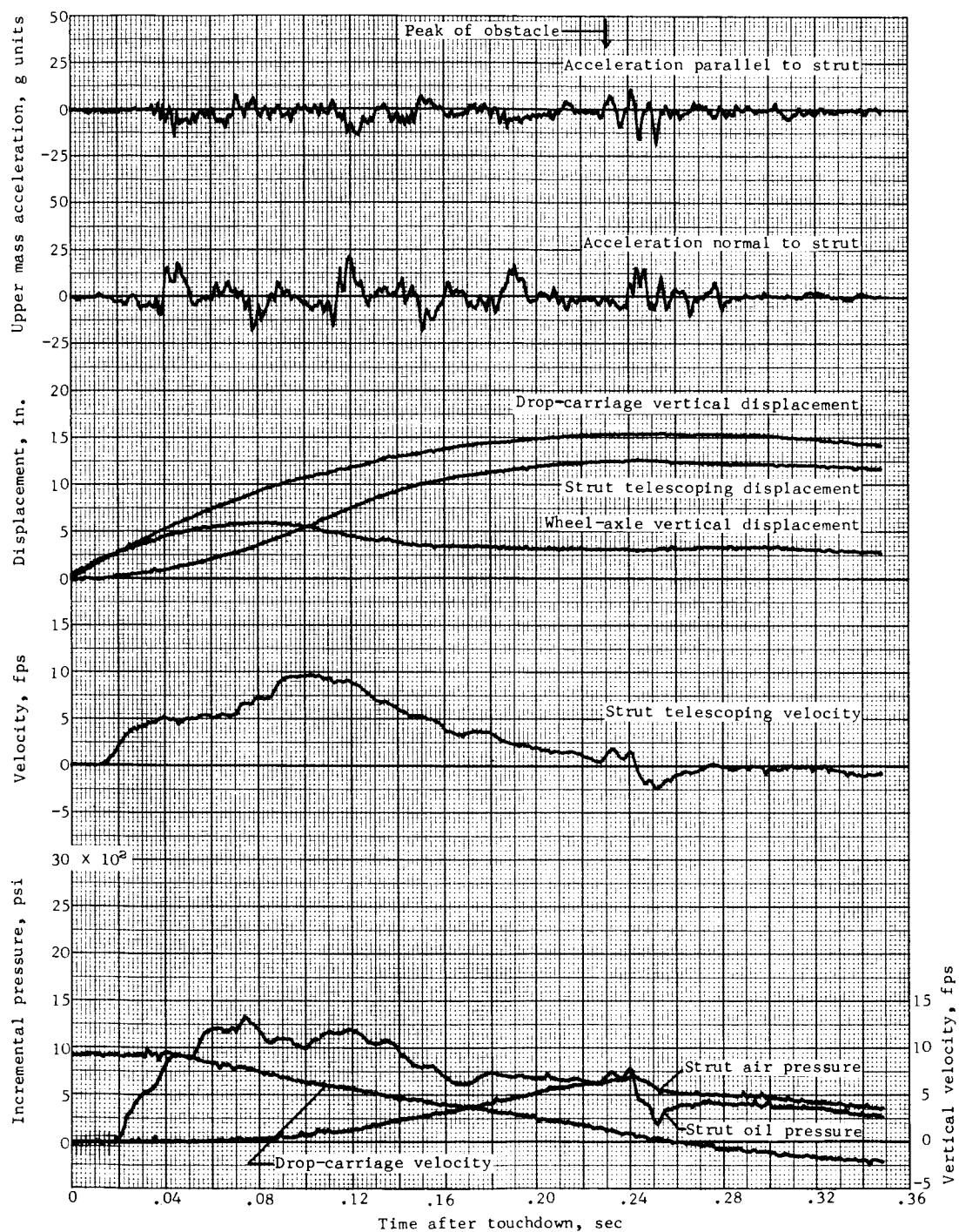
(a) Concluded.

Figure 21.- Continued.



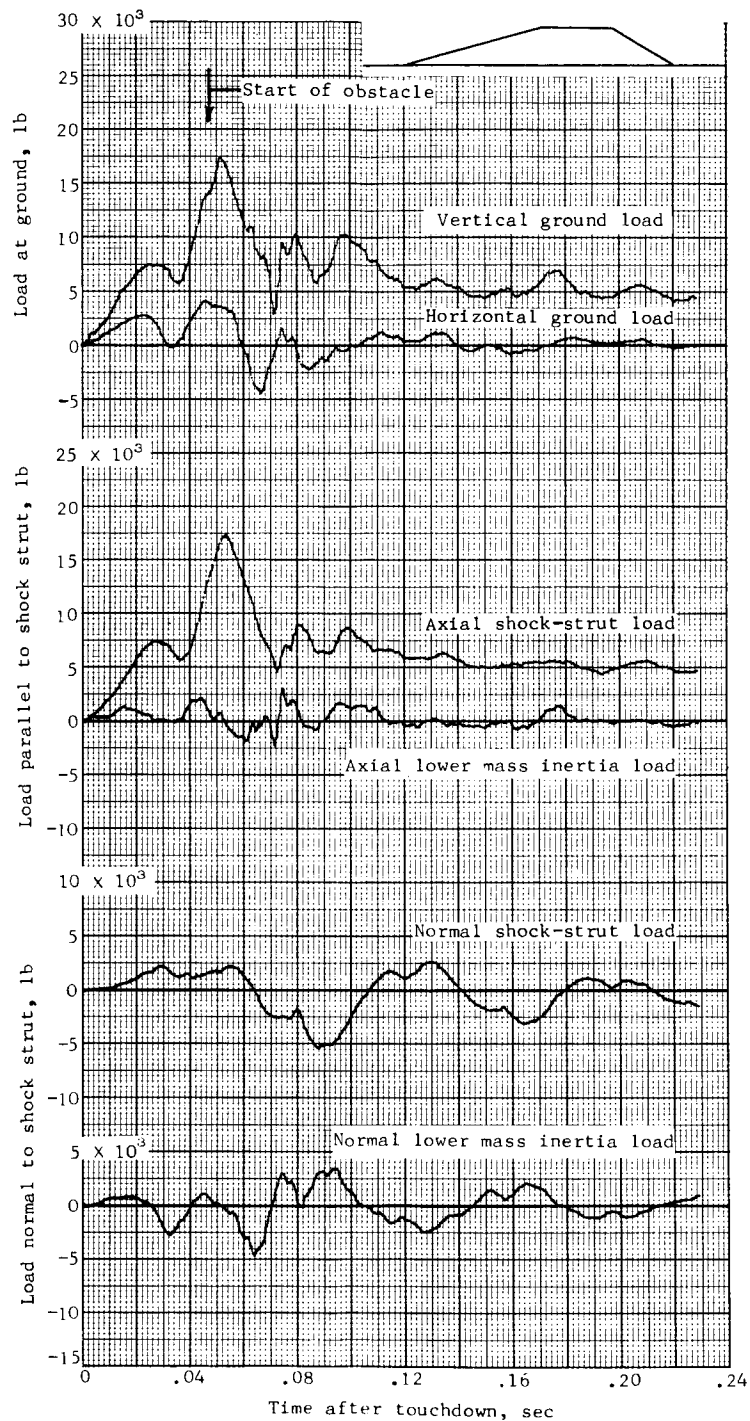
(b) Test 32.

Figure 21.- Continued.



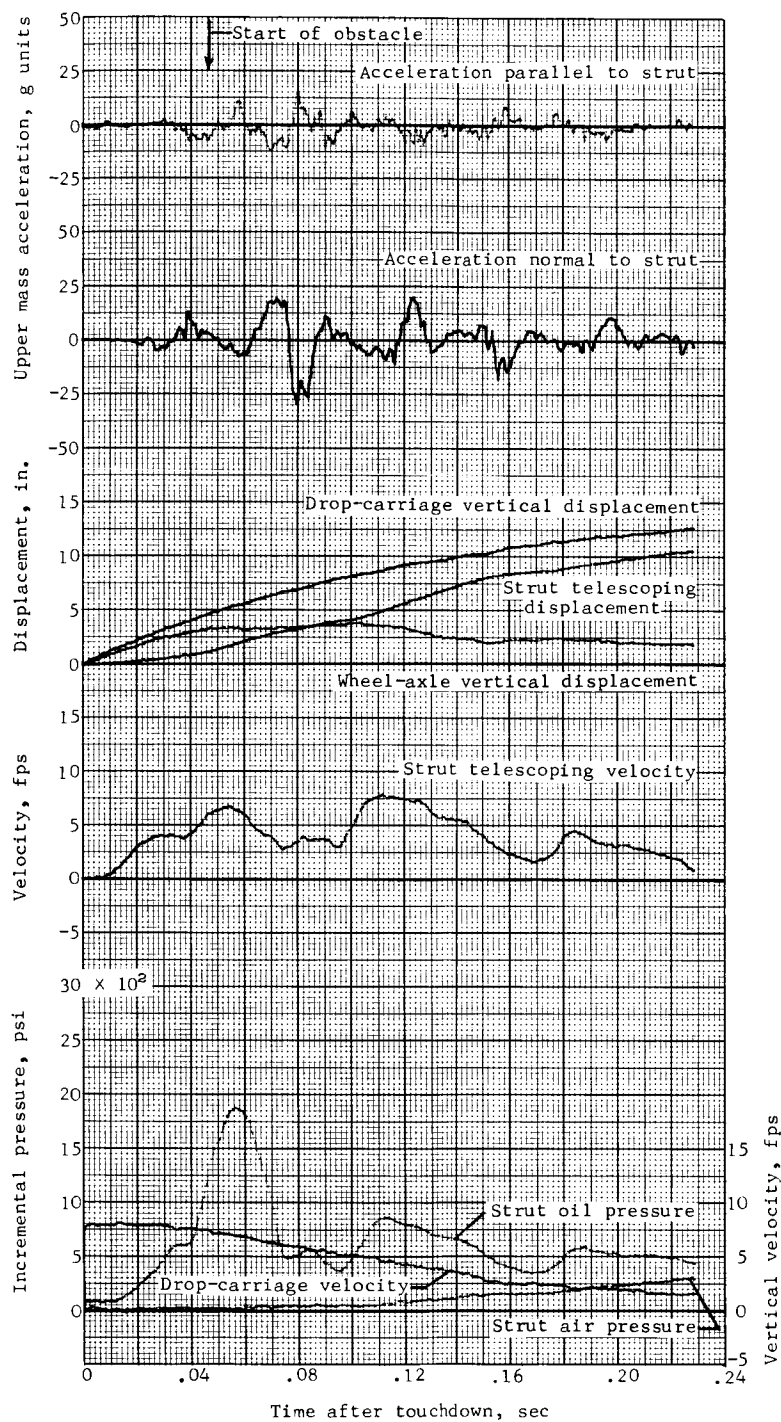
(b) Concluded.

Figure 21.- Concluded.



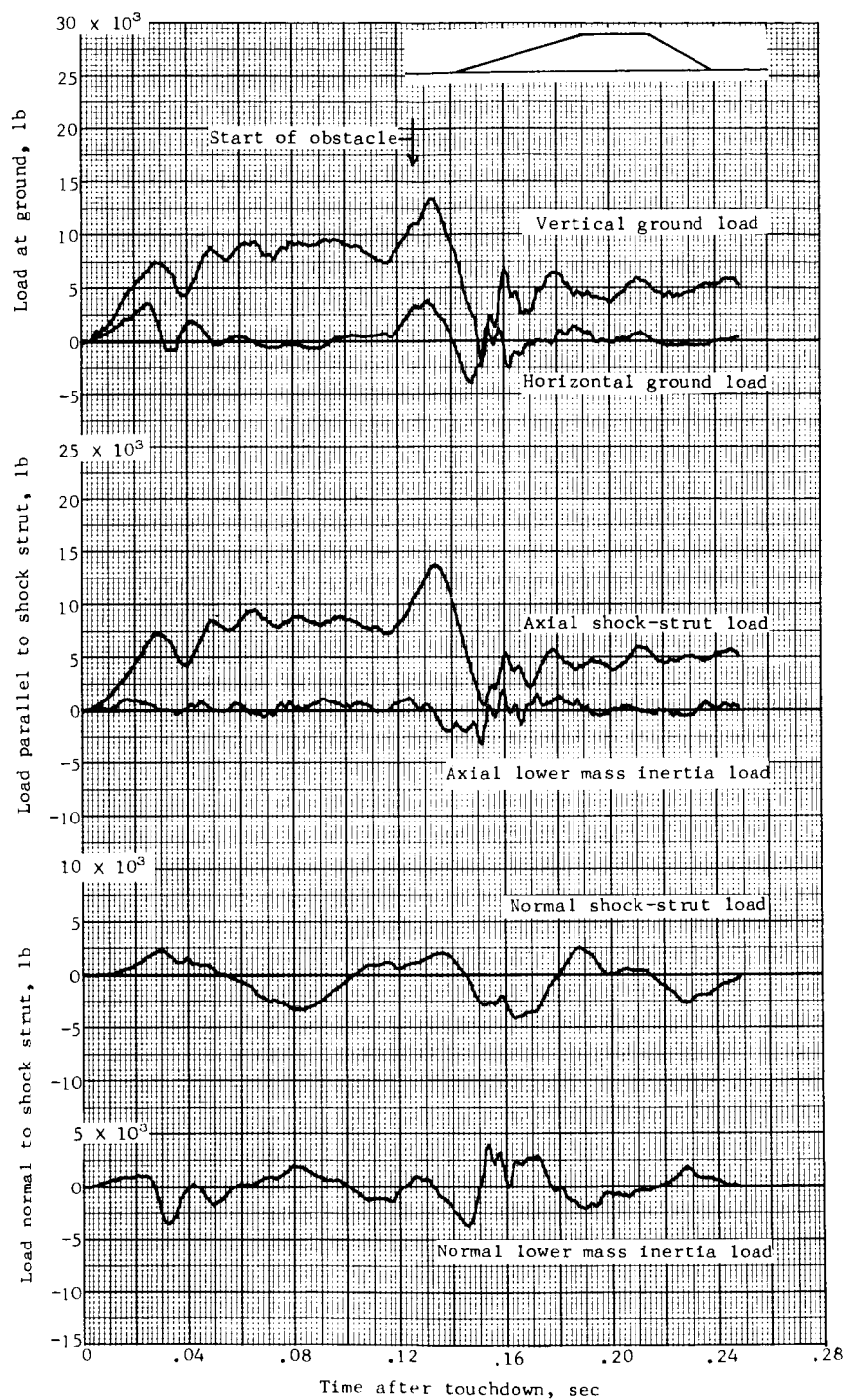
(a) Test 33.

Figure 22.- Time histories of loads and other quantities obtained during landing impact over a ramp, 3 inches high and 21 inches long.



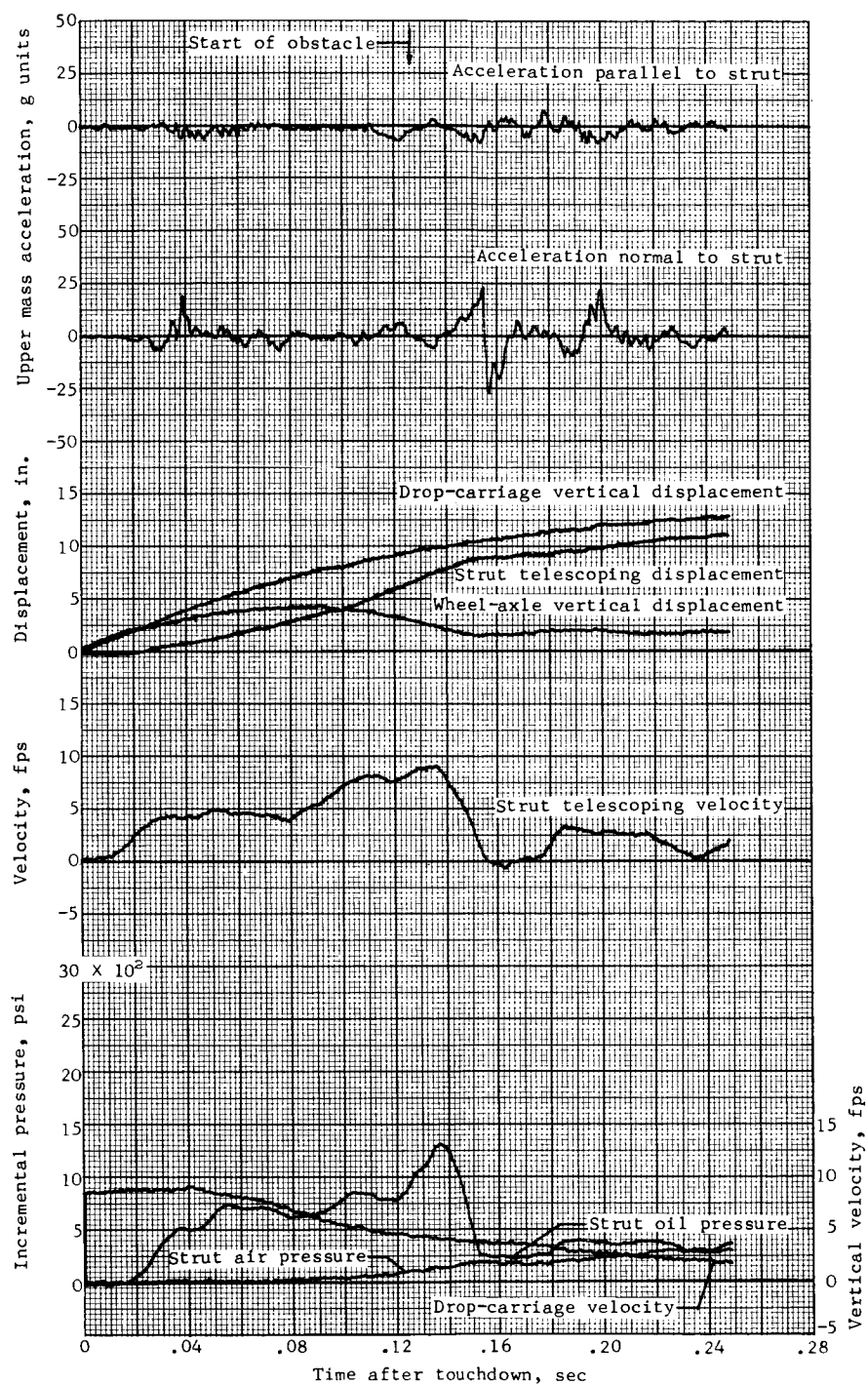
(a) Concluded.

Figure 22.- Continued.



(b) Test 34.

Figure 22.- Continued.



(b) Concluded.

Figure 22.- Concluded.

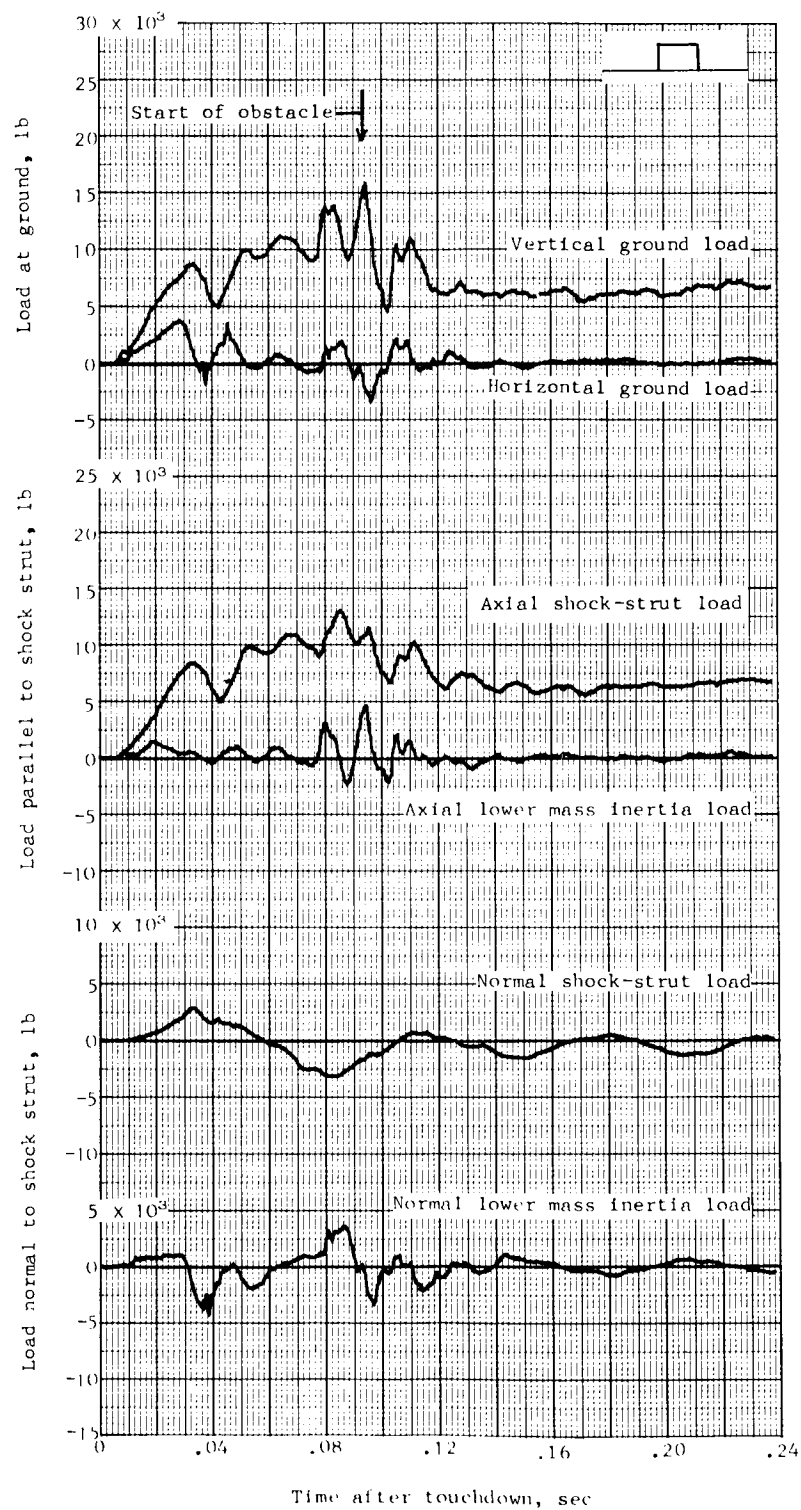


Figure 23.- Time histories of loads and other quantities obtained during landing impact over a step, 2 inches high and 3 inches long. Test 35.



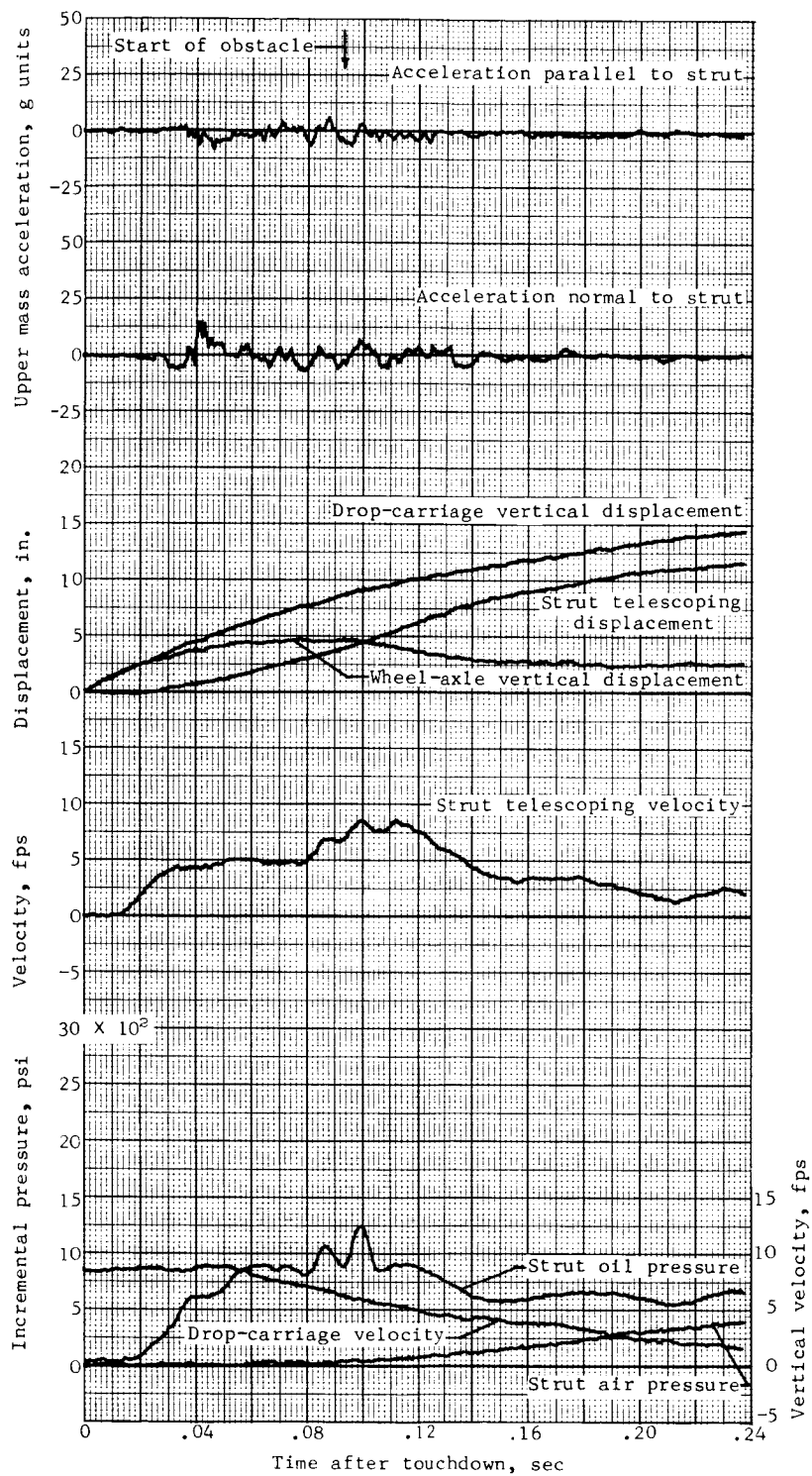
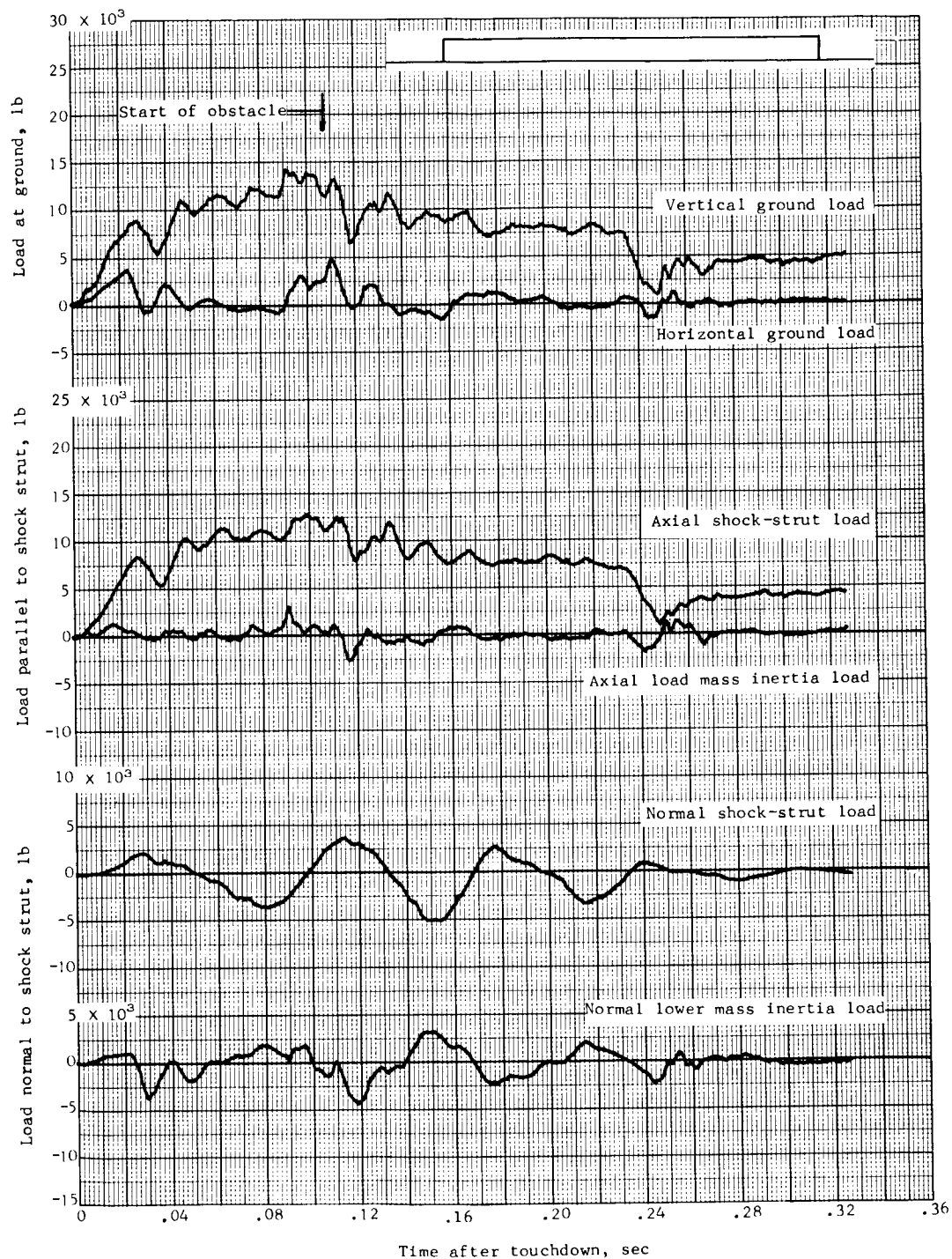
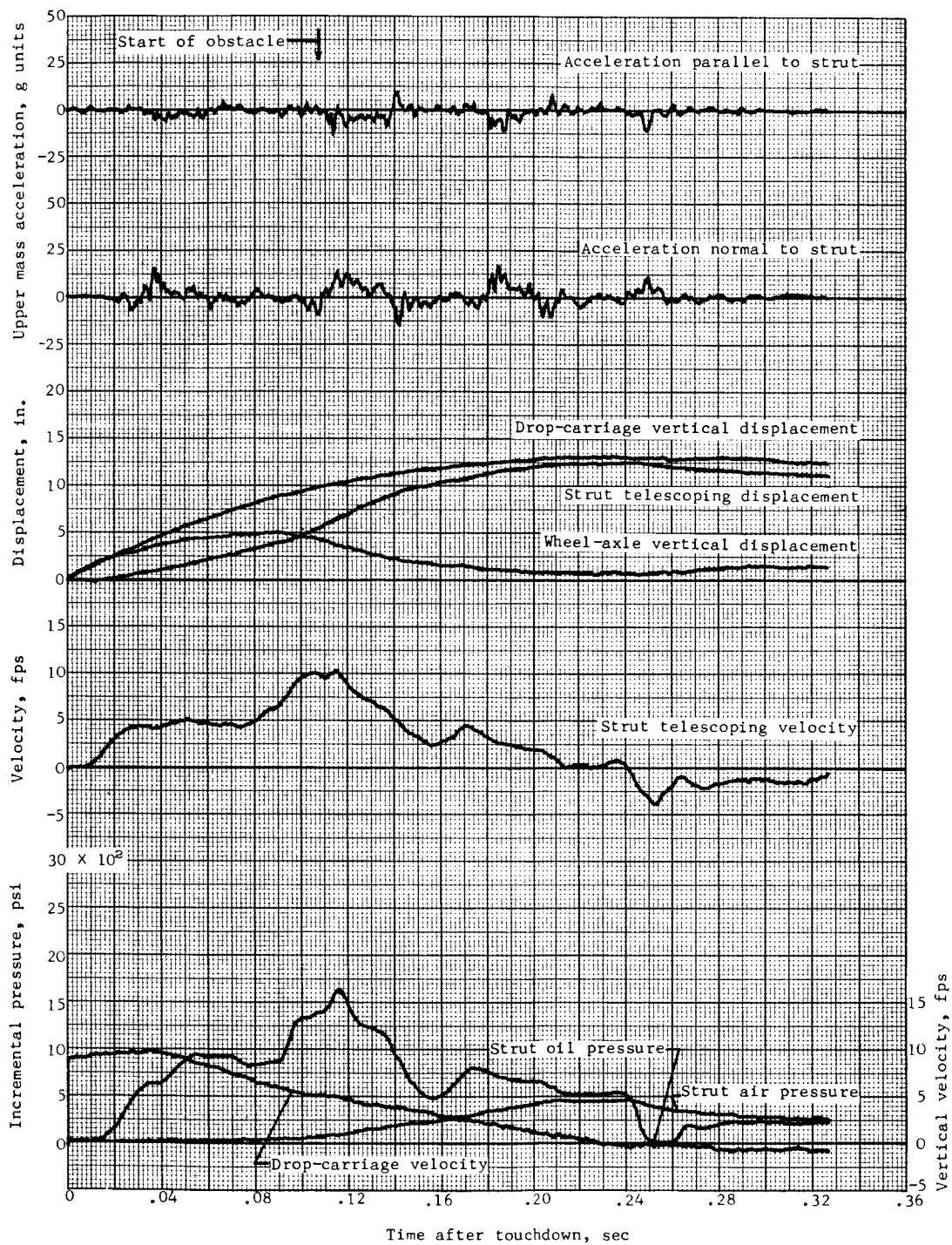


Figure 23.- Concluded.



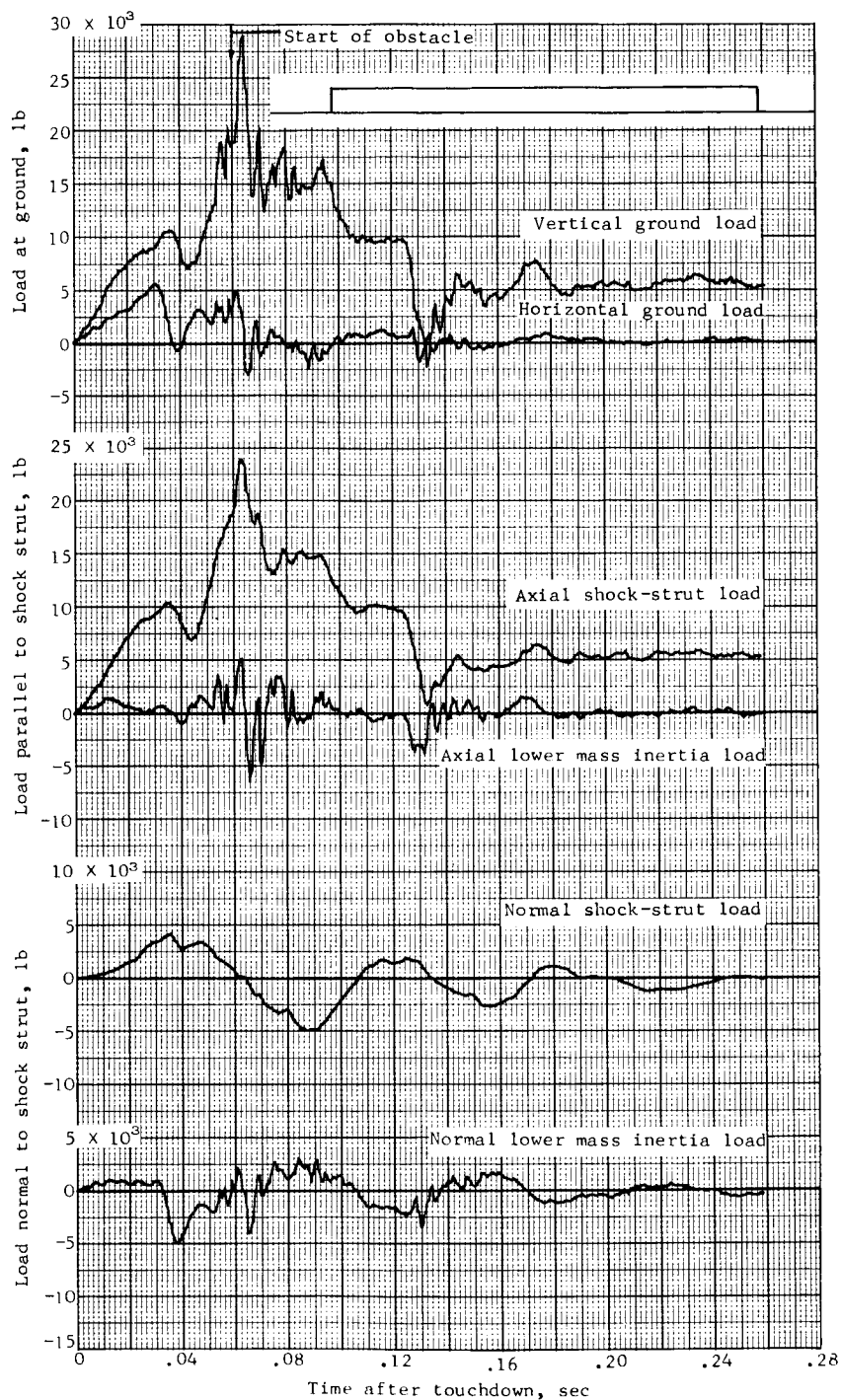
(a) Test 36.

Figure 24.- Time histories of loads and other quantities obtained during landing impact over a step, 2 inches high and 120 inches long.



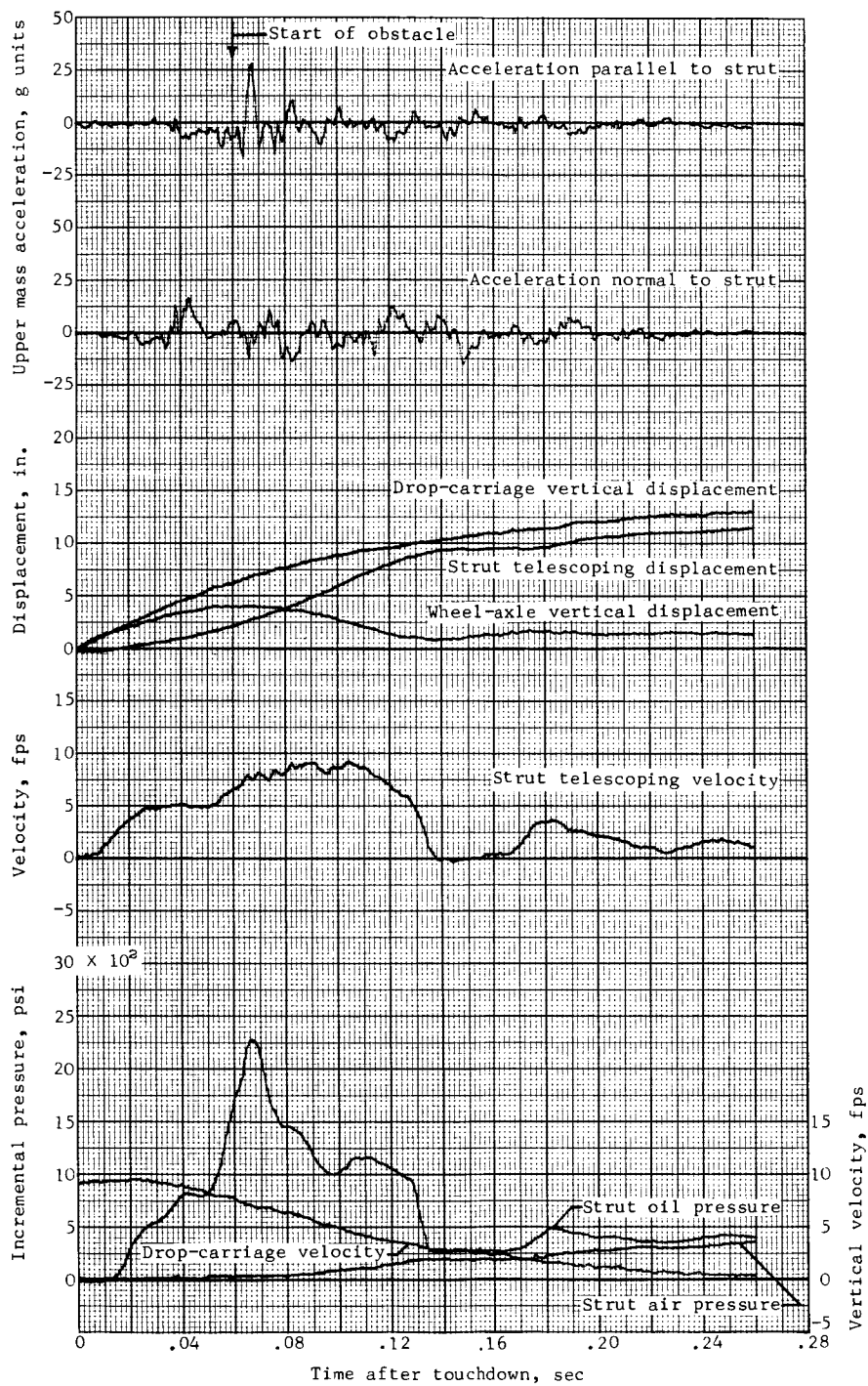
(a) Concluded.

Figure 24.- Continued.



(b) Test 37.

Figure 24.- Continued.



(b) Concluded.

Figure 24.- Concluded.

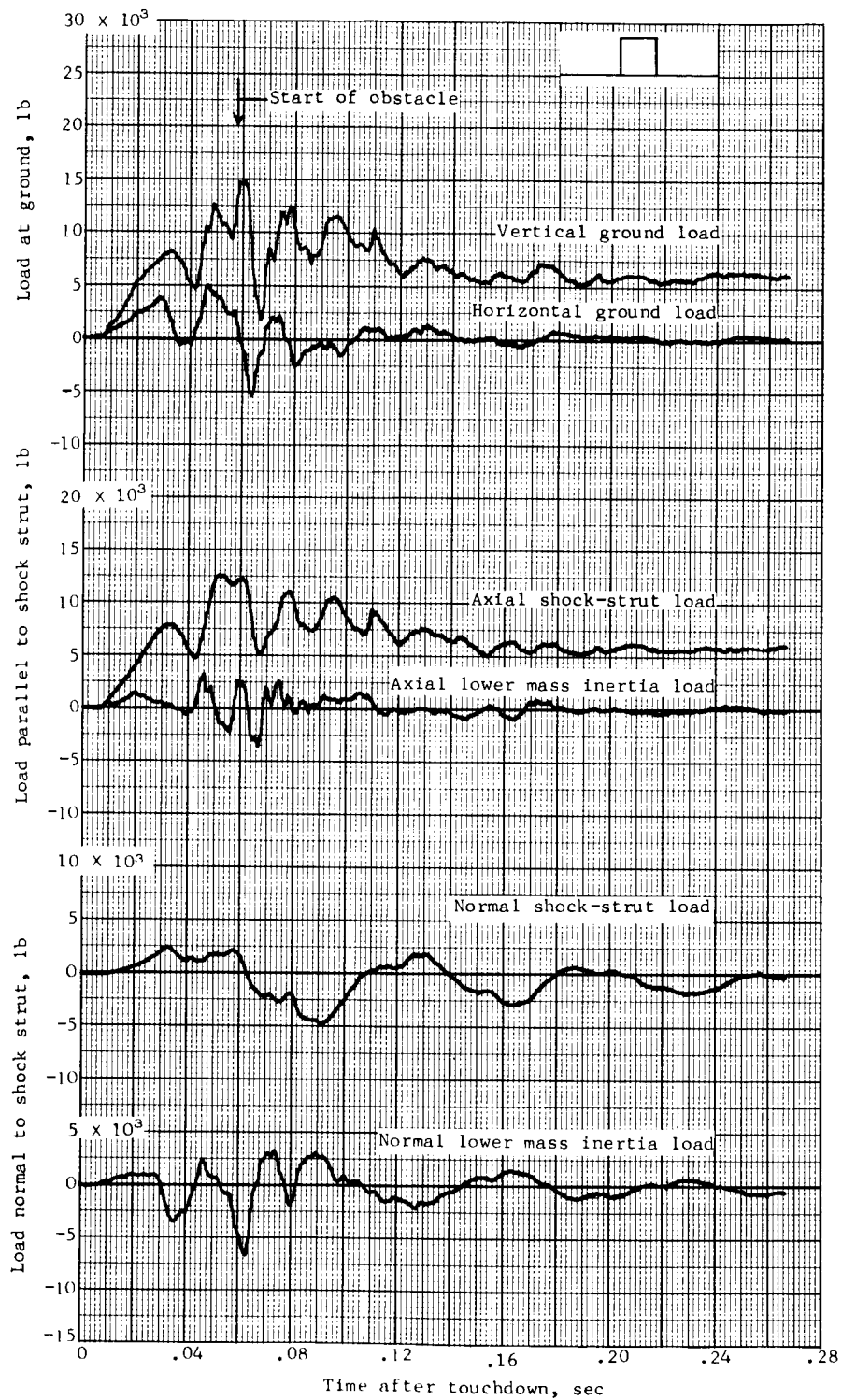


Figure 25.- Time histories of loads and other quantities obtained during landing impact over a step, 3 inches high and 3 inches long. Test 38.

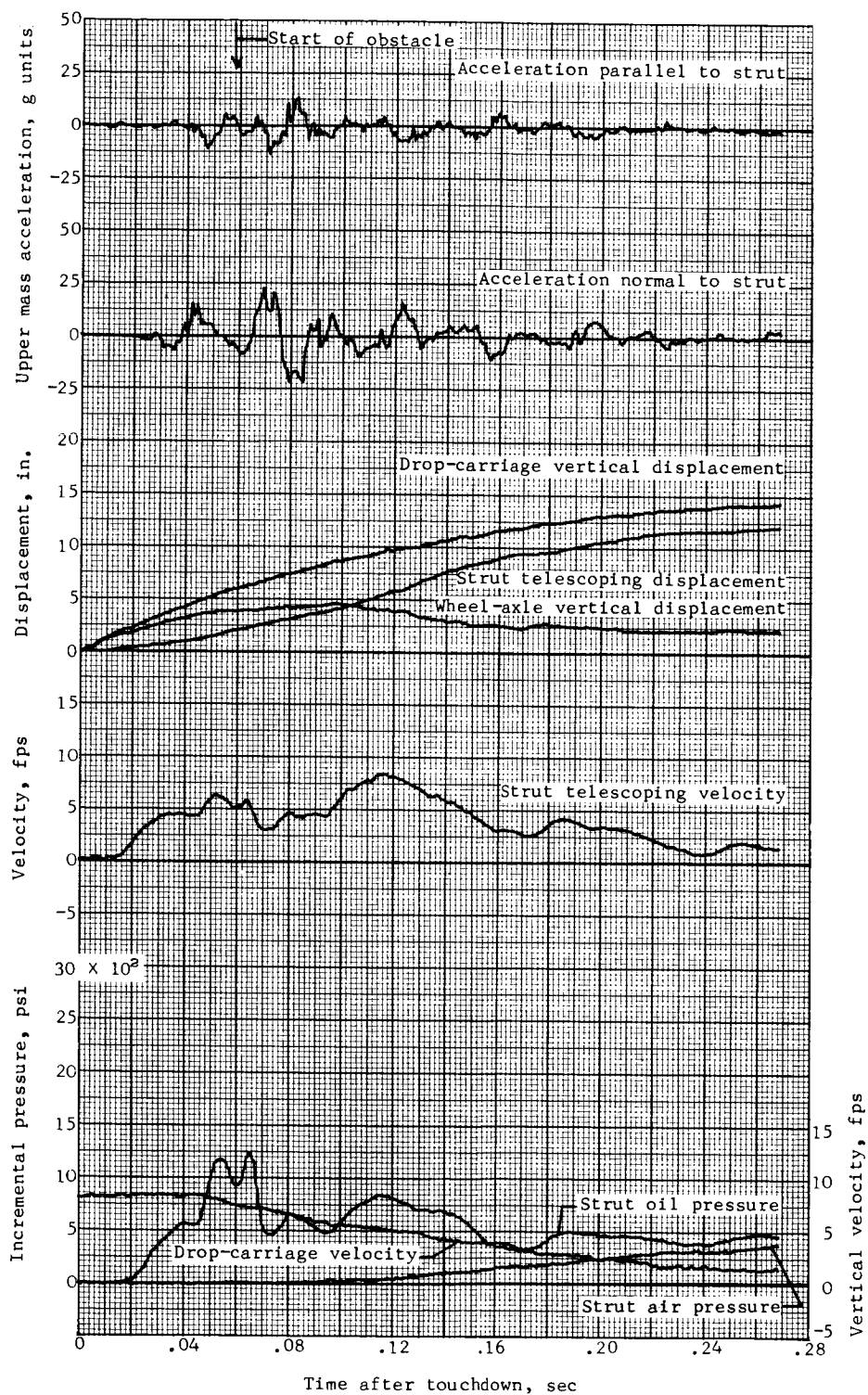
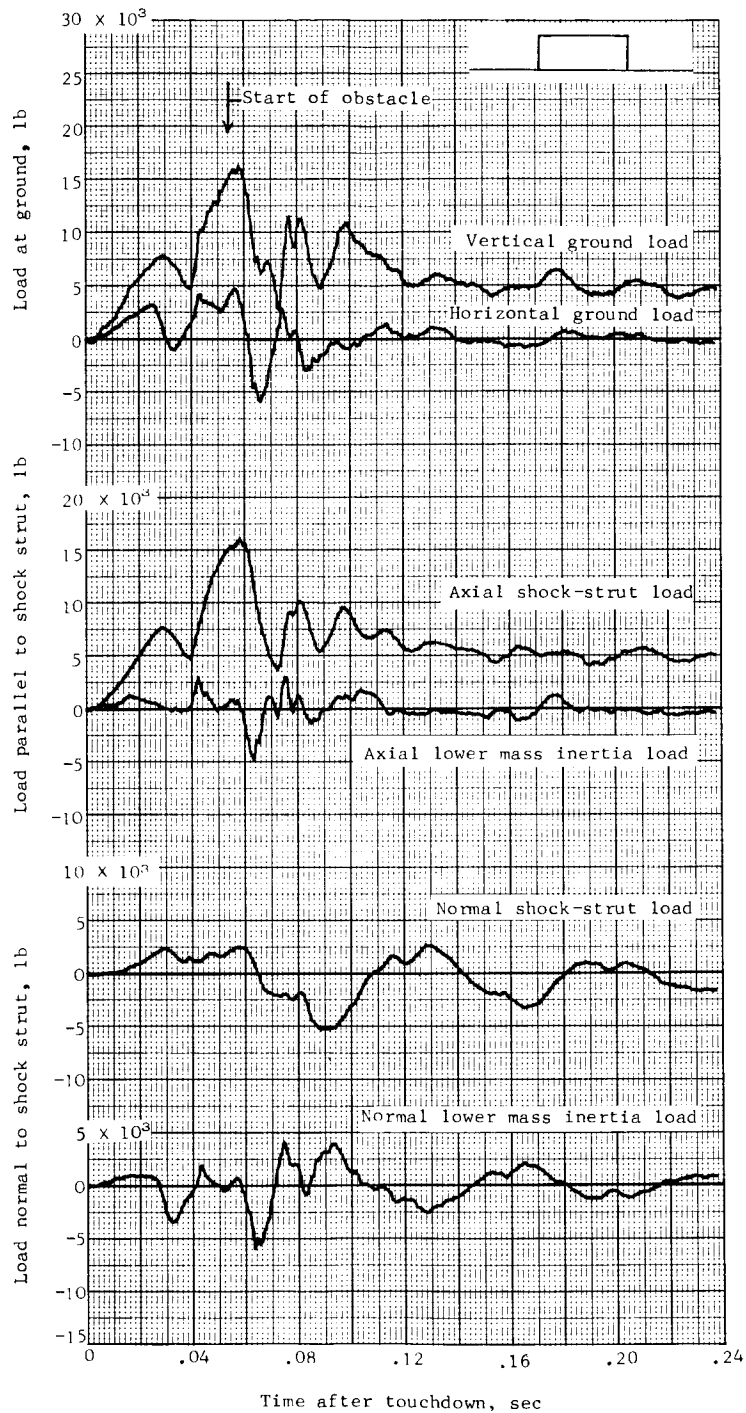


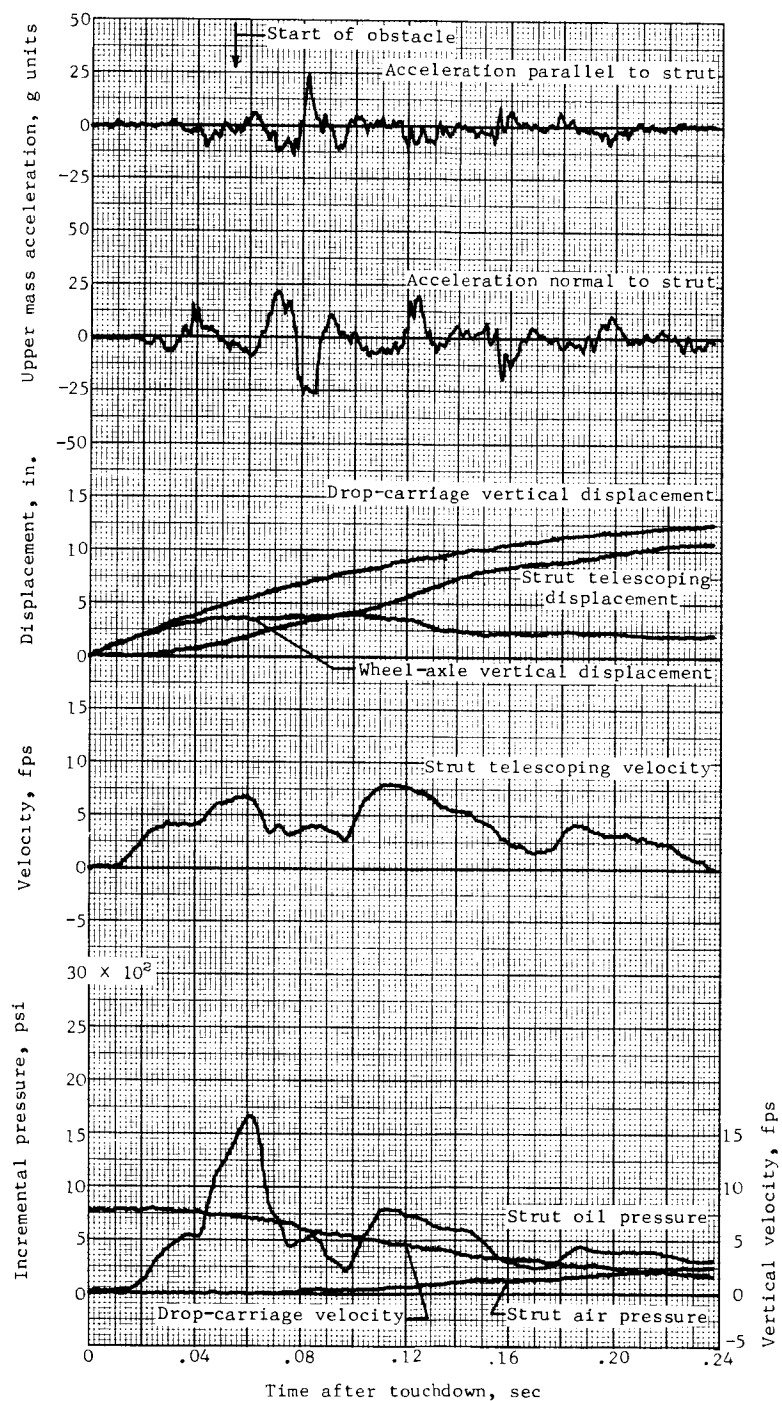
Figure 25.- Concluded.



(a) Test 39.

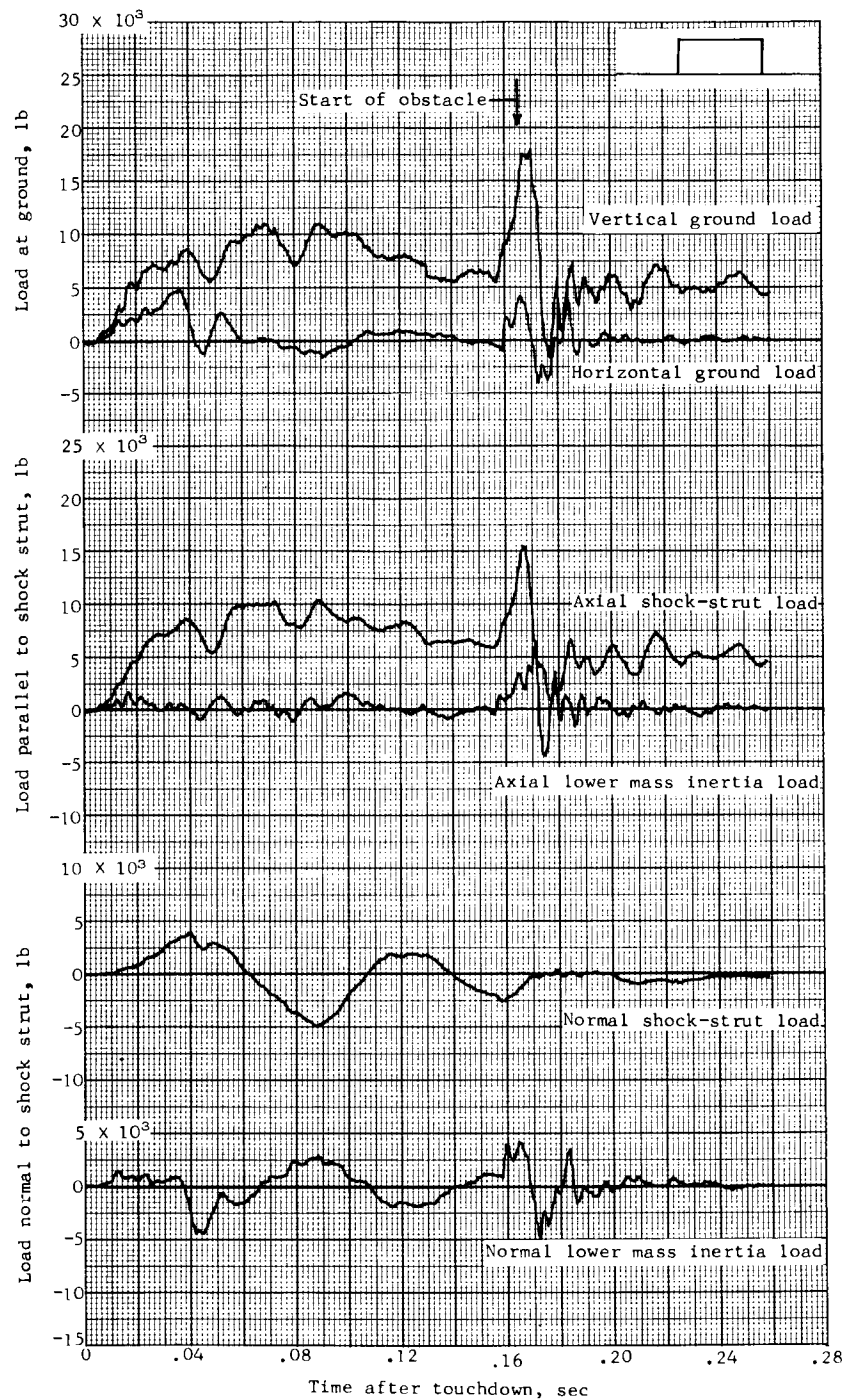
Figure 26.- Time histories of loads and other quantities obtained during landing impact over a step, 3 inches high and  $10\frac{1}{2}$  inches long.





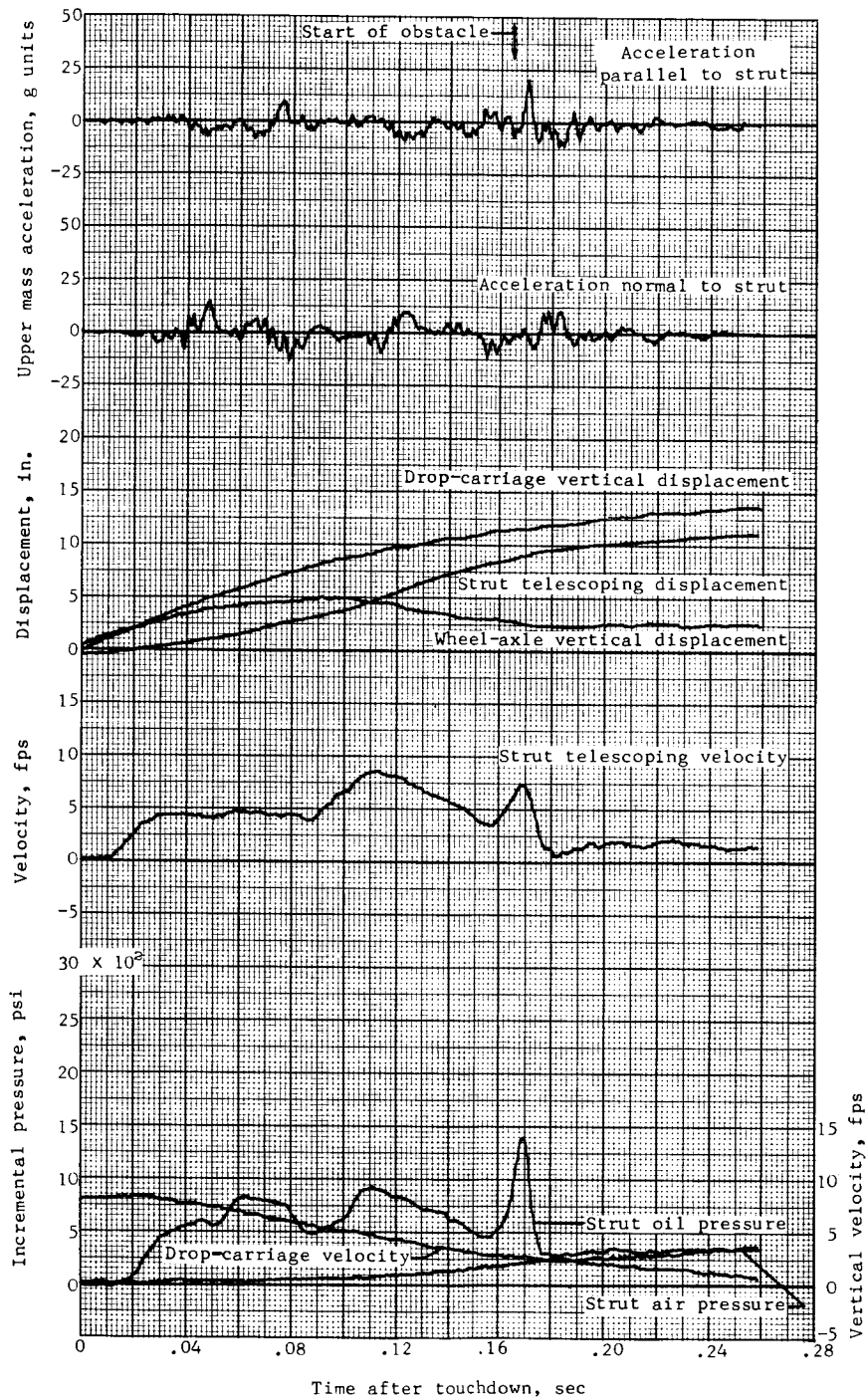
(a) Concluded.

Figure 26.- Continued.



(b) Test 40.

Figure 26.- Continued.



(b) Concluded.

Figure 26.- Concluded.

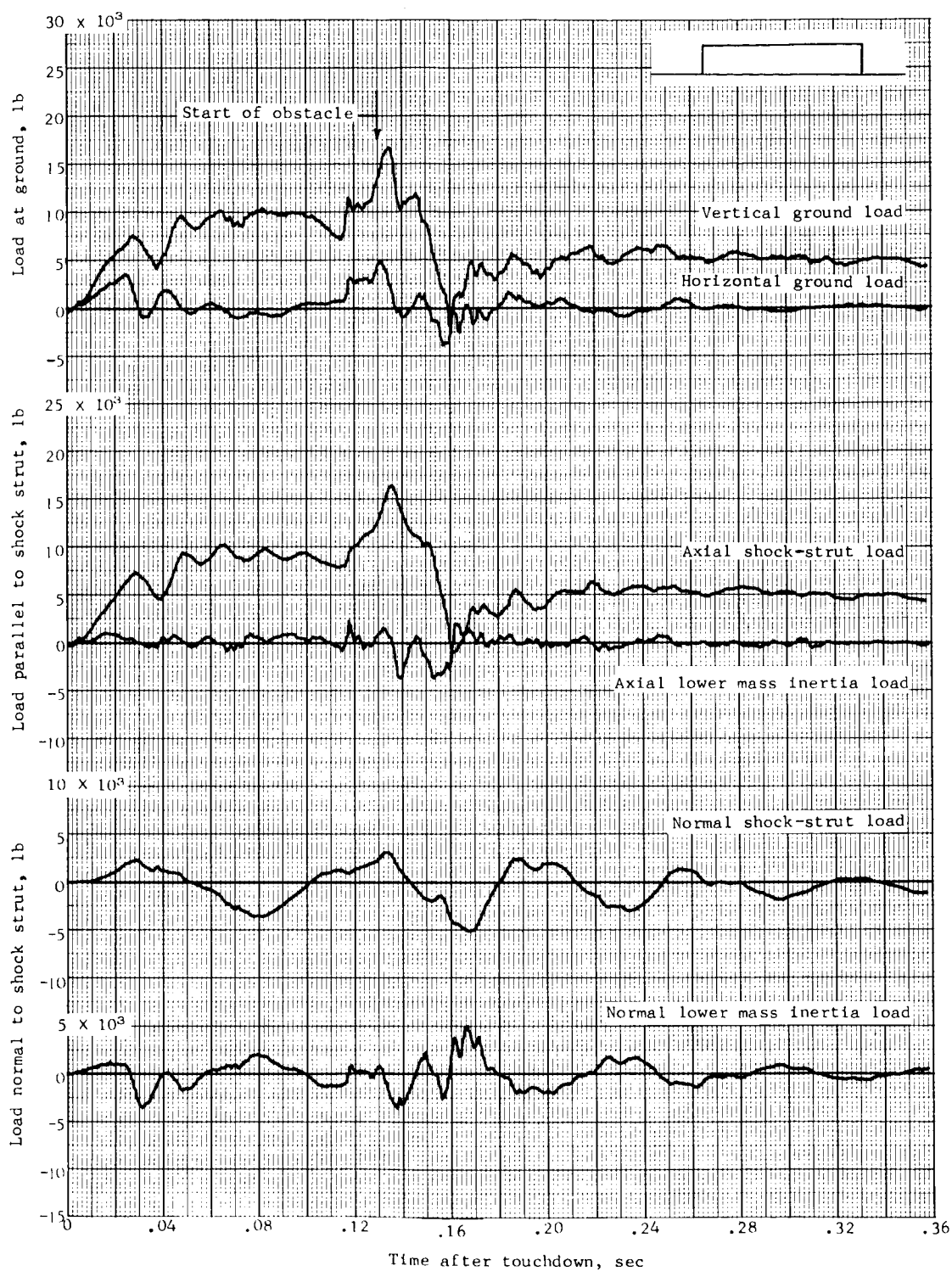


Figure 27.- Time histories of loads and other quantities obtained during landing impact over a step, 3 inches high and 24 inches long. Test 41.

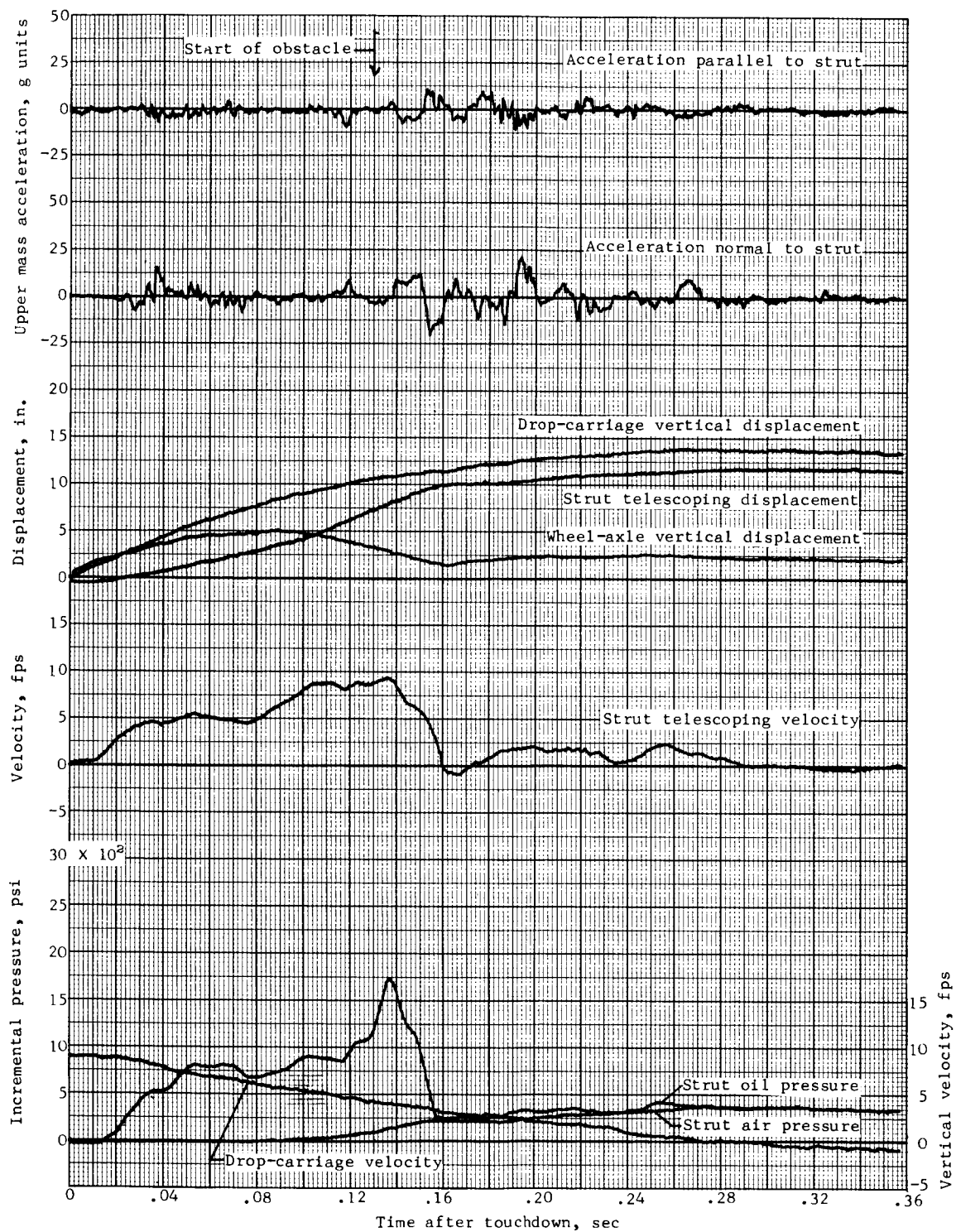


Figure 27.- Concluded.

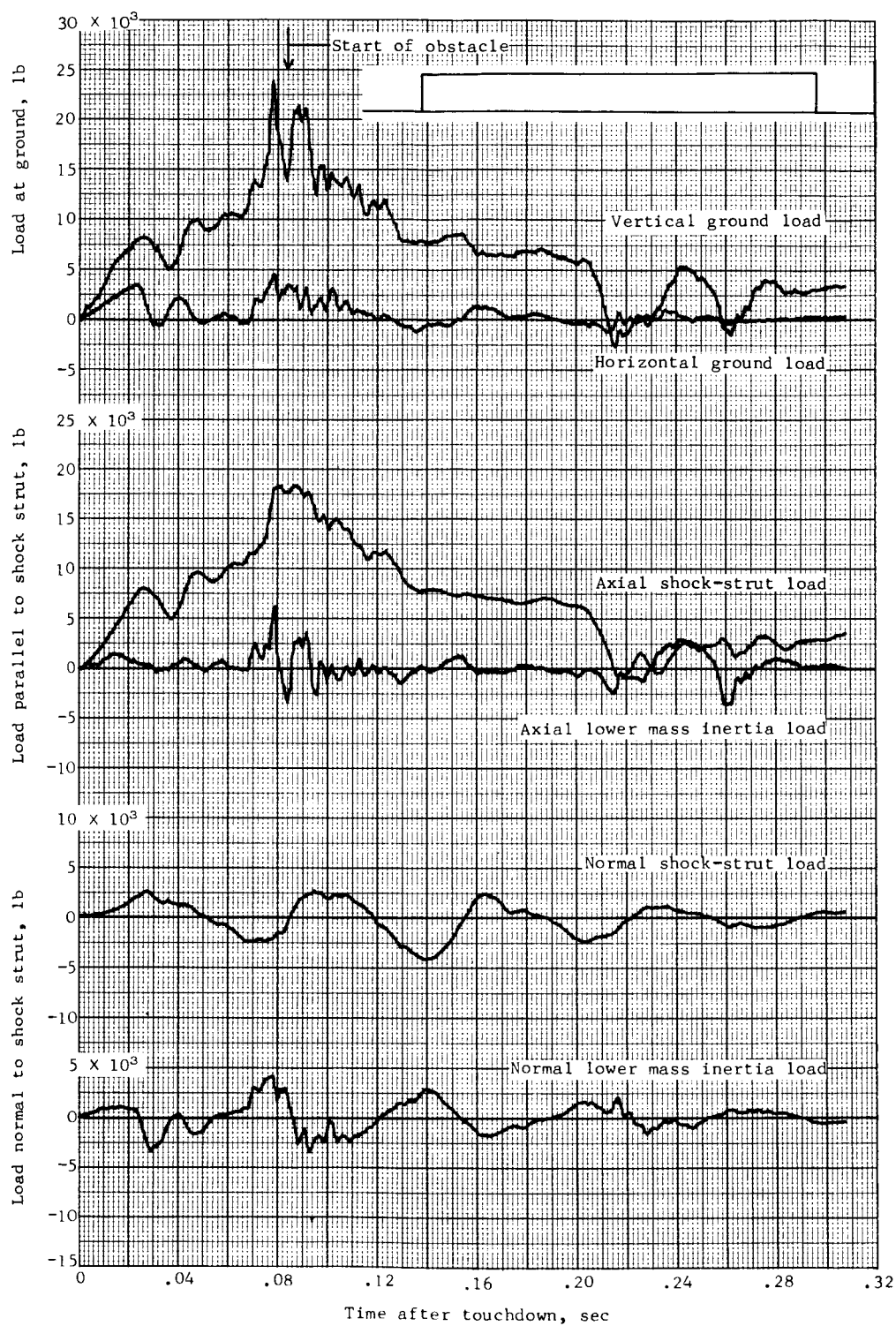


Figure 28.- Time histories of loads and other quantities obtained during landing impact over a step, 3 inches high and 120 inches long. Test 42.

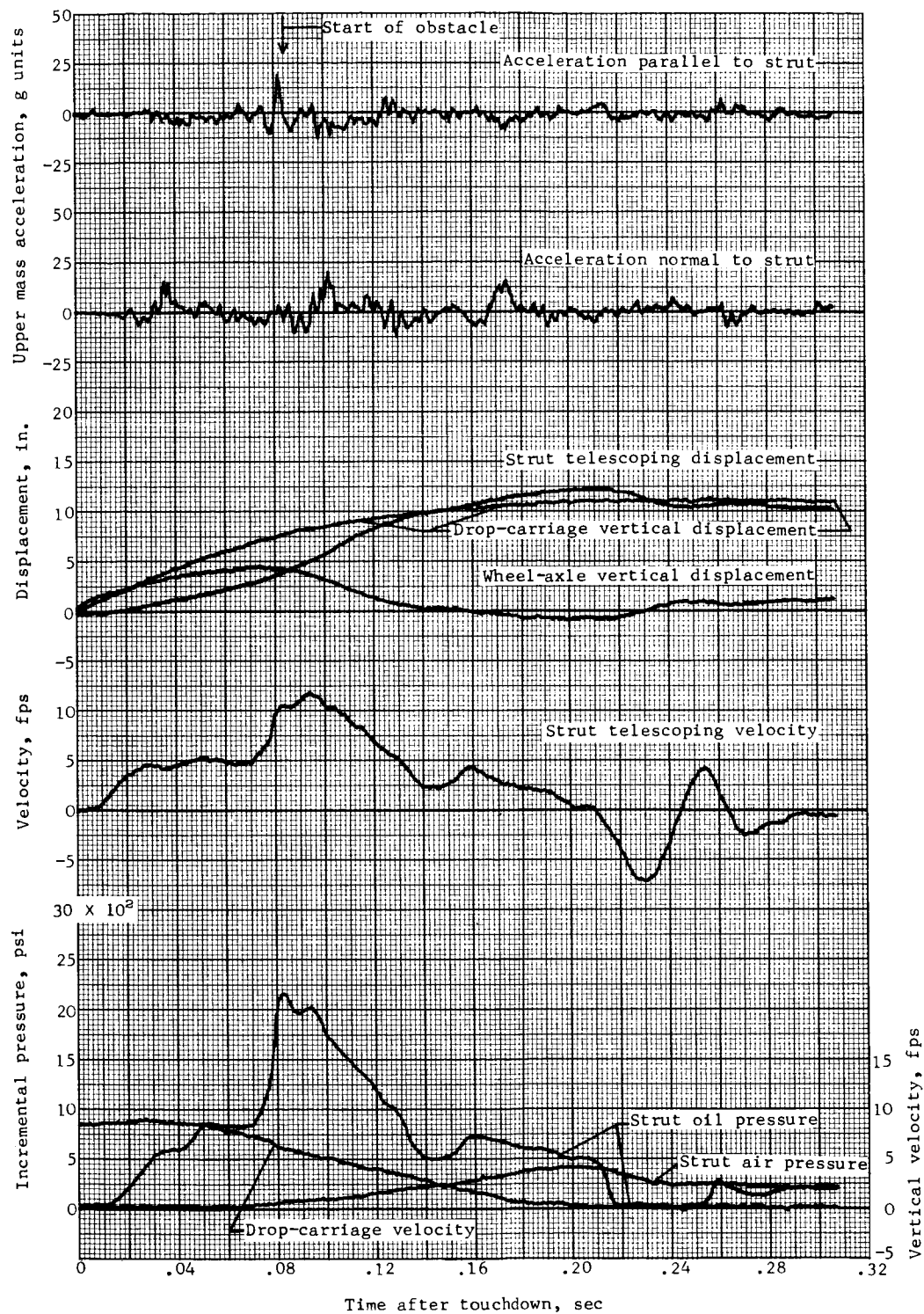


Figure 28.- Concluded.



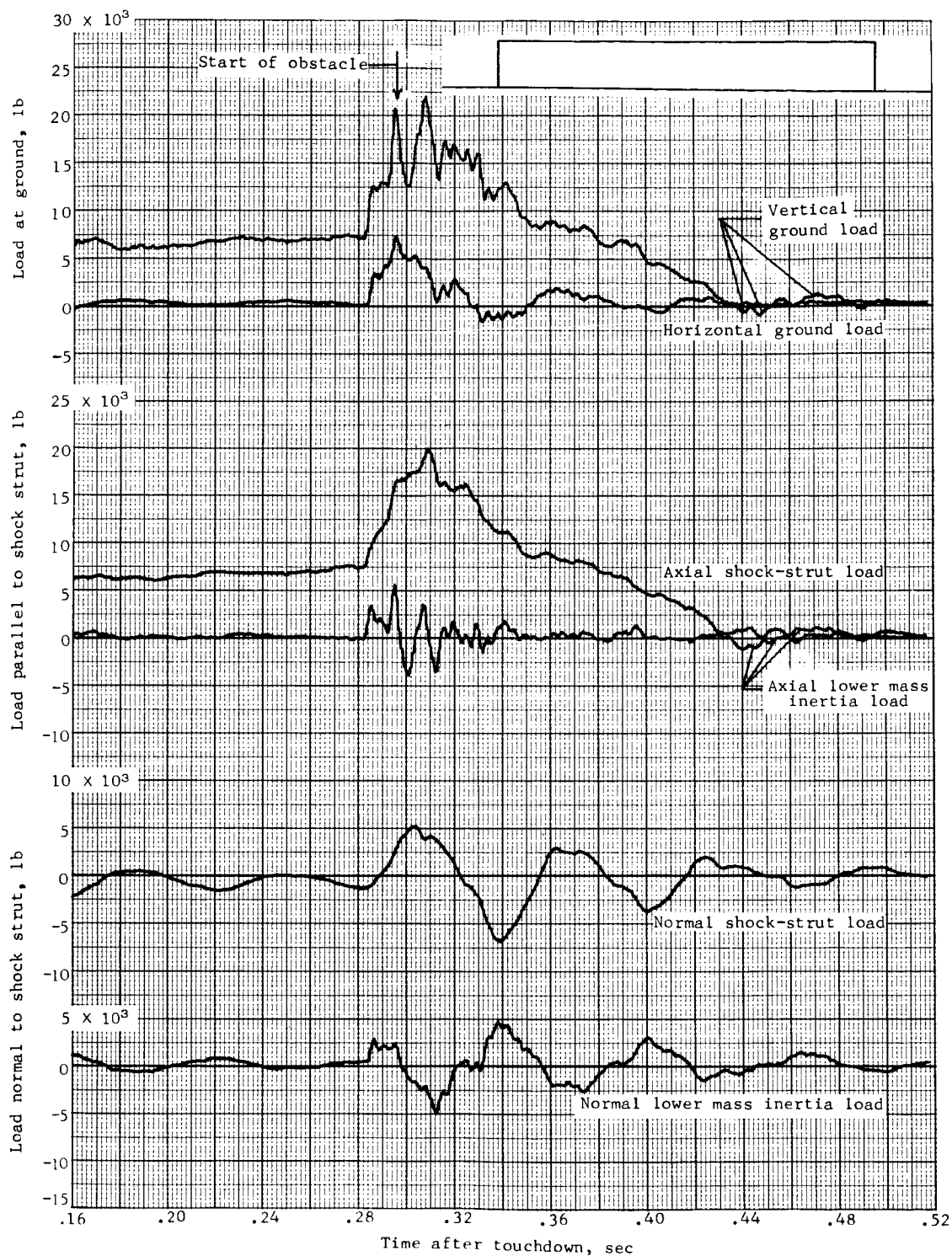


Figure 29.- Time histories of loads and other quantities obtained during landing impact over a step, 4 inches high and 120 inches long. Test 43.



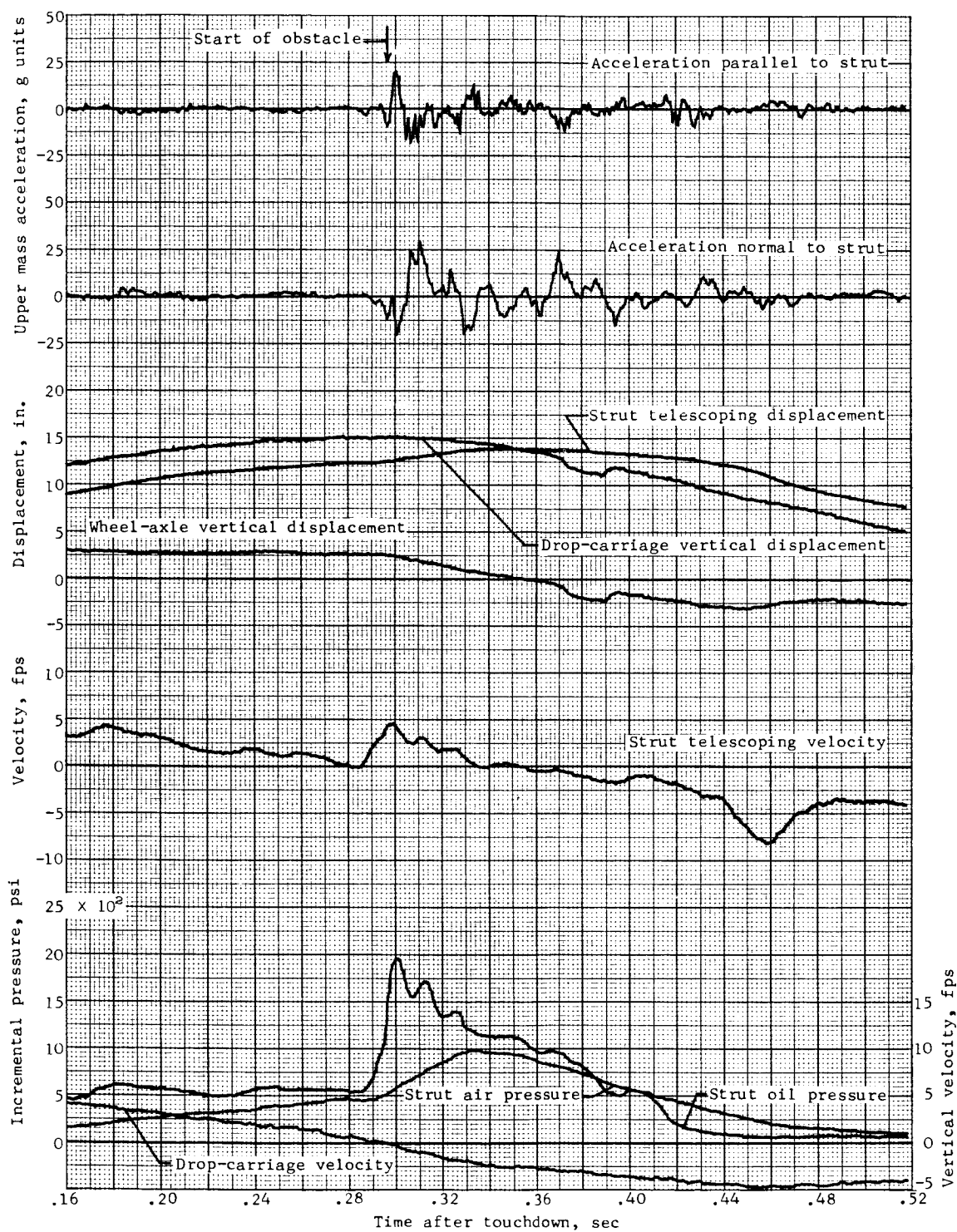


Figure 29.- Concluded.

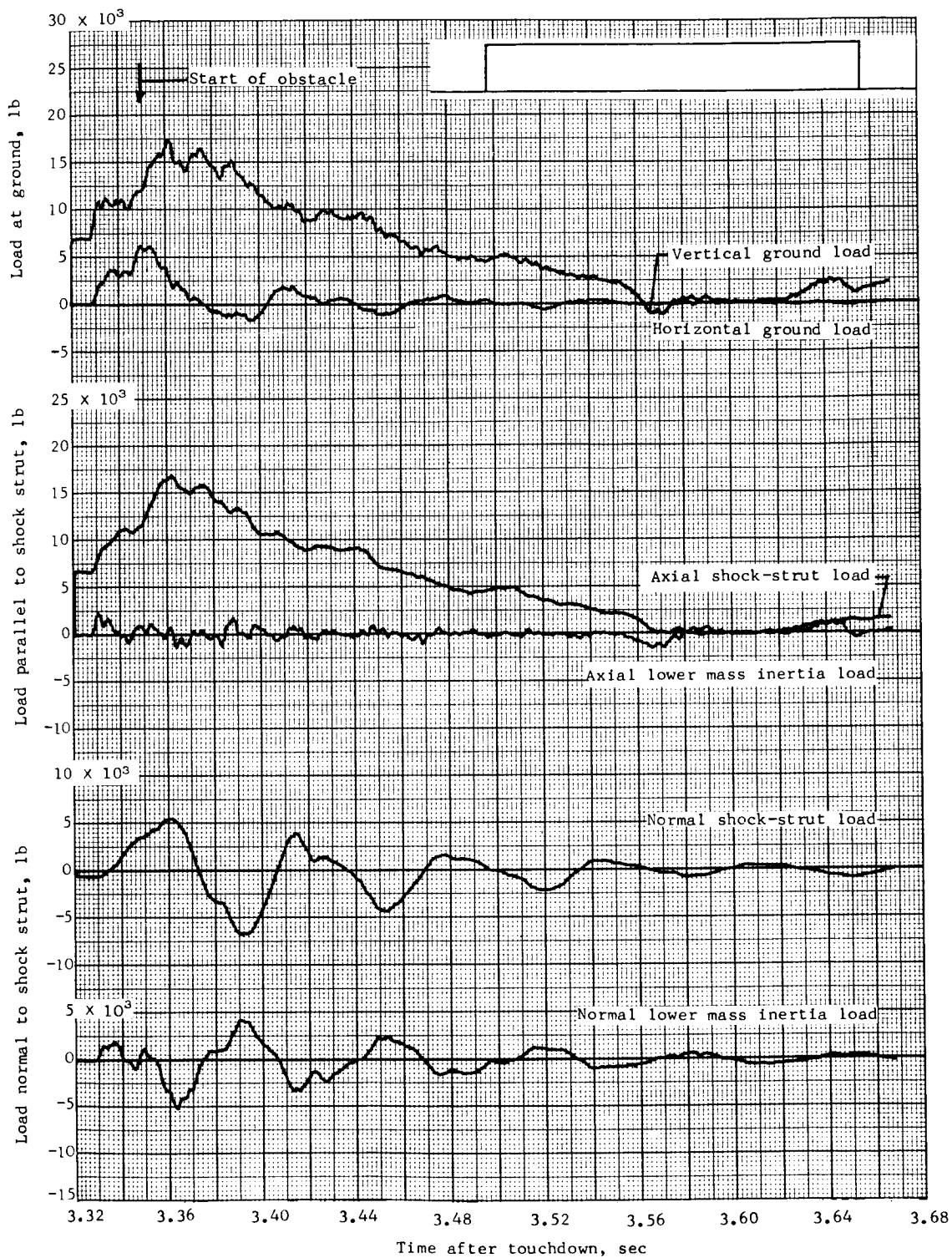


Figure 30.- Time histories of loads and other quantities obtained during taxiing over a step, 4 inches high and 120 inches long. Test 44.

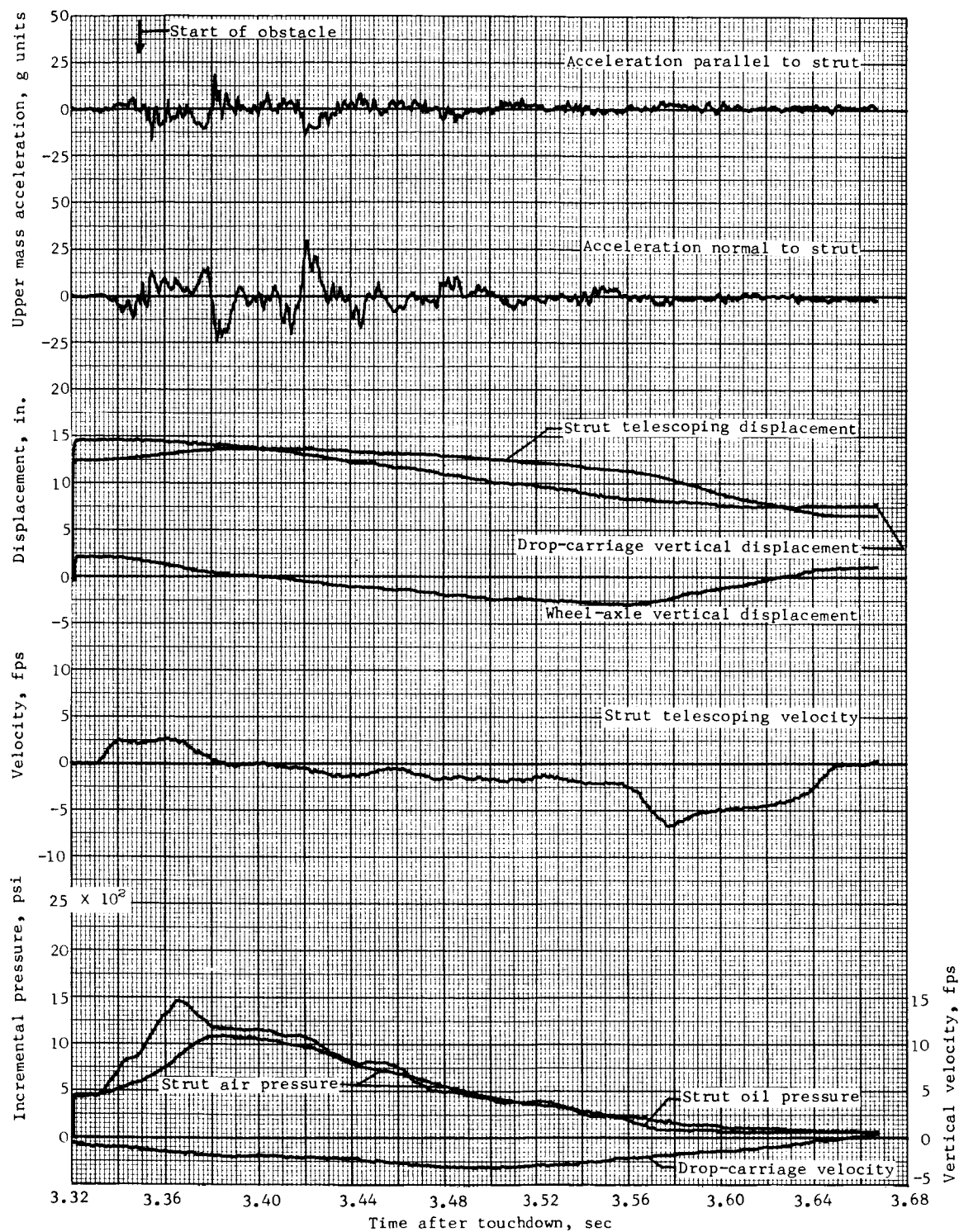


Figure 30.- Concluded.

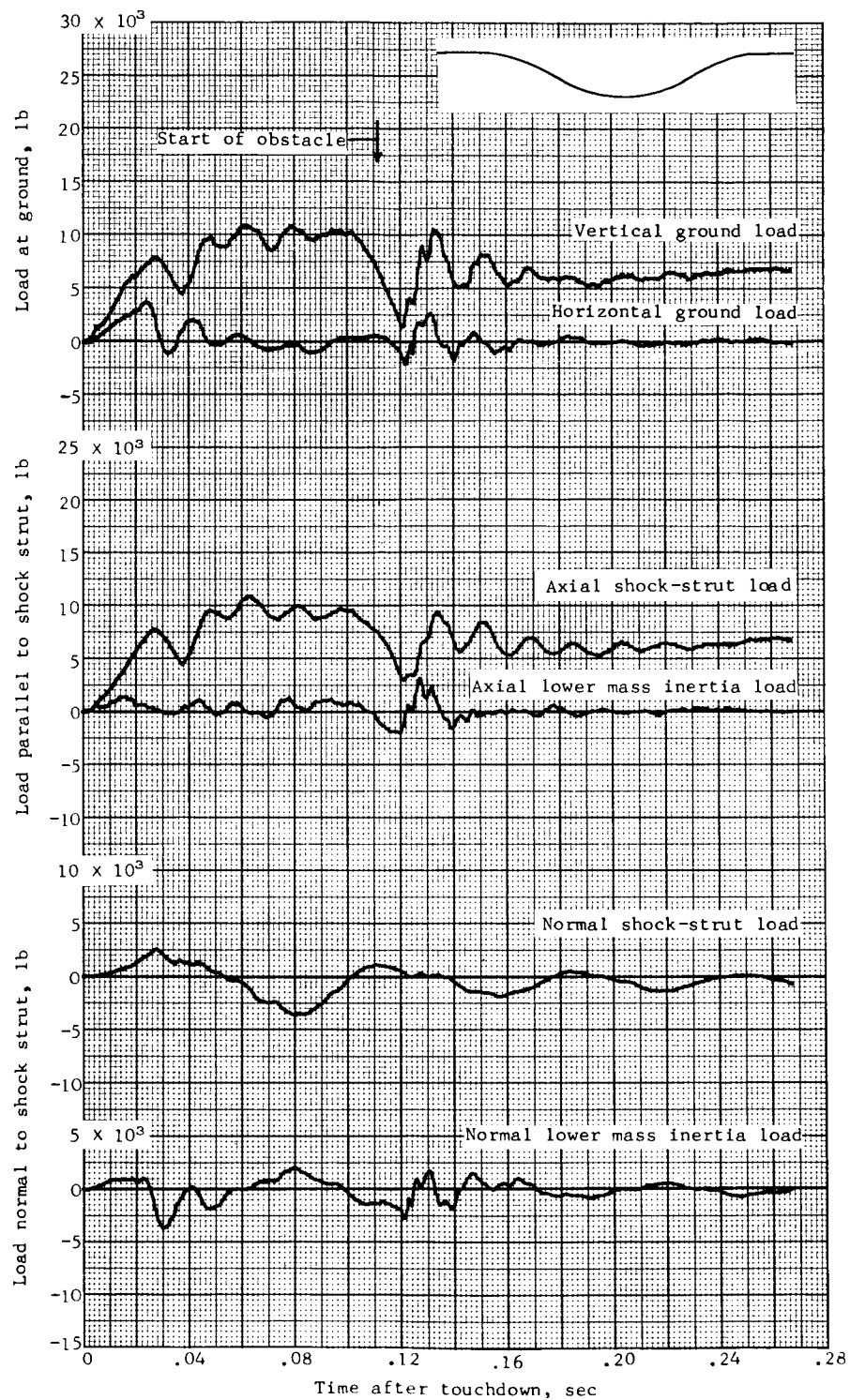


Figure 31.- Time histories of loads and other quantities obtained during landing impact over a 1 - cos hole, 3 inches deep and 15 inches long. Test 45.

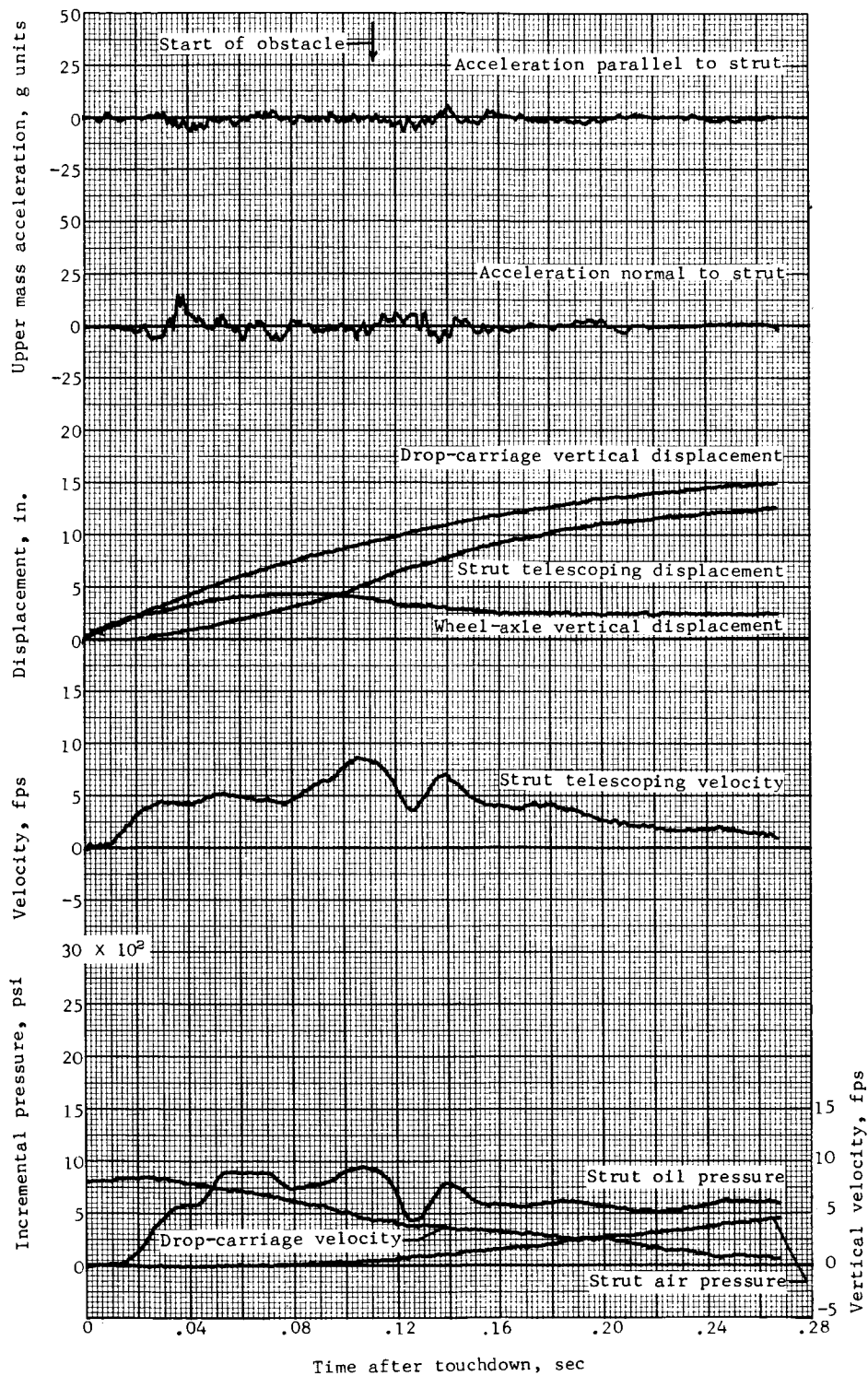
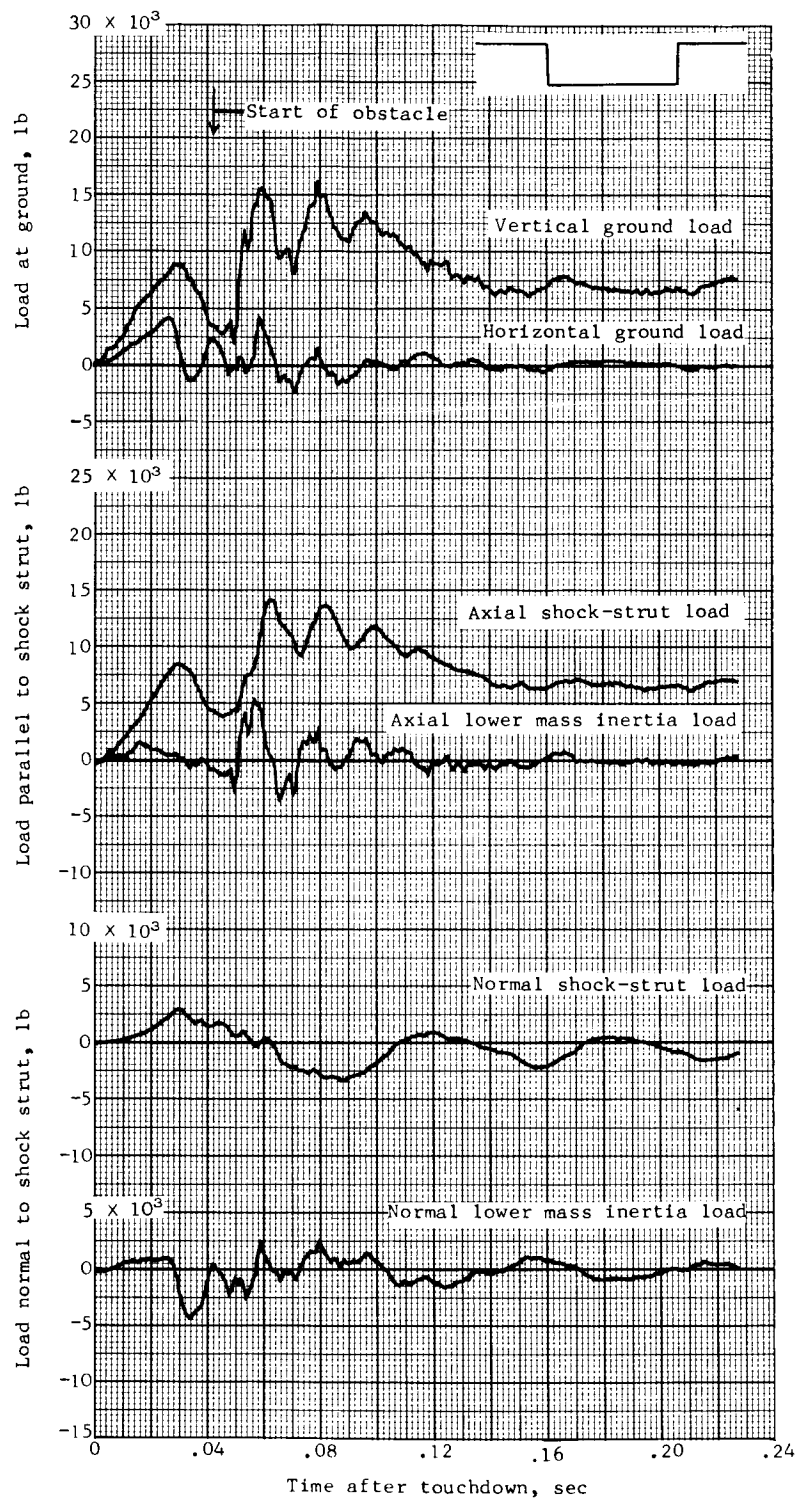
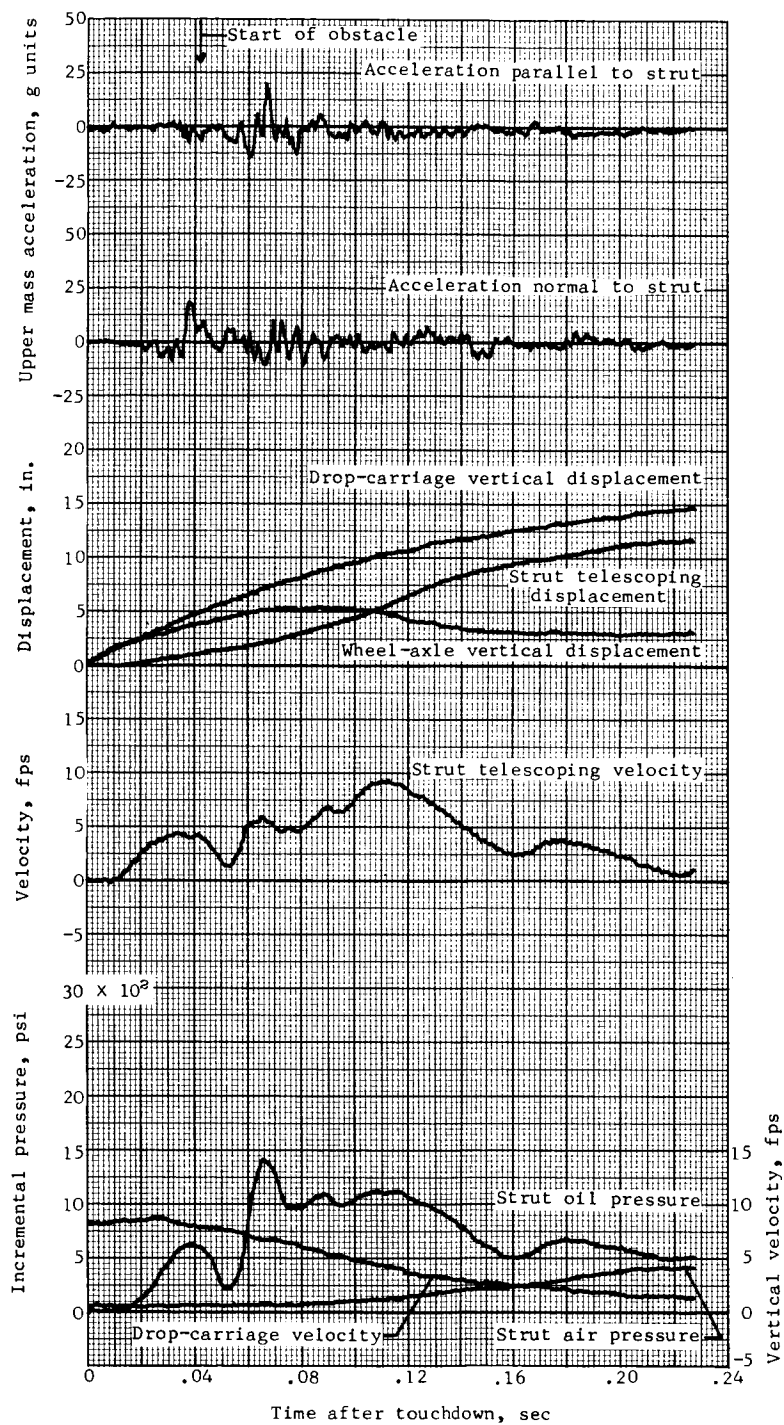


Figure 31.- Concluded.



(a) Test 46.

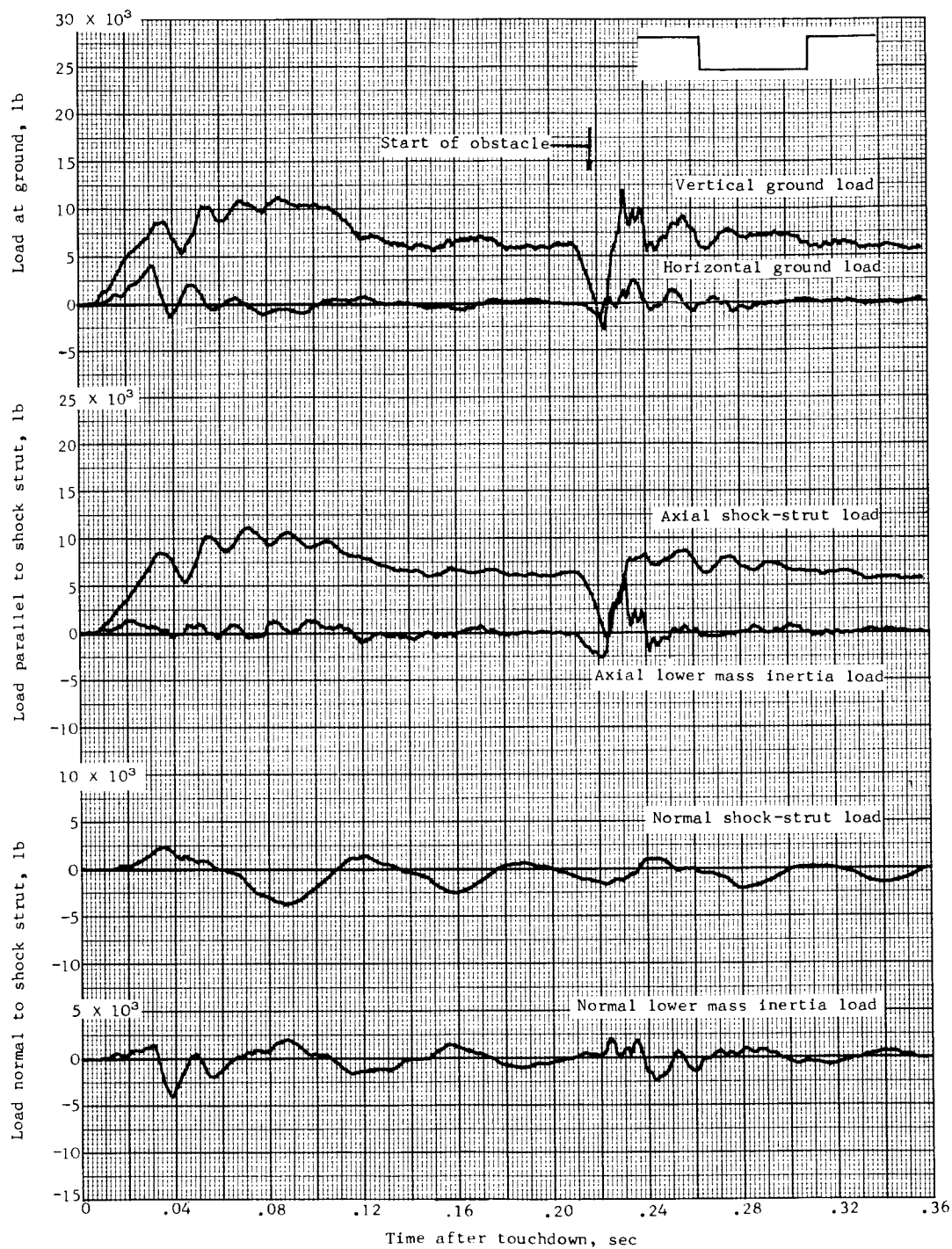
Figure 32.- Time histories of loads and other quantities obtained during landing impact over a step hole, 3 inches deep and 15 inches long.



(a) Concluded.

Figure 32.- Continued.

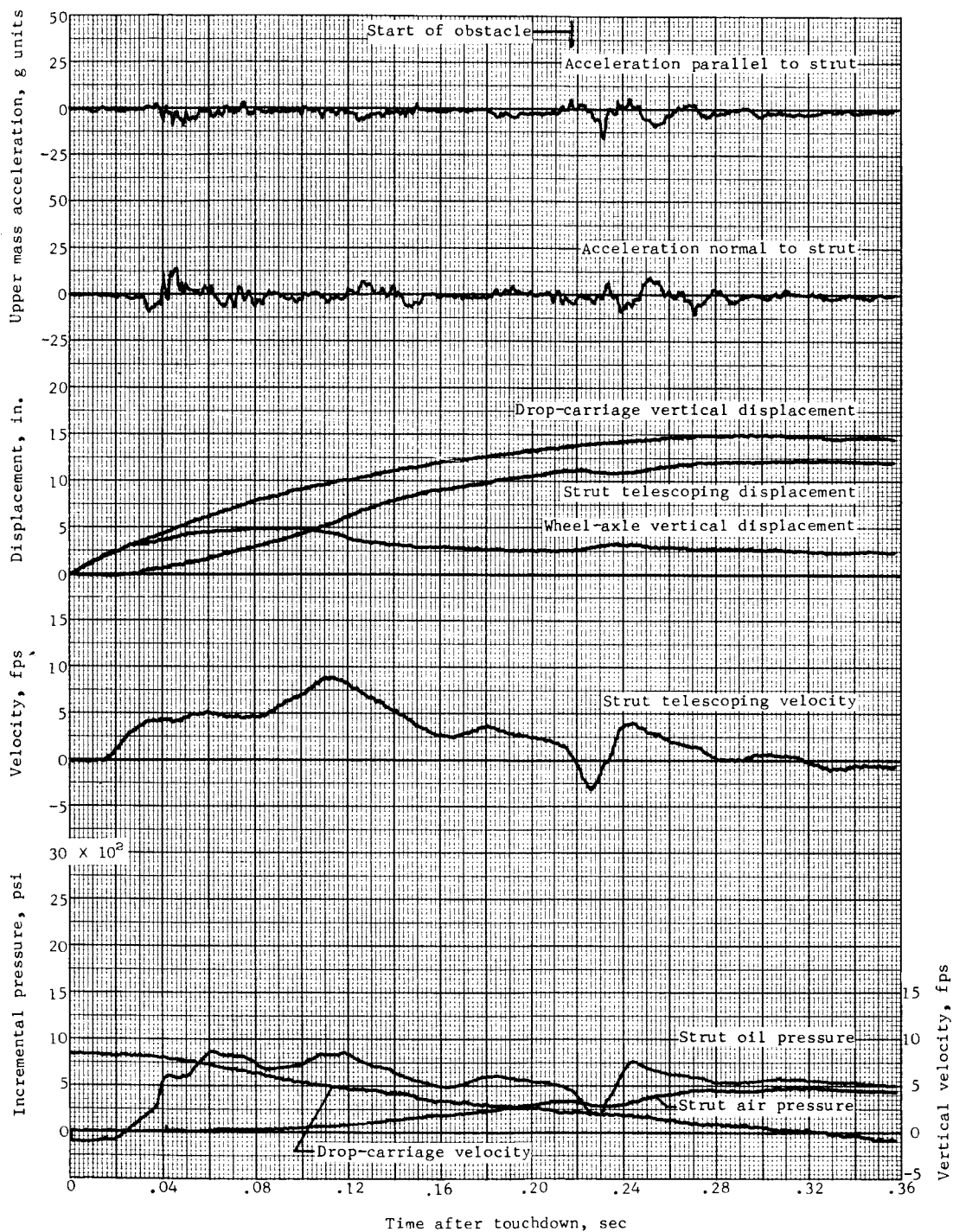




(b) Test 47.

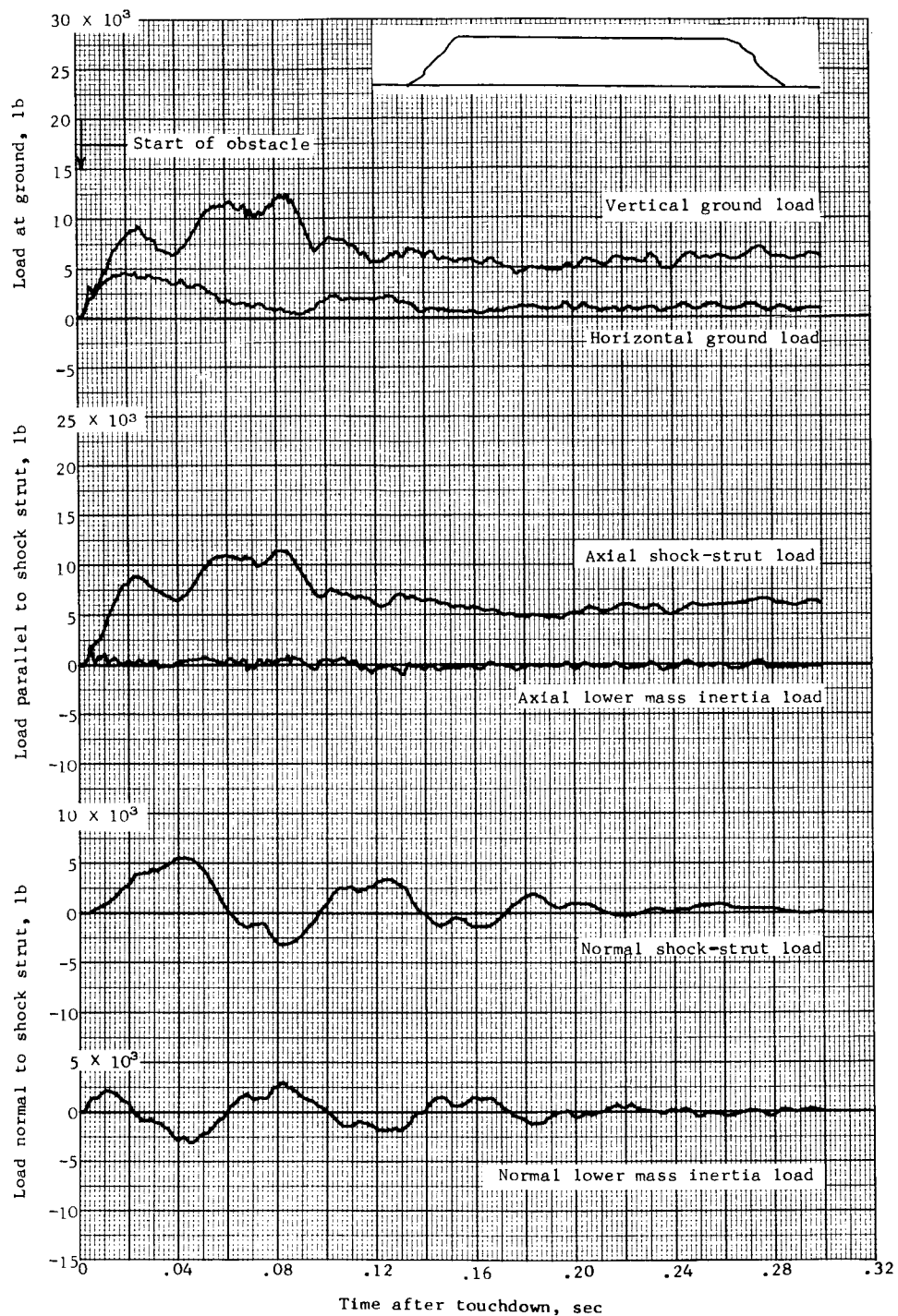
Figure 32.- Continued.





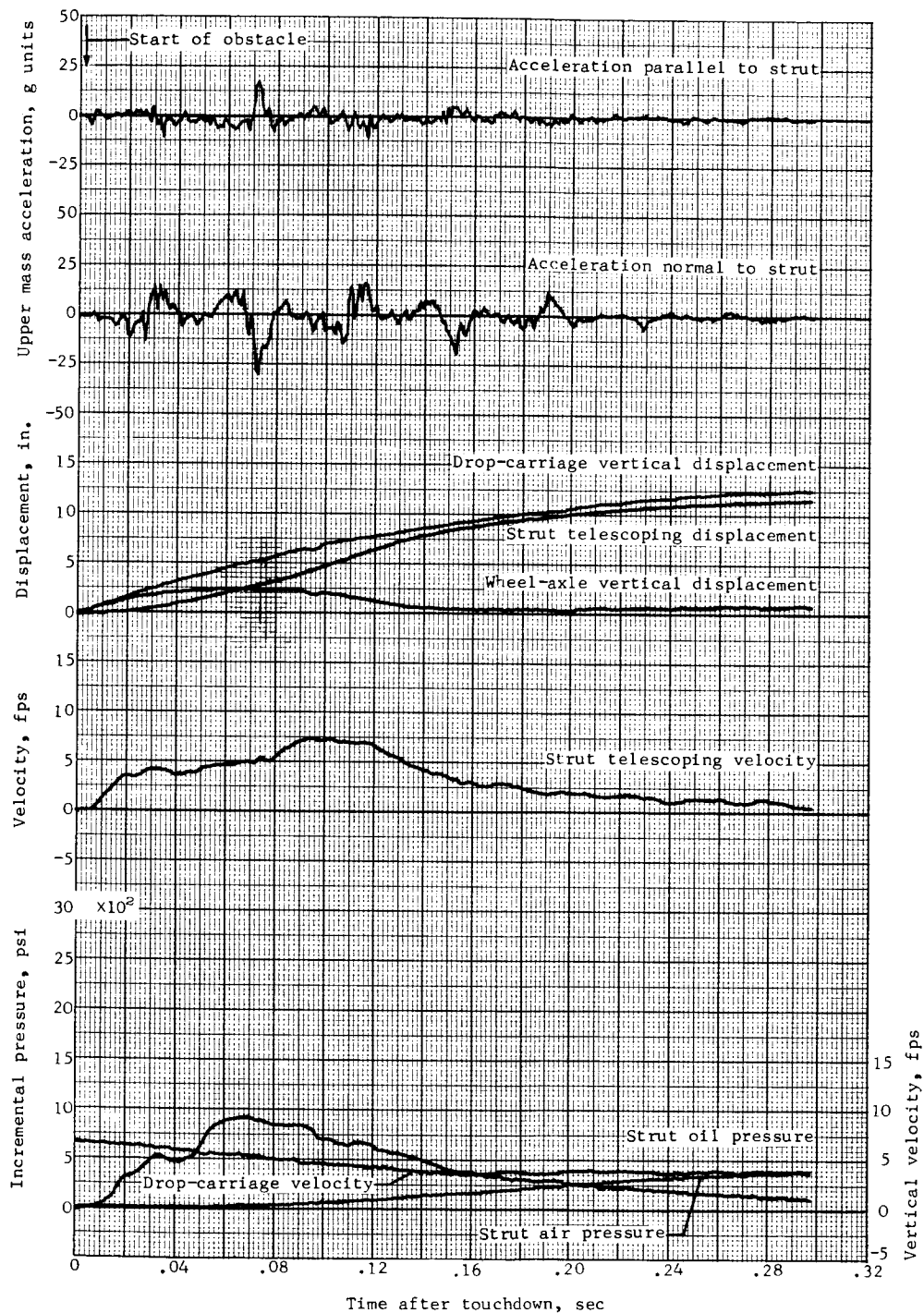
(b) Concluded.

Figure 32.- Concluded.



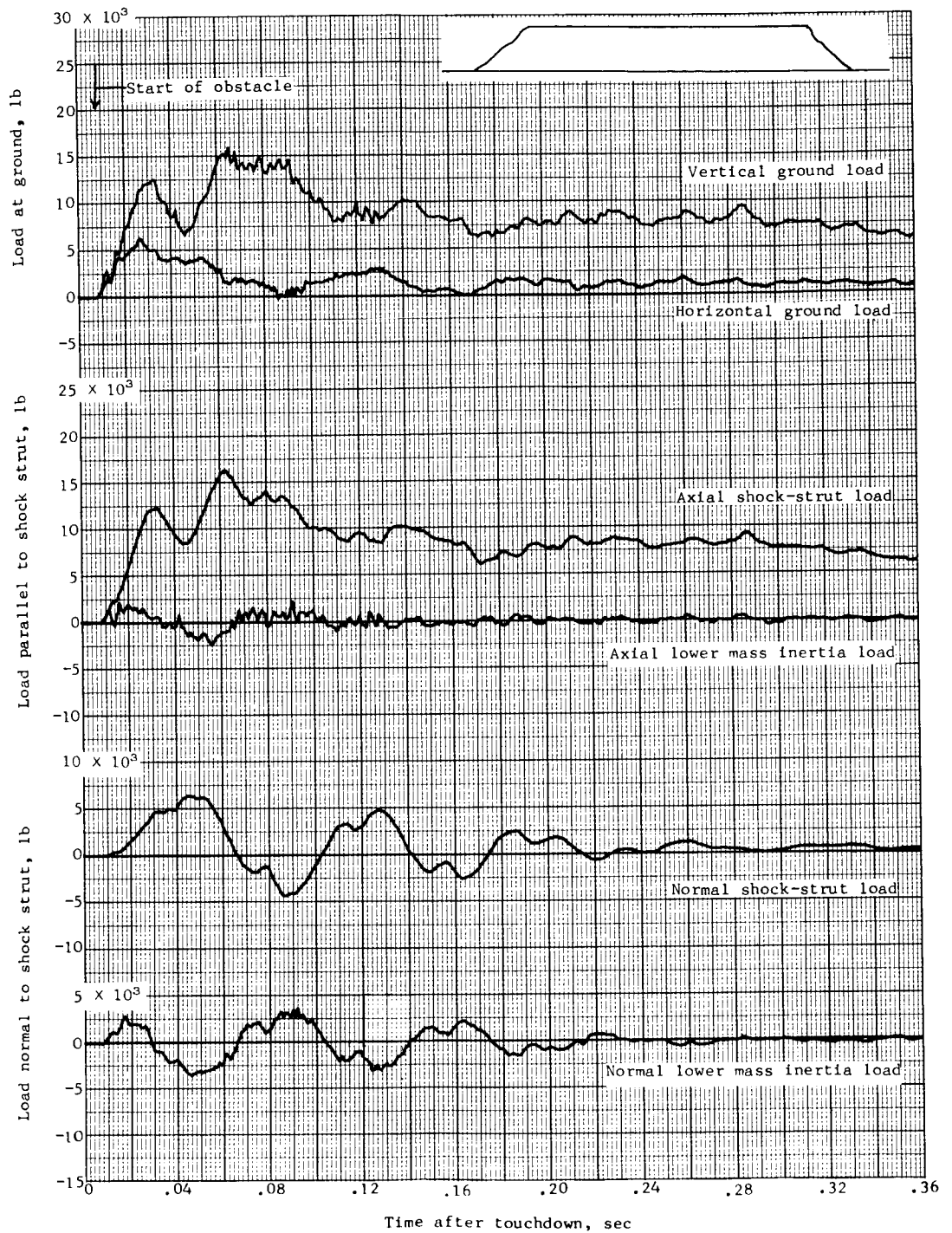
(a) Test 48.

Figure 33.- Time histories of loads and other quantities obtained during landing impact in sand, 8 inches deep and 720 inches long.



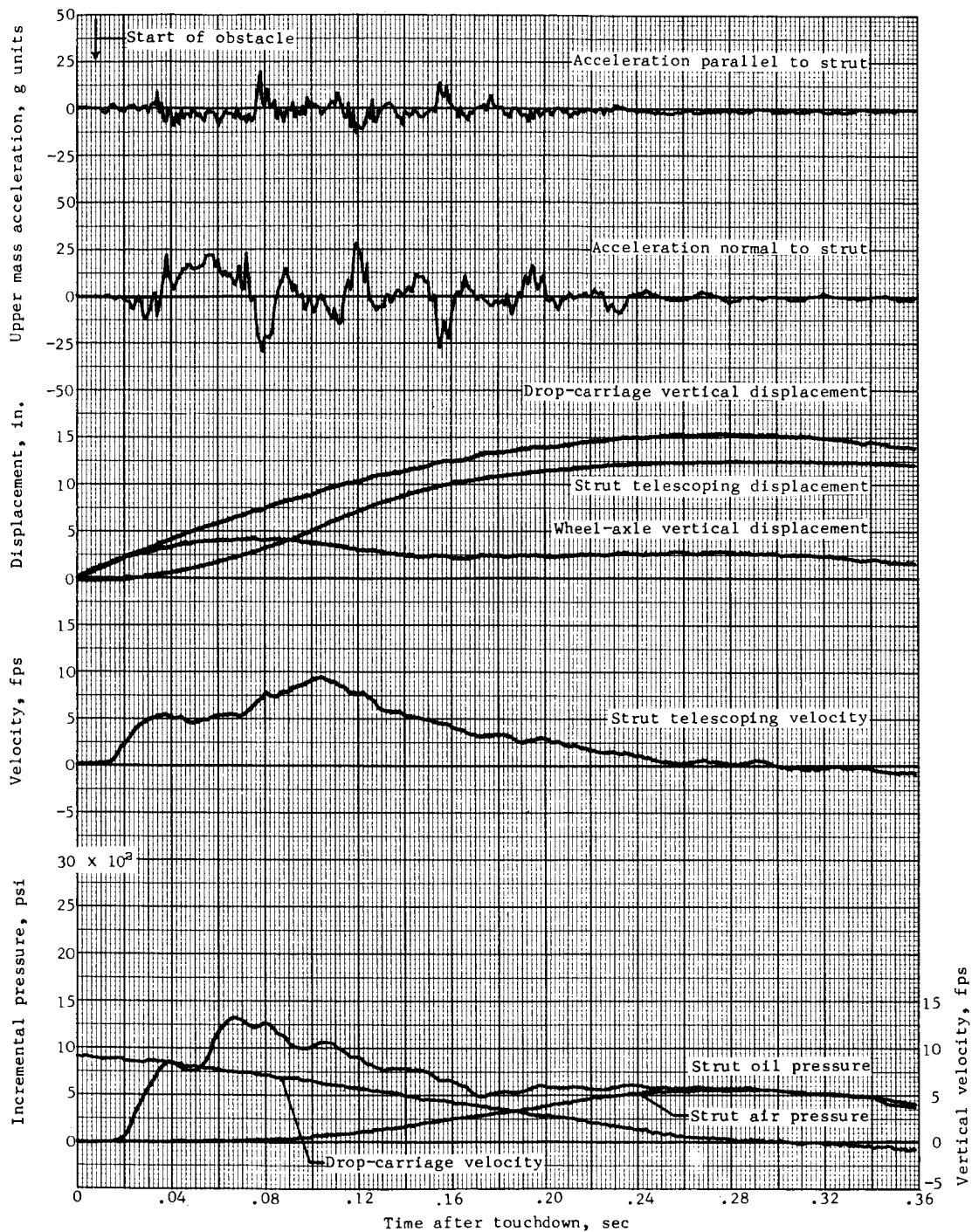
(a) Concluded.

Figure 33.- Continued.



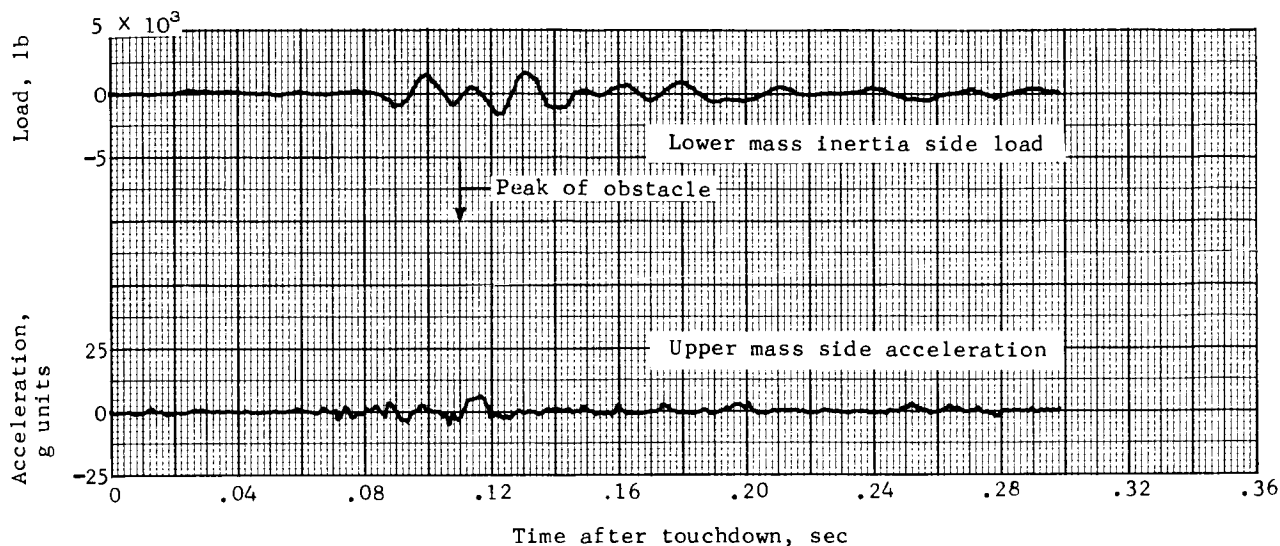
(b) Test 49.

Figure 33.- Continued.

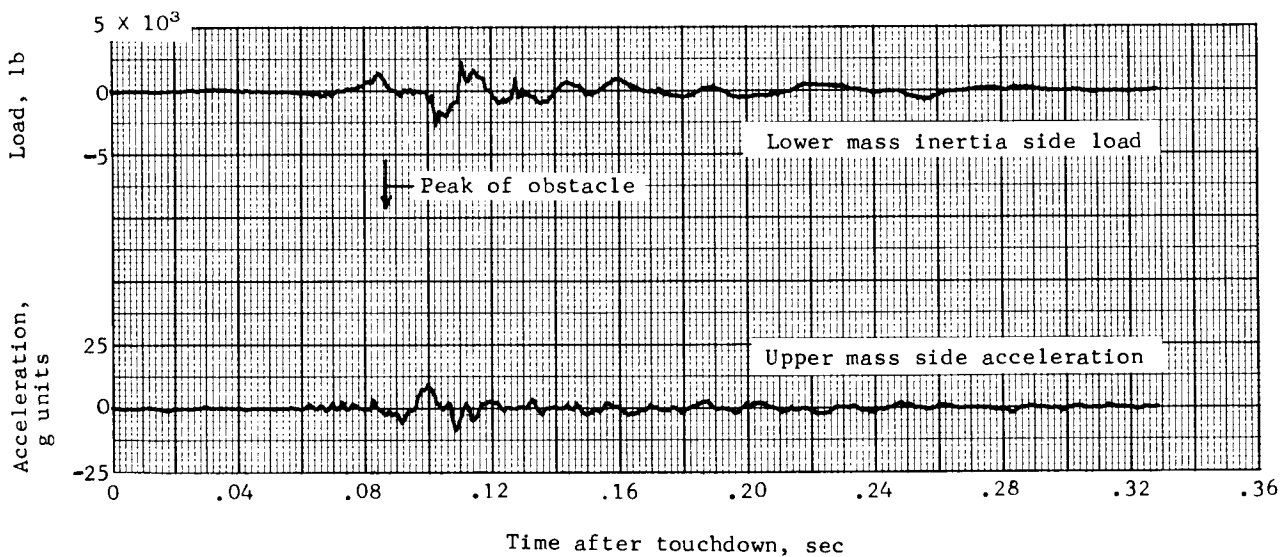


(b) Concluded.

Figure 33.- Concluded.



(a) 1 - cos, 2-inch-high, 30-inch-long obstacle. Test 6.



(b) 1 - cos, 2-inch-high, 30-inch-long obstacle oriented  $45^\circ$  to runway. Test 18.

Figure 34.- Time histories of lower mass inertia side loads and upper mass side accelerations obtained during landing impact tests over two different obstacles.

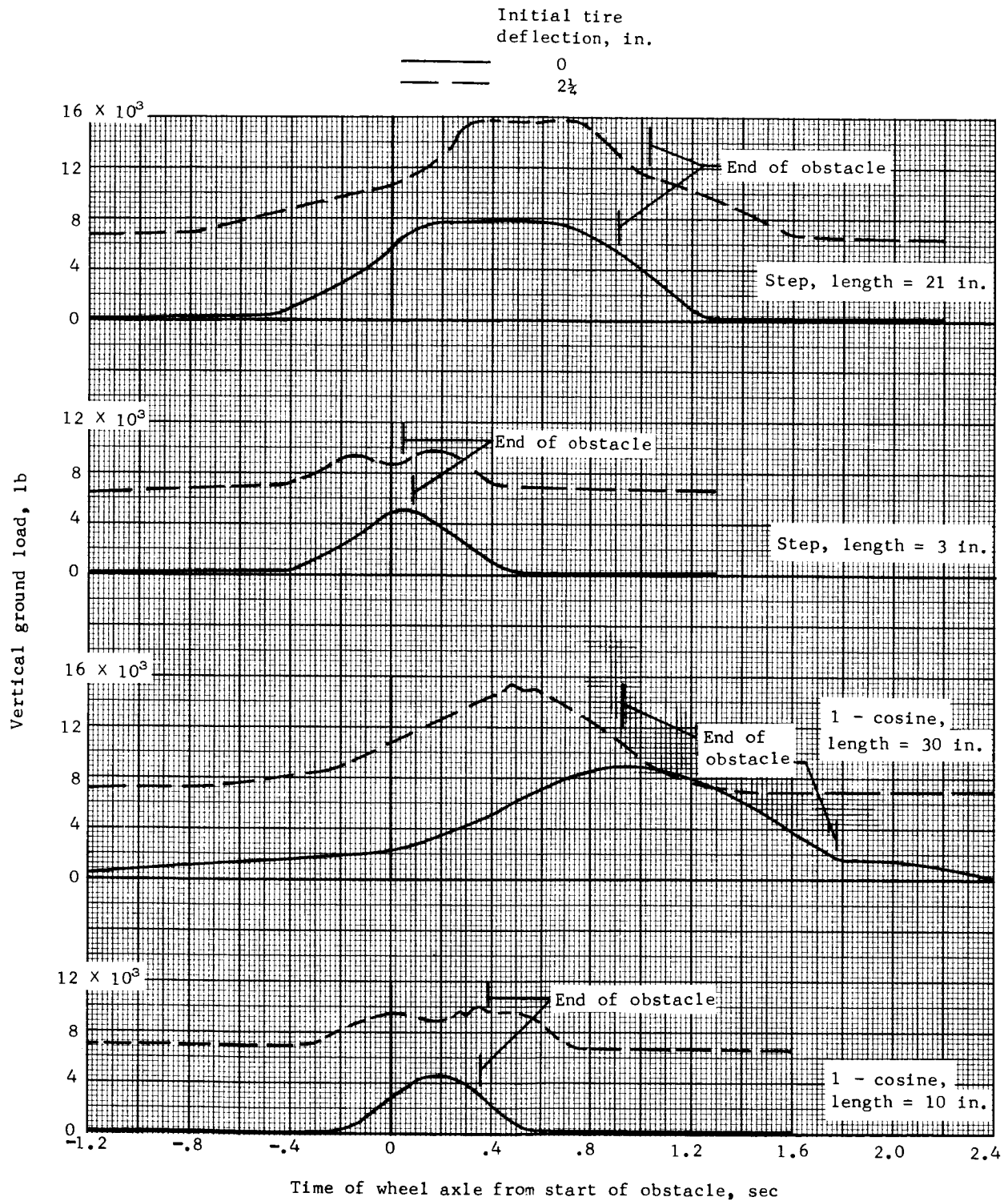


Figure 35.- Time histories of vertical ground loads obtained during slow-rolling tests over four different obstacles. Forward speed  $\approx$  2 feet per second.